IV. DETERMINATION OF VEGETATION COVER IN THE CALIFORNIA SOUTH COAST AIR BASIN FROM AERIAL IMAGERY

A. Introduction and Background

To assemble an emission inventory for vegetative hydrocarbons for that portion of the Los Angeles Basin designated as the study area, a biomass estimate was required. This estimate in turn depended upon analysis of the vegetation composition and distribution within the study area. In view of the paucity of relevant data of this kind for CSCAB vegetation and inherent limitations in the time and resources which could be devoted to this program, an integrated study was designed involving areal mapping of vegetation from high-resolution photographs and the acquisition of ground-based data by UCR botanists.

Previous studies designed to assemble natural hydrocarbon emission inventories have used various data bases to obtain information about vegetation. The Association of Bay Area Governments (ABAG), in preparing a biogenic hydrocarbon emission inventory for the San Francisco Bay Area, used digital Landsat data for a vegetation inventory (Hunsaker 1981, Hunsaker and Moreland 1981). Land cover classification was based on Landsat spectral data which had been clustered (a computer-assisted aggregation of data) by the California Department of Forestry (CDF). The Landsat data were used to describe location, area and percent composition of 23 different land cover classes. Most classes were expressed as percentages of four basic vegetation types: hardwood, conifer, grass and brush in 1 km x 1 km grid cells (Hunsaker 1981, Hunsaker and Moreland 1981).

A study supported by the Environmental Protection Agency (EPA) to determine the impacts on air quality of emissions of hydrocarbons from indigenous species of vegetation in the Tampa/St. Petersburg, Florida area determined vegetation types and distribution primarily from Level II land use and planning maps (Zimmerman 1979a). These maps were developed by the U. S. Geological Survey for the Land-Use and Land-Cover Data Analysis System (LUDA). LUDA maps are based primarily upon land use or function, in addition to ground cover. The Tampa/St. Petersburg study area was divided into a grid and overlayed on the 1:250,000 LUDA maps. The percentage occupied by each land use category was then visually estimated for

each grid cell. The result was a set of LUDA categories and their percent coverage for each grid cell in the study area (Zimmerman 1979a). These results were combined with experimentally determined emission rates.

A more detailed approach to obtaining a vegetation inventory was taken in an EPA-sponsored study of natural sources of ozone in Houston (Zimmerman 1980). Here, the approximate vegetative composition was estimated from 1:20,000 scale aerial photographs for the 1,610 km^2 study area. Although it was recognized that land use changes had taken place since the aerial photographs were taken, no effort was made to update the data since more recent information was unavailable. Percent ground cover was visually estimated for trees, pasture, cropland and lawn, water surfaces and barren land (houses, roads and highways). Again, these data were combined with appropriate hydrocarbon emission rates.

In reviewing these previous studies it was felt that there was a significant lack of the detailed information on vegetation-type which is required for a more accurate calculation of biogenic emissions. While much emphasis was placed on the measurement of emission rates, relatively minor consideration was given to the reliability of calculations for total biomass of the study area. Since this is a critical link in assembling the ultimate emission inventory, it was decided that a greater emphasis should be placed upon the vegetation mapping exercise and field assessments in the present study.

B. Delineation of the Study Area

As noted earlier, the area investigated in this study was that portion of the CSCAB containing essentially all of the anthropogenic sources of reactive organics in the western and middle portion of the Basin (i.e., the "source" region) - or about 75% of the total reactive organic emissions in the entire CSCAB (see Figure II-2) - plus surrounding areas of natural vegetation. Defining the study area in terms of hydrocarbon emissions from vegetation required consideration of physiographic as well as climatic factors. The so-called "coastal plain" on which Los Angeles stands is the largest continuous plain of the many lowlands of Southern California. Its length along the coast from the Santa Monica mountains on the northwest to the San Joaquin hills to the southeast is 80 km, and its breadth from the sea to the Puente and Chino hills is approximately 30 to

40 km. The area is bounded on the north by the Santa Monica and San Gabriel mountains, on the east and southeast by the Santa Ana mountains and San Joaquin hills, and on the west by the Pacific Ocean.

An important factor governing the mixing and transport of biogenic (as well as anthropogenic) hydrocarbons is the local meteorology, which is affected, to some extent, by the topography and geography of the area. In the Los Angeles basin, a diurnal pattern occurs characterized by a sea breeze (onshore) in the daytime and a land breeze (offshore) at night (DeMarrais et al. 1965). This means that, in general, the air moving into the study area during the day comes from over the ocean. This is indicated by the streamline airflow chart shown in Figure IV-1. Consideration of the full set of such streamline charts (DeMarrais et al. 1965) suggested that the transport of hydrocarbons produced in another area and transported via air flow into the study area should be of minor consideration for daytime hours. Typically, relatively clean marine air is transported into and through the source area in the morning, accumulates hydrocarbon and oxides of nitrogen emissions, and then continues on to the receptor sites east and north of the Los Angeles coastal plain.

The study area was delineated from assessments of these local topographic and meteorological conditions. As noted, three mountain ranges constitute the most important parts of an almost continuous boundary of mountains and foothills around the study area, namely the Santa Monicas, San Gabriels, and the Santa Anas. The Santa Monica mountains were divided along the ridgeline since the southerly facing slopes would be contributing hydrocarbons to the study area from westerly winds. In the San Gabriels and Santa Anas, the 3600 foot contour line was chosen as the upper boundary. This altitude is well above the approximate average height of the summer inversion layer in the coastal plain (DeMarrais et al. 1965) and therefore provides a "worst" case with respect to the contribution of vegetative hydrocarbons from these slopes. These natural boundaries were connected with lines which were consistent with treating this portion of the air basin as the "source" area for primary pollutants. The actual boundaries of the project study area are plotted on the Universal Transverse Mercator coordinate system shown in Figure IV-2.

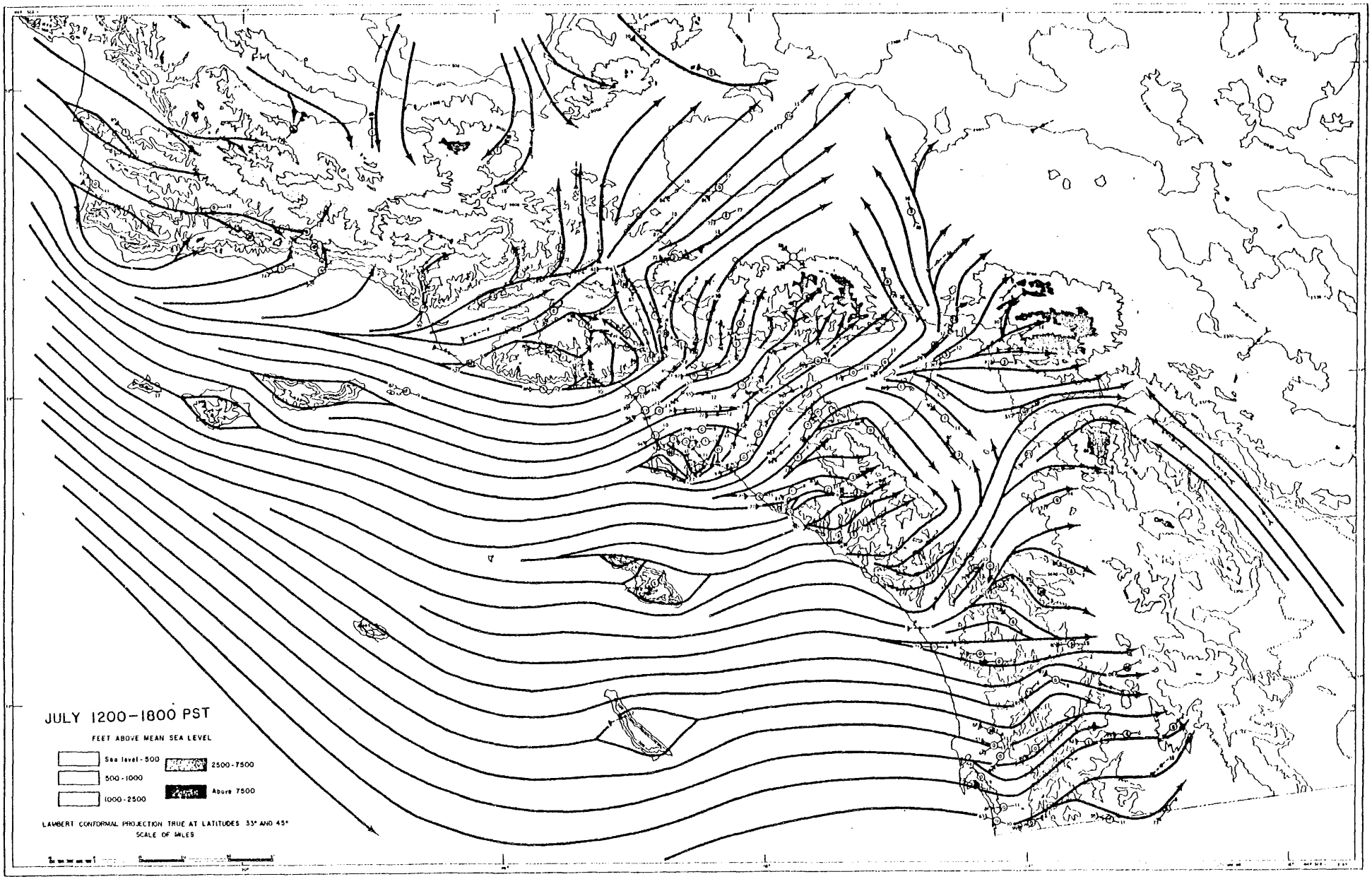

Figure IV-1. Streamline chart for southern California for July, 1200-1800 PST (from DeMarrais et al. 1965).

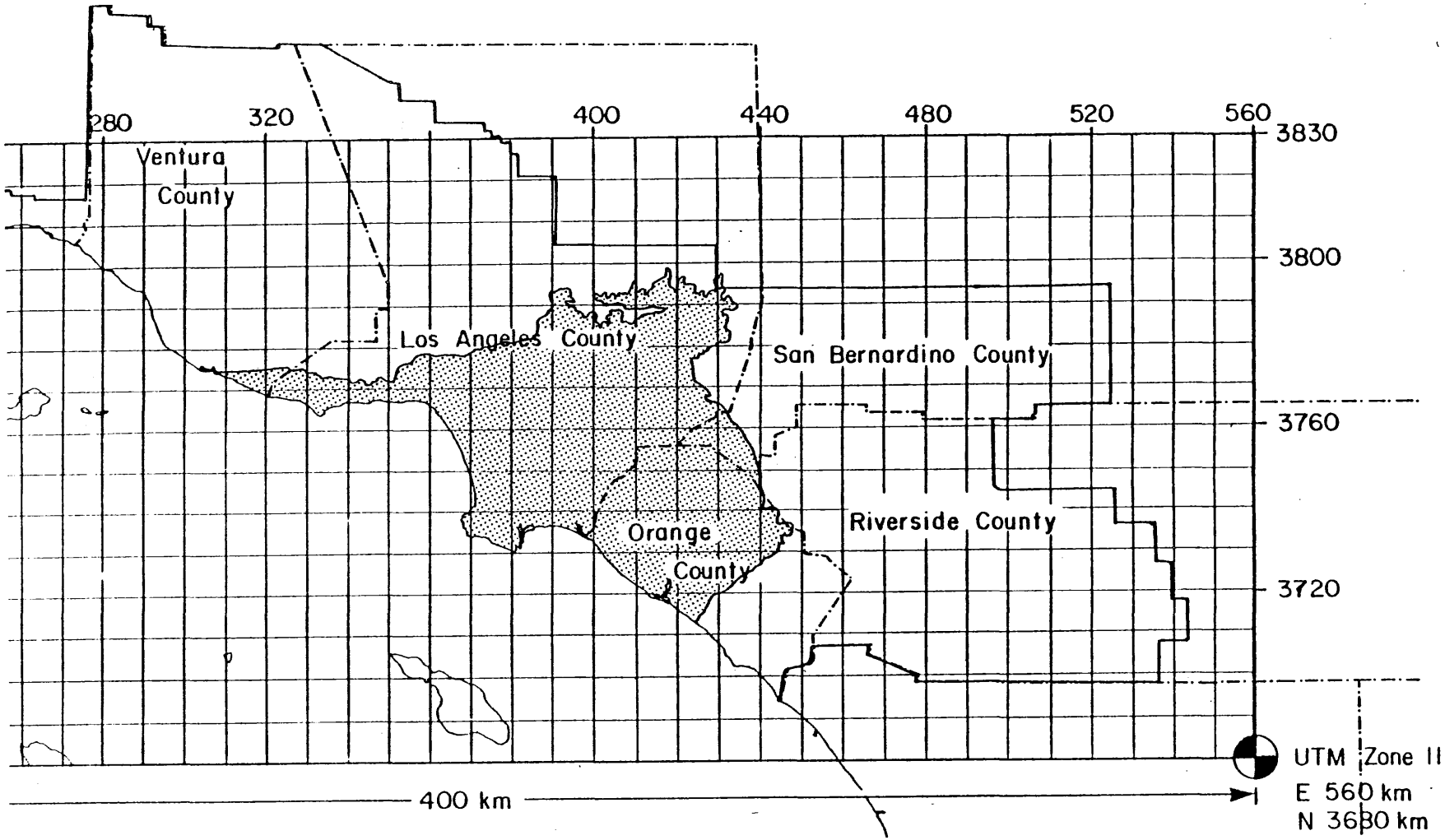

Figure IV-2. Universal Transverse Mercator (UTM) coordinate system showing project study area defined by coastline and 3600' contour (or ridgelines) of mountains and hills surrounding the Los Angeles coastal plain.

C. Use of Remotely-Sensed Data as a Map Base

An important decision in any mapping exercise is the choice of the data base upon which the subsequent analyses will be dependent. Also, the data base used to make a vegetation map must be representative of the vegetation itself. A land use map, therefore, which is constructed from an interpretation of land use or land cover, cannot be used reliably to analyze vegetation since a quantitative analysis cannot be based on inference. Since urban vegetation is so complex, no detailed vegetation maps exist for the Los Angeles area. Thus, it was decided to use aerial photography to map the composition and distribution of the vegetation within the study area.

Two forms of aerial imagery were immediately available for complete coverage of the study area: satellite imagery (Landsat) and high altitude (NASA/U-2 aircraft) photographs. There are distinct disadvantages to employing Landsat imagery to describe the vegetation for this study which could be avoided by using photographs. Specifically, when dealing with a large scale (small areal coverage) photograph, one can see actual objects, in this case, plants. This enables many techniques of interpretation (including color, tone, shape, size, association with other objects, texture, etc.) to be used to characterize the entity mapped. Many of these useful interpretive attributes are lost when resolution is reduced to a cell that averages many reflective tones as in the case of Landsat imagery. Interpretation of satellite imagery is dependent solely upon the tone of the pixel cell since, due to poor resolution, no objects less than 60 m x 80 m can be seen. For this study resolution was of prime importance.

For those reasons it was decided to use high-resolution U-2 color infrared (CIR) imagery for a regional breakdown of vegetation by physiognomic (structural) category and for a detailed analysis of the urban vegetation within the study area.

D. Distribution of Broad Physiognomic Classes of Vegetation in the California South Coast Air Basin

Color infrared imagery is extremely valuable for vegetation analysis because plants are high reflectors of infrared radiation. A mosaic of 15 CIR images taken in July 1972 by a NASA U-2 aircraft and covering the LA

Basin and surrounding areas was used to determine boundaries of urban, natural and agricultural vegetation in the CSCAB. (This imagery is on file in the Department of Earth Sciences at UCR.) Any boundary changes were updated using current (June 1981) Landsat imagery on an International Imaging Systems color combiner. Boundary variations between 1972 and 1981 were found to be limited, involving primarily urbanization of small agricultural areas.

A map of the three broad physiognomic classes of vegetation, urban, natural and agricultural, (as well as non-vegetated areas) is reproduced in Figure IV-3. From this map, it can be seen that urban vegetation is by far the largest class within the study area. This urbanized portion of the basin is surrounded by natural vegetation on mountain slopes and rolling hills. Agricultural vegetation is limited to small areas in canyons (mainly citrus) and a larger area in southern Orange County (mostly vegetable crops with some citrus). In addition to the vegetative classes, another class termed non-vegetated is included as a scattered distribution within the urban area. This class encompasses the larger central business districts, airports and extensive industrial areas that have relatively little or no vegetative cover as observed on the imagery. It was therefore felt that these areas could be safely eliminated from further investigation.

Areal calculations of the three vegetation classes were made utilizing a Talos Class IV floating cursor digitizer. With this instrument areas are calculated by moving a hand-held cursor around the perimeter of a polygon. The areas of each vegetative class (and the non-vegetated regions) were calculated and summed to produce a total acreage. The results of these calculations are shown in Table IV-1.

From these data it was determined that the four classes constitute a total study area of about 4500 km^2. It was also noted that the urban class formed over half of the entire study area (58%). Natural vegetation constituted one-third (33%) of the study area, with agricultural and non-vegetated classes as minor elements. From these data, it became obvious that a biomass calculation would require a more detailed analysis as to the character of the urban and natural vegetation.

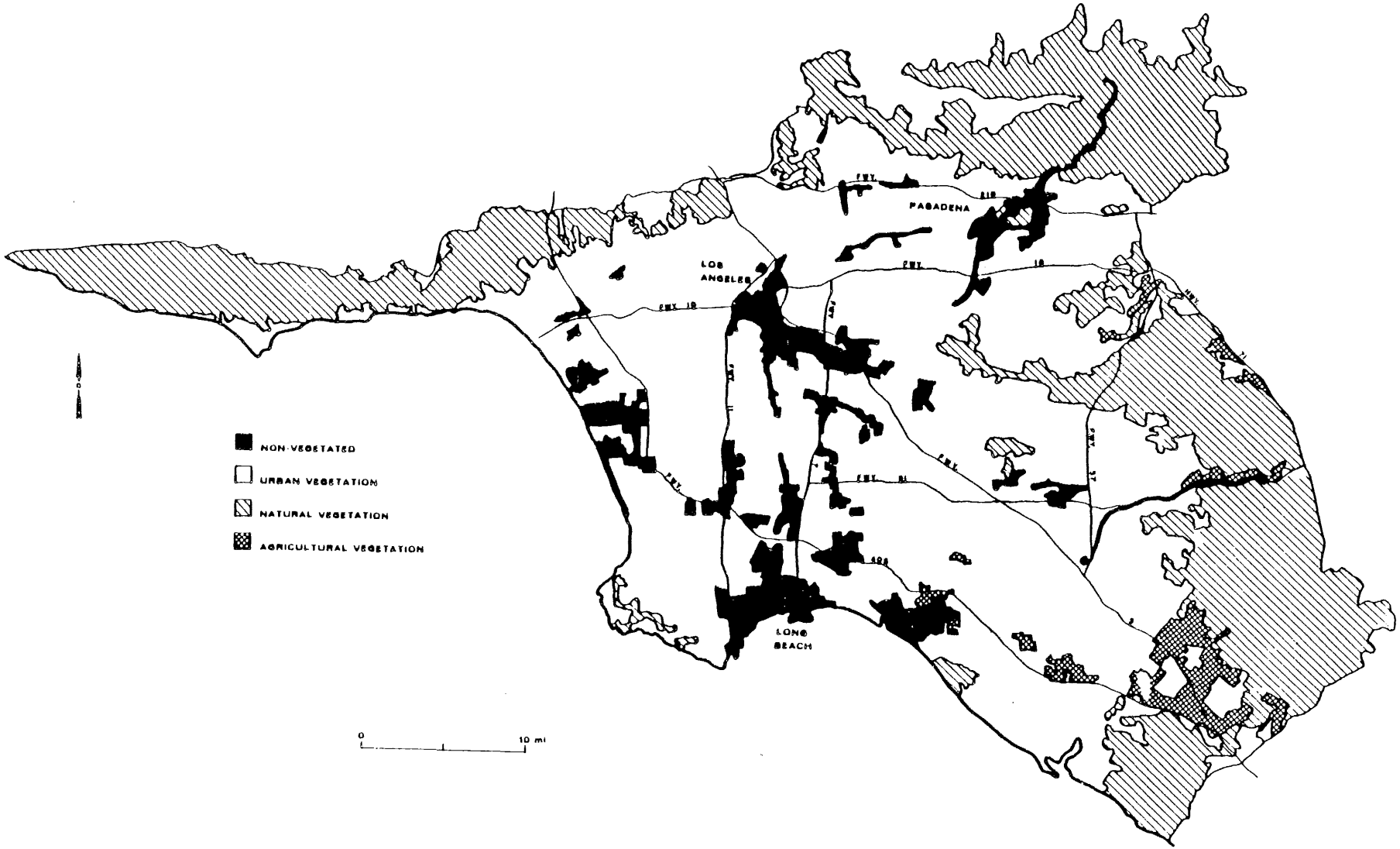

Figure IV-3. Distribution of natural, agricultural, and urban vegetation (and non-vegetated areas) in the study area. Mapped from a mosaic of 15 color infrared images obtained by a NASA U-2 overflight of the CSCAB in 1972 at a scale of 1:131,000.

Table IV-1. Area Totals for Natural, Agricultural and Urban Vegetation

	Area		Percent of Study Area
	km^2	mi^2	
Natural	1476	570	33
Agricultural	105	40	2
Urban	2626	1014	58
Non-vegetated	297	114	7
Total study area	4504	1738	100

E. Detailed Study of Urban Vegetation

Although studies have been made of the natural vegetation of southern California (Mooney 1977, Hanes 1977), no detailed, quantitative study of the urban vegetation had been carried out prior to the present work. Previous biogenic emission studies have dealt primarily with natural and agricultural vegetation (Taback et al. 1978, Zimmerman 1979a,b, Hunsaker 1981, Hunsaker and Moreland 1981). Urban vegetation has typically been ignored or given minor consideration because their biogenic emission contribution was considered minimal with respect to other vegetated areas, or possibly because urban vegetation was considered too complex for analysis. However, in the present study, urban vegetation is the major component on an areal basis, and must be taken into account. Because of the enormous size of the area to be studied, a comprehensive vegetation analysis was inconceivable. It was therefore decided that the detailed analysis required for the urban component should be based on random sampling procedures designed to be as comprehensive and statistically valid as possible within the limited time and resources of this investigation.

1. Stratified Random Sampling Approach

It had been noted that distinct variations in reflective intensity and tone existed within urban areas on the U-2 imagery. These variations were interpreted as differences in leaf mass and species composition. On this basis the urban vegetation class was subdivided into 20 polygons based on their relative tone and reflective intensity (Figure IV-4). These polygons were assumed to be relatively homogeneous in vegetation composition to enable a stratified, random sampling analysis of urban vegetation.

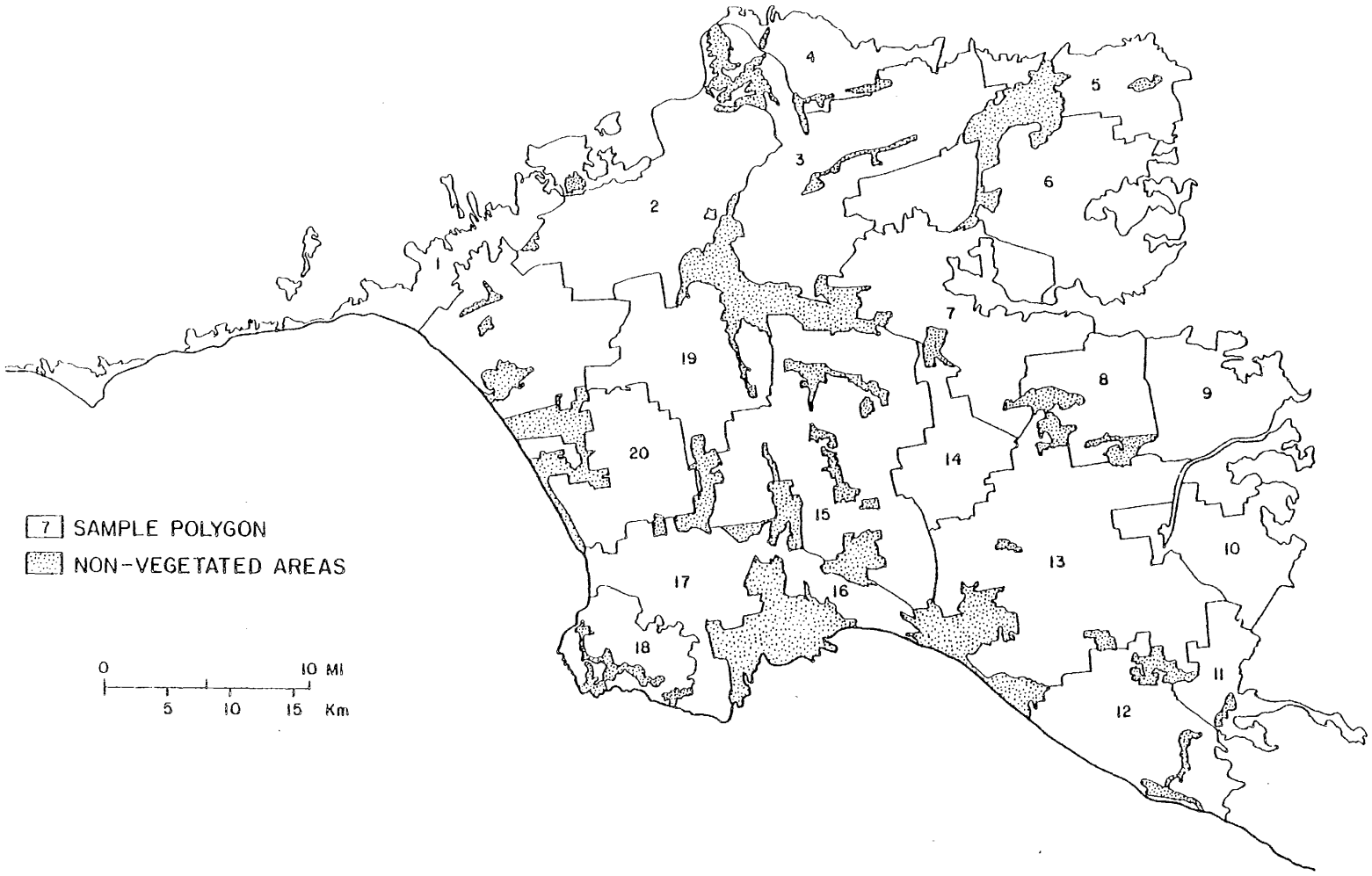

Figure IV-4. Division of urban vegetation in study area into 20 polygons based on their relative tone and reflective intensity on NASA U-2 color infrared imagery.

As noted above, the purpose of the sample survey design was to maximize the amount of information obtainable within the time and funding constraints of this study. Random sampling usually provides good estimates of population quantities. As depicted in Figure IV-5 (after Paysen 1978) a stratified random sample is one obtained by separating the population elements into non-overlapping groups called strata, and then selecting a simple random sample from each stratum (Mendenhall et al. 1971).

To implement the stratified random sampling of the urban vegetation it was necessary to randomly select a sample cell for each of the 20 polygons. It was decided that large scale high resolution (1:3,000) photographs would be taken within each polygon to determine the character of the urban vegetation. A grid was constructed to cover the entire urban area, with each grid cell the size of the photography to be obtained from a low altitude flight. The grid was laid out by latitude and longitude over four 1:250,000 scale U. S. Geological Survey (USGS) sheets covering the Los Angeles basin. Random numbers (Rand Corporation 1955) were converted by computer to latitude and longitude coordinates of sample cell size and a list of randomly selected cells was generated.

These cells were then consecutively plotted on the grid overlaying the urban study area and the 20 polygons. The first cell plotted in each polygon was designated as a sample site. Cells were plotted until each of the 20 polygons contained at least one sample site. The locations of the resulting 20 sample sites in the CSCAB are shown in Figure IV-6 and the latitude and longitude coordinates of the center point of the rectangularly shaped sample sites are listed in Table IV-2 along with the community containing this point. These 20 sample sites were then plotted on 7.5 minute U. S. Geological Survey maps by their latitude and longitude coordinates. An example of a Survey map plot is shown in Figure IV-7 (for Polygon No. 1). All twenty such plots are given in Appendix A.

Because of summer cloud cover the aerial photography could not be obtained until October 6, 1981. The sample flightlines were photographed on that date at approximately 1:3,000 scale with color infrared film by Western Aerial Surveys, Inc., of Riverside, California.

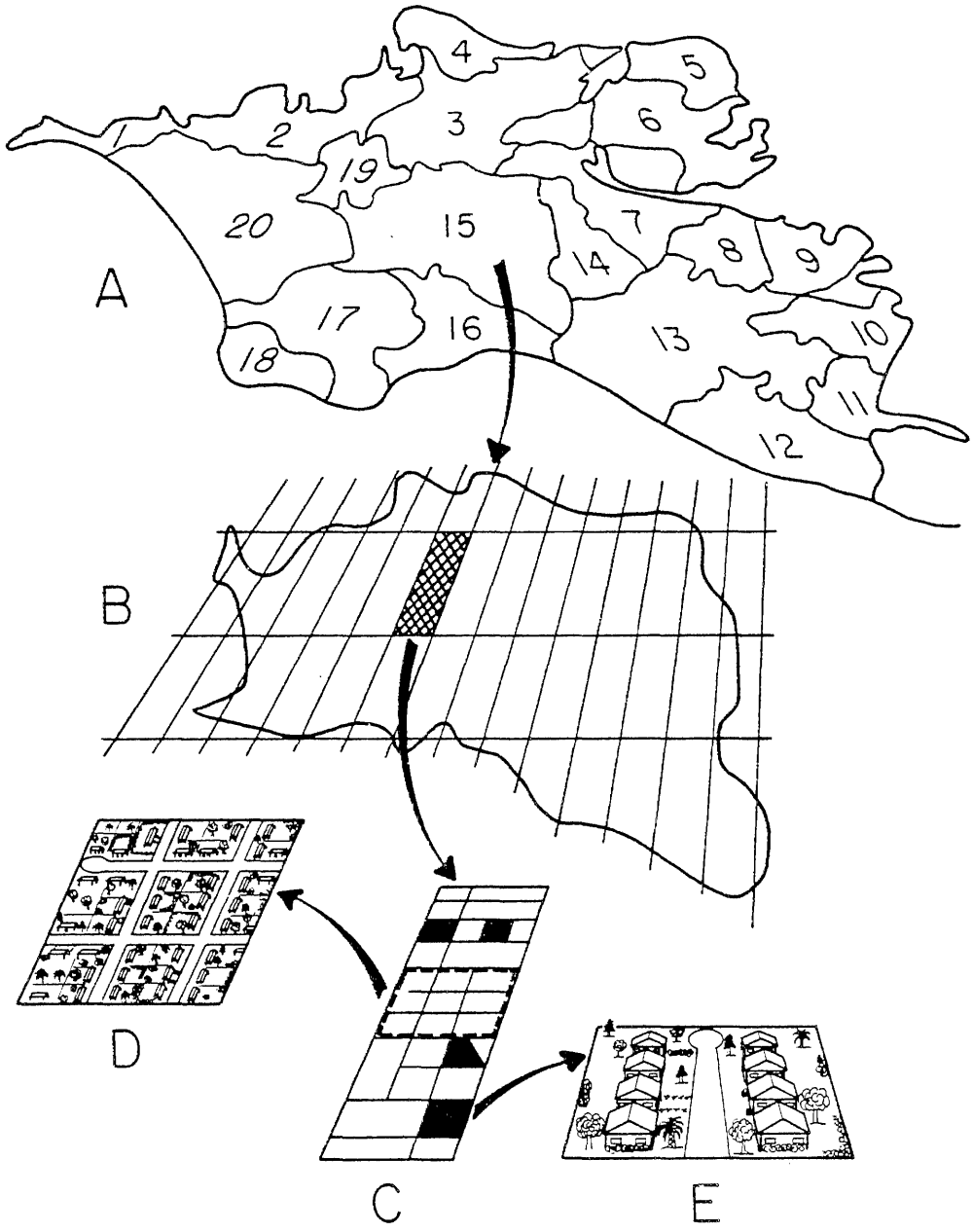

Figure IV-5. Depiction of the three-stage, stratified, random sampling design used in this study. A. Twenty stratified polygons covering urban portion of study area; B. Polygon with sample cell grid and randomly selected cell; C. Randomly selected sample cell showing center frame of color infrared imagery (dashed line) and randomly selected subplots (darkened); D. Color infrared imagery area mapped for vegetation cover; E. Subplot randomly selected for vegetation inventory.

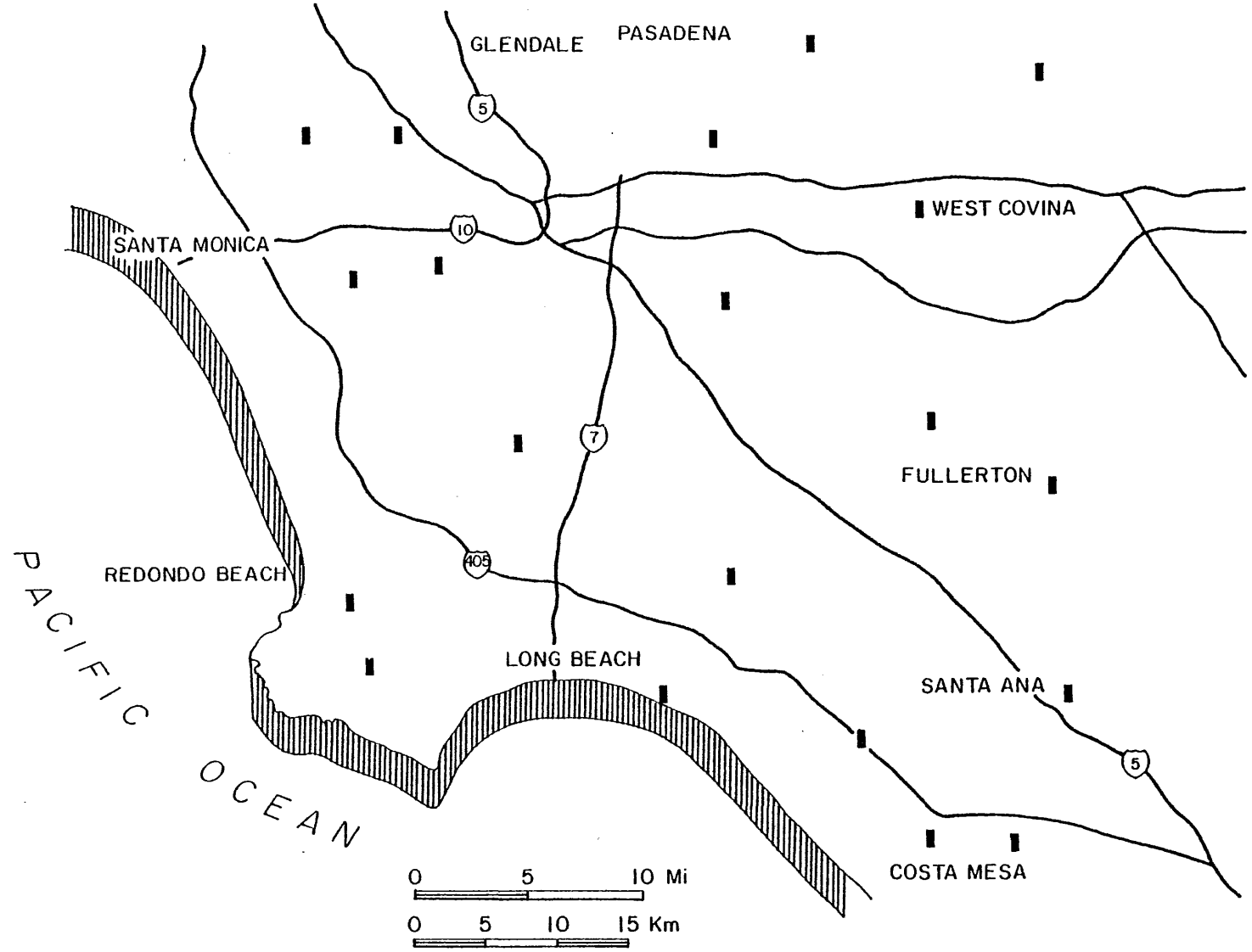

Figure IV-6. Randomly selected sample sites for which high-resolution aerial imagery was obtained and field survey of vegetation was conducted (not to scale).

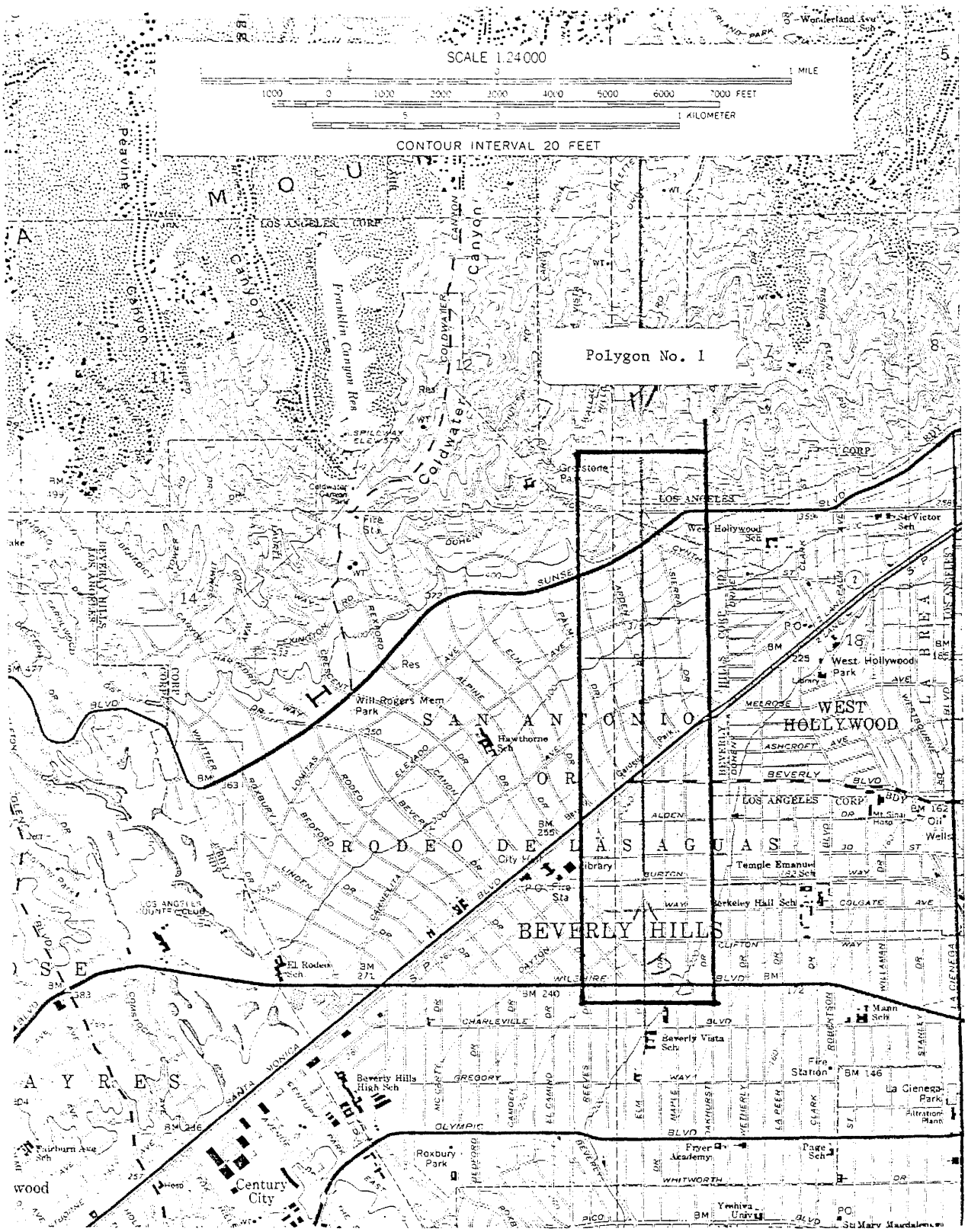

Figure IV-7. Portion of 7.5 minute U.S. Geological Survey Map for Beverly Hills Quadrangle. Rectangular area corresponds to randomly selected location in Polygon 1 for which aerial photography was taken and in which field survey was conducted.

Table IV-2. Random Sample Sites Chosen for Aerial Imagery and Field Studies

Polygon Number	Community Containing Center Point	Quadrangle Map	Coordinates of Center Point	
			Latitude	Longitude
1	Beverly Hills	Beverly Hills	34°05'00"	118°23'36"
2	Hollywood	Hollywood	34°05'36"	118°19'42"
3	San Gabriel	El Monte	34°05'36"	118°05'54"
4	Arcadia	Mt. Wilson	34°09'12"	118°01'42"
5	Glendora	Glendora	34°08'00"	117°51'30"
6	West Covina	Baldwin Park	34°03'12"	117°56'36"
7	Montebello	Montebello	34°00'48"	118°06'30"
8	La Habra	La Habra	33°55'24"	117°56'00"
9	Placentia	Yorba Linda	33°53'00"	117°50'54"
10	Santa Ana	Orange	33°45'12"	117°50'00"
11	Newport Beach	Tustin	33°39'48"	117°52'06"
12	Costa Mesa	Newport Beach	33°38'36"	117°56'00"
13	Huntington Beach	Newport Beach	33°43'24"	117°59'00"
14	Long Beach	Los Alamitos	33°49'24"	118°05'00"
15	Compton	South Gate	33°54'12"	118°14'36"
16	Long Beach	Los Alamitos	33°45'48"	118°07'06"
17	Palos Verdes Estates	Torrance	33°48'12"	118°21'48"
18	Rolling Hills	Torrance	33°45'48"	118°20'54"
19	Los Angeles	Hollywood	34°00'48"	118°17'54"
20	Baldwin Hills/ Hawthorne[a]	Hollywood	34°00'12"	118°21'48"

[a]See text.

2. Mapping and Classification of Sample Sites

For each of the twenty randomly chosen sample sites five frames of imagery (with 30% overlap between frames) were obtained covering the areas plotted on the 7.5 minute USGS maps as given in Appendix A. In all but one case the imagery fell within or greatly overlapped the plotted rectangles. In Polygon 7 the imagery center point fell just outside the plotted rectangle. The specific frame of imagery lying over, or closest to, the center point of each sample site, was designated as the area to be mapped. A portion of a center frame of color infrared imagery (necessarily reproduced in black and white) is shown, as an example, in Figure IV-8 for the Glendora site (Polygon 5).

Time and funding constraints limited mapping to the center frame of imagery obtained for each polygon. The vegetation was then mapped

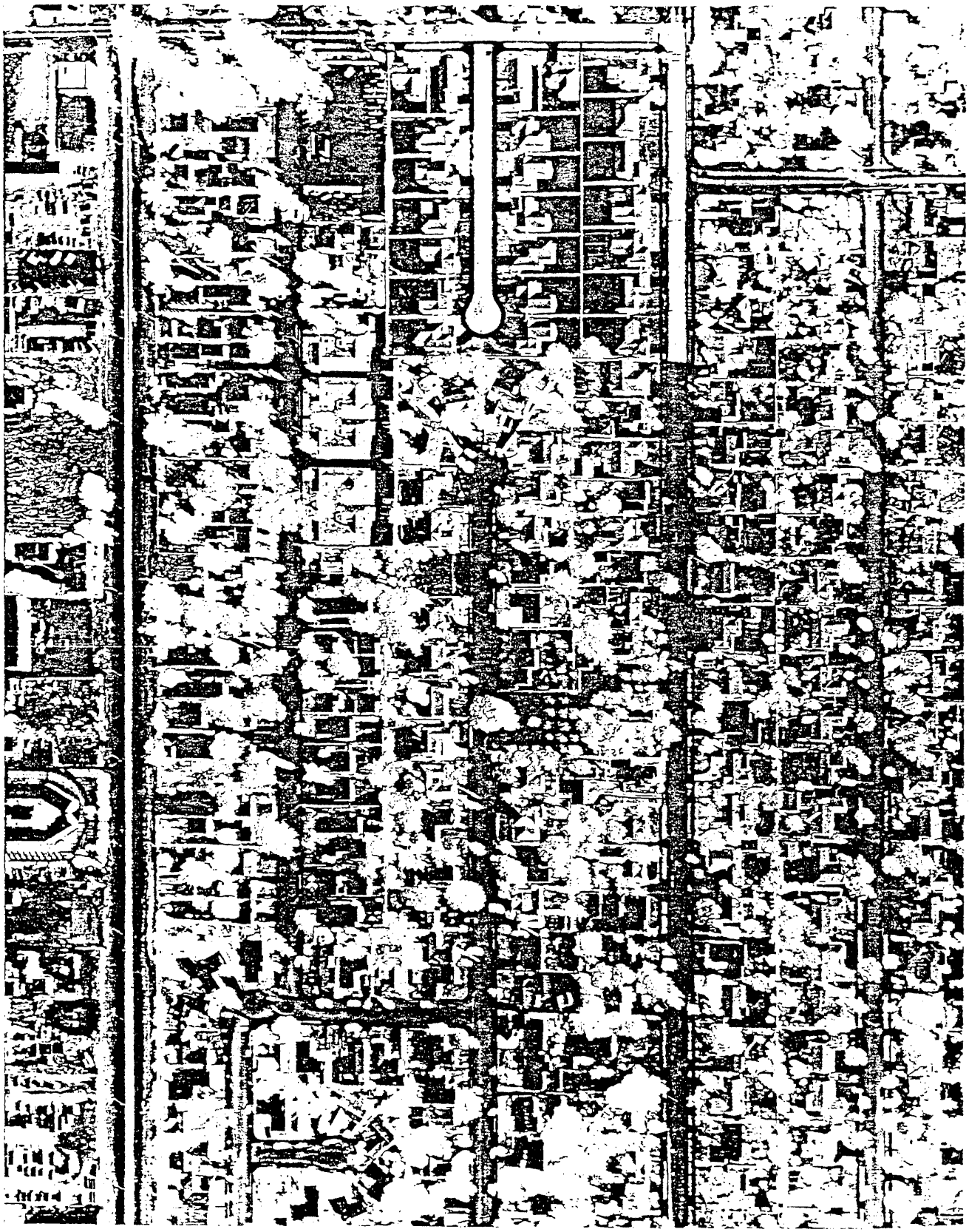

Figure IV-8. Black and white print of high resolution color infrared imagery obtained from overflight of CSCAB. Shown is a portion of the center frame of imagery for Polygon No. 5 (Glendora).

directly from this frame as shown in Figure IV-9 (for Polygon 5 - the Glendora site). Only 60% of each center frame was mapped due to inherent distortions at the edges of the photographs which would affect the plant cover calculations. The areas of those portions of the center frames mapped averaged ~0.3 km^2 but ranged from 0.16 to 0.64 km^2 due to variations in scale (see third column from the right in Table IV-2).

Examination of the imagery showed that five physiognomic (structural) vegetation categories could be consistently recognized and recorded. Vegetation categories were interpreted on the basis of color, tone, size (areal), shape, shadow, texture, and height (aided by stereoscope viewing). The five vegetational categories consisted of trees (deciduous and conifer), palm trees, shrubs, ground cover and grass.

The resulting vegetation maps were digitized as previously described, and the areal cover of individual plants summed for each of the five vegetation classes within their respective sample areas. Table IV-3 shows this for each of these vegetation classes along with the area mapped and the sum of the vegetational area in each sample plot. As noted above, the areas mapped varied with each sample because of the fluctuations in the scale of the photographs. Differences in ground level and in the airplane height at each sample site when the imagery was taken resulted in scales from 1:2,200 (sample plot 13) to 1:4,400 (sample plot 18). These variations in scale resulted in an even wider range of mapped areas since the area varies as the square of the linear scale. This is exemplified in the total area mapped for polygon samples 13 and 18. Scale variations were of course taken into account when calculations were made to convert areas on the map to area on the ground ("actual" area). The sum of the areas actually mapped for the 20 sites was 6.2 km^2, or about 0.2 percent of the total urban area.

It can be seen from Table IV-3 that the total and percent vegetative cover vary with each sample plot. These differences represent actual variations in vegetative cover over the urban area. Determining this actual variation in plant cover was the object of this survey. Low values of about 10 percent occur in business districts or light industrial areas (for example, sample sites in Polygons 2 and 4). These contrast with the heavily vegetated plots of 47 percent cover in Beverly Hills (Polygon 1) and 58 percent for a sample plot which includes a golf course (Polygon

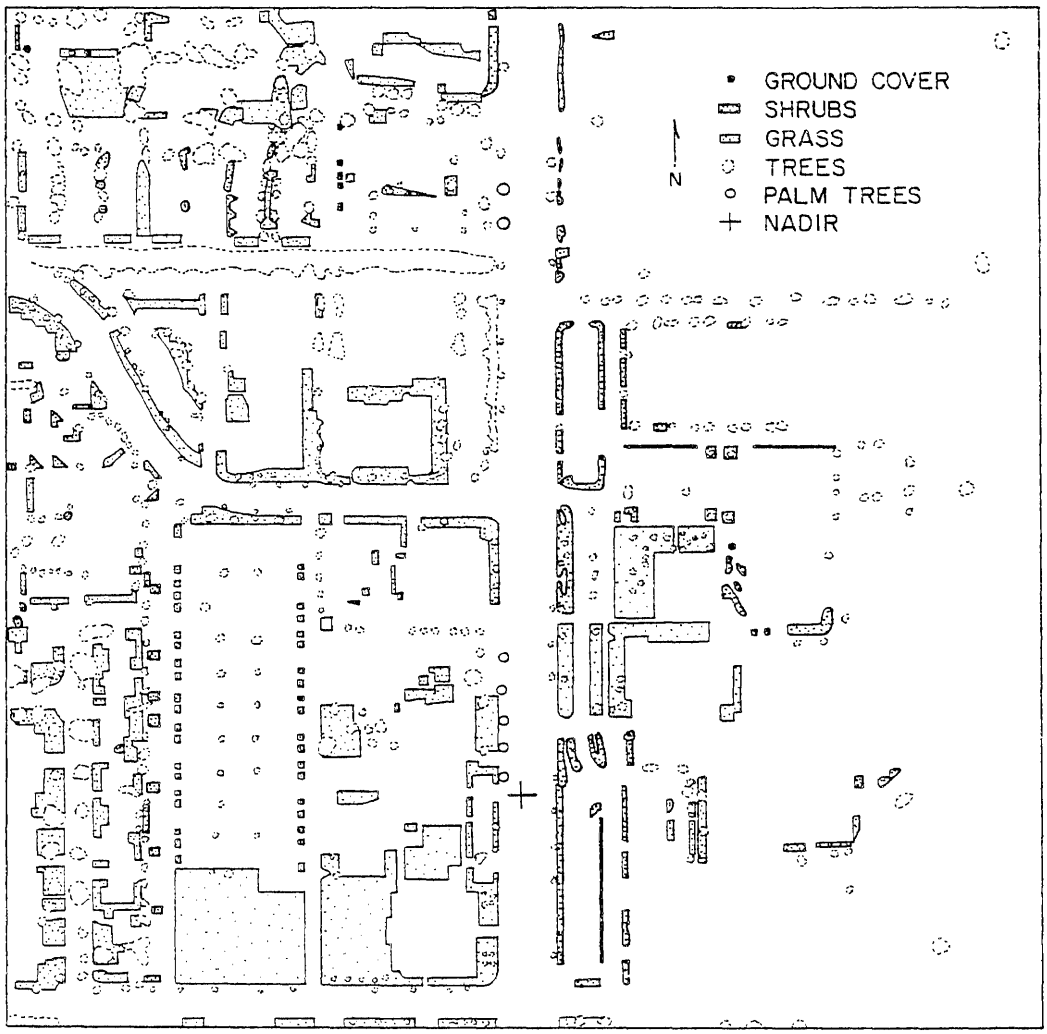

Figure IV-9. Vegetation map produced from aerial imagery (center frame) for Polygon 5 - Glendora. (Map re-drafted for clarity.)

Table IV-3. Areal Cover (m^2) by Vegetation Group (Center Frame of Imagery)

Polygon Sample No.	Trees	Palm Trees	Shrubs	Ground Cover	Grass	Area Mapped	Total Area of Vegetation	Percent Vegetative Cover
1	87,310	2,904	21,362	1,188	71,887	392,757	184,651	47.0
2	17,006	605	4,920	1,895	7,277	373,549	31,703	8.4
3	38,045	807	7,095	1,297	40,553	288,456	87,796	30.4
4	16,690	675	6,504	2,669	6,274	361,880	32,812	9.1
5	20,539	1,119	7,021	1,657	47,051	342,892	77,387	22.7
6	28,963	806	6,523	1,148	27,875	286,449	65,315	22.8
7	20,185	143	4,075	131	55,897	280,137	80,431	28.7
8	1,907	25	3,505	999	18,783	194,157	25,219	13.0
9	26,618	632	5,880	2946	75,618	296,276	111,694	37.7
10	10,716	0	4,355	0	21,885	272,186	36,956	13.6
11	18,701	0	3,528	940	28,004	325,670	51,173	15.7
12	22,605	431	5,773	29	77,611	339,654	106,449	31.3
13	12,882	309	4,374	2,517	32,452	166,865	52,534	31.5
14	17,499	145	9,985	6,858	146,602	311,229	181,089	58.2
15	17,075	802	3,258	59	46,836	231,852	68,030	29.3
16	573	73	5,965	5,862	1,866	346,997	14,339	4.1
17	33,428	27	11,237	16,436	13,672	215,341	74,800	34.7
18	155,784	271	47,382	30,578	21,188	641,863	255,202	39.8
19	15,352	1,878	3,746	0	20,256	227,948	41,232	18.1
20	34,020	230	10,814	16,795	37,649	337,477	99,508	29.5

14). In general, most values fall in the 20 to 30 percent range for residential areas throughout the study area. The data for vegetation cover were used along with field measurements to assign biomass values to each physiognomic category (see Section V). Sample site data were ultimately extrapolated to each polygon and summed for the urban area. The protocol described in the foregoing sections is graphically depicted in the flow diagram shown in Figure IV-10.

F. Natural Vegetation Data Base

1. Introduction

Data similar to that required for the urban area were also needed for the naturally occurring vegetation within the study area. After assessment of the urban vegetation, an evaluation was therefore made of the natural vegetation which, as previously shown, constitutes 33 percent of the study area.

The use of aerial photography to map natural plant communities has been documented and demonstrated to be very useful (Minnich et al. 1969, Orme et al. 1971), but as with urban vegetation, an up-to-date comprehensive vegetation map for the natural areas in question does not exist. Most current studies of the natural vegetation of southern California deal with the individual species or vegetative communities in limited areas. A sampling scheme analogous to that employed for the urban vegetation analysis might not accurately represent species composition because the natural communities have more-or-less definite boundaries, unlike the continuous urban vegetation. Such an undertaking as previously described was neither practical or necessary to obtain the data needed in this study. Fortunately, a set of vegetation maps published by the U. S. Forest Service in the 1930's was available. These detailed maps were made exclusively from field surveys and show vegetation as it existed in its natural communities or types (these maps are subsequently called Vegetation-Type maps). Plant geographers and other researchers currently using these maps feel that for the most part they are still applicable today.

Naturally occurring species inhabit semi-predictable areas that reflect the tolerance limits of the individual species. Plants in similar habitats are presumed to have similar tolerances and to occur together in a mapable vegetation type. Within the study area, there are five such

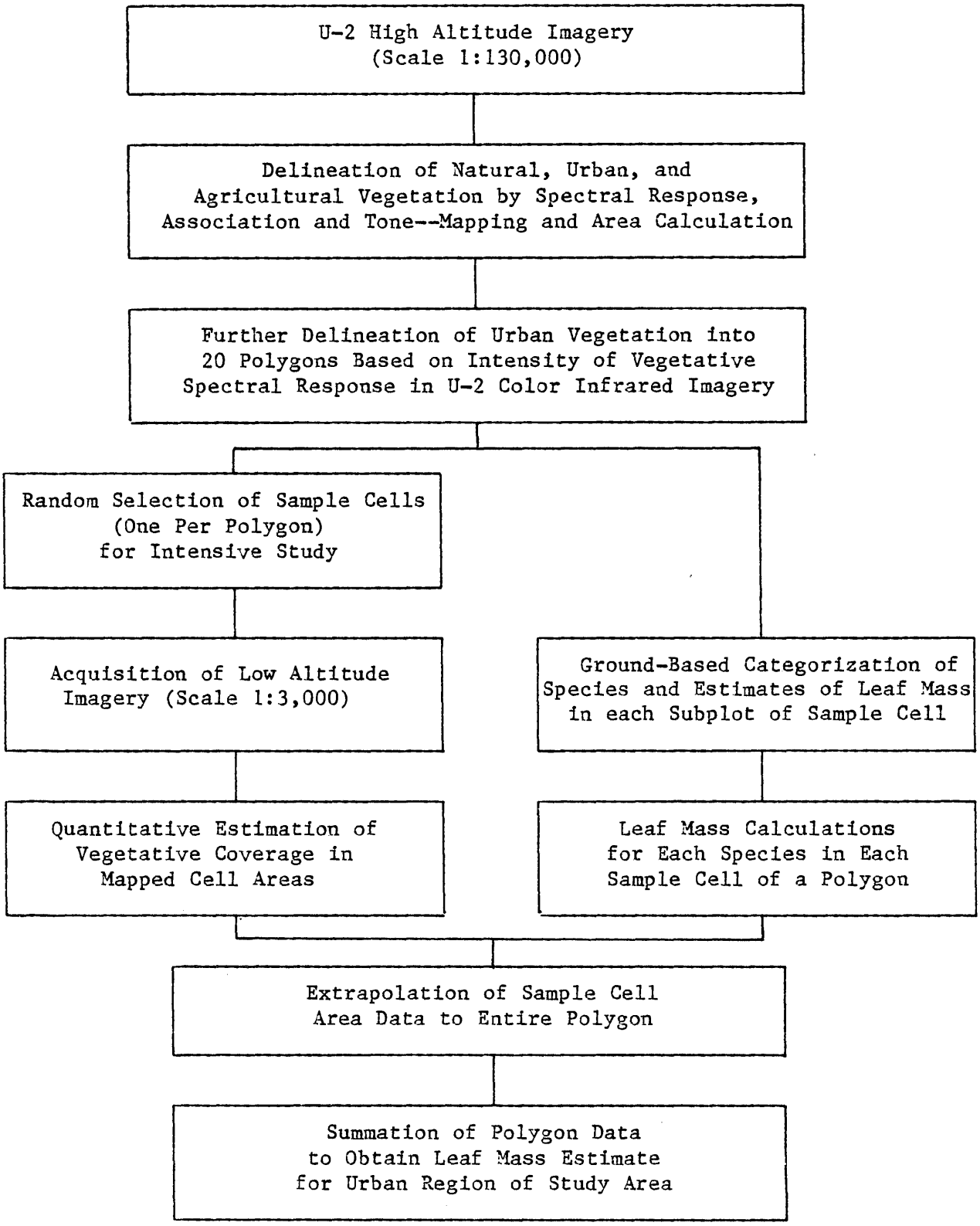

Figure IV-10. Protocol for obtaining leaf mass estimate for urban portion of the study area.

vegetation types: grassland, sagebrush, chamise chaparral, chaparral and woodland.

Grasslands are generally adjacent to cultivated or urban areas. They are commonly the result of previous cultivation or frequent burning. Sagebrush is found in the low elevations and recent burn areas within chaparral vegetation. Chamise chaparral and chaparral may occupy similar elevations with chamise on the dryer south facing slopes, and the larger chaparral species becoming increasingly abundant at higher (wetter) elevations. In addition to these types, woodland tree species frequently inhabit the larger streambeds and washes (woodland species may have been under-represented in the final analysis; because of their limited distribution they were not frequently sampled for the Type maps).

In summary, these vegetation types inhabit relatively stable areas which, although subject to fluctuations or disturbance, return to their original species composition in a relatively short period of time. It is reasonable to assume that disturbances such as fires occur today just as they did when these maps were made, with similar results.

Having established the current credibility of these Vegetation-Type maps, it was also recognized that more information than type distributions would be needed for biomass calculations. As with urban vegetation data, actual plant cover by each species would be necessary. Original data compiled by the Forest Service for the Type maps included hundreds of field sample plots covering the areas mapped. The sample plot data, which are currently held at the Pacific Southwest Forest and Range Experiment Station in Berkeley, California, include information concerning species composition and percent cover. These data, when combined with area calculations from the Type maps, gave areal cover by species suitable for the biomass calculations.

2. Mapping and Area Calculations

Data for species and percent cover were transcribed from the sample plot cards (see for example Figure IV-11) for a total of 106 plots within the study area boundaries. These data included field plots within all vegetation types described. Each sample plot covered 100 milacres, the total of 106 giving a combined field sample of 10.6 acres or 0.04 km^2. Because the species composition may change within a type that occurs in a different geographical area, the data were grouped into five sets,

FRONT

B-2-16 Form CFES-1

CALIFORNIA FOREST AND RANGE EXPERIMENT STATION

SAMPLE PLOT VEGETATIVE TYPE MAP

Plot No. 58 Quadrangle Triunfo Pass

2 Miles W. + 1½ mi. N. of Castro Pk.

Geographic Location (reference to mountain, stream, town, etc.)

Elevation 2300 Sec. 2 T. 1S R. 19W.

Taken by P.H.J. Date 5-8-31

BRUSH AND GROUND COVER PLOT 100 MILACRES

Cb	Sm	As	Cer	Af
Ef	Cer	Af	Sm	Sm
Cb	Cb	Sm	Cer	As
Af	Sm	Cer	Cer	Af
Sm	As	As	Cer	Af
Ef	Sm	Sm	Ef	As
Sm	Af	Af	As	Af
Cer	Rl	Cer	Cer	Cb
Af	Cb	Ef	Sm	Cer
Af	Af	Sm	Af	As
Cer	Sm	Cer	Cer	Sm
Af	Af	Af	Cer	As
As	Cer	Cer	Sm	Cb
Af	Cer	Cm	Cer	Cb
Af	Sm	Cb	As	As
Ef	Cer	Cer	Cer	As
Sm	Rl	Cer	Cer	Af
Cb	Sm	As	Af	Af
Cm	Ef	Sm	Af	Cer
Af	As	As	Sm	Af

SUMMARY BRUSH AND GROUND COVER PLOT

Species	%	Ht. Feet	Litter Depth Inches	Species	%	Ht. Feet	Litter Depth Inches
Af	22	7	1/8				
As	16	10	1/2				
Cm	2	7	3/4				
Cer	24	6	3/4				
Sm	19	5	1				
Ef	6	1	1/16				
Cb	9	7	1/8				
Rl	2	6	1/4				
				Total	100		

*TREE TALLY..2 ACRES

Species	Diameter Classes					Ht Feet
	4-11	12-23	24-35	36+	Total	
Total						

*Strip 2 x 1 chains

BACK

Type Chamise (5)

Exposure East Slope per cent 60%

Year of last burn Old

Site Index —

Penetrability (indicate by check ✓)

easy — medium ✓

difficult — impenetrable

SOIL

(Check terms applicable ✓)

Depth: Shallow ✓ (under 1') — Medium (1'-3') — Deep (over 3')

Character: Rocky ✓ — Loam ✓ — Gravelly ✓ — Silt — Adobe — Sandy — Clay

Origin (Parent rock)

Igneous	Sedimentary	Metamorphic
felsite	alluvium	schist
basalt	sandstone	gneiss
granite	shale	slate
gabbro	limestone	quartzite
porphyry	Conglaverate	serpentine
tuff		
obsidian		

Additional Ground Cover Species

Remarks

(OAKLAND-9-22-34-25,000)

Figure IV-11. Example of Forest and Range Experiment Station sample plot card with information concerning species composition and percent cover in a portion of the study area containing natural vegetation.

one for each naturally vegetated region within the study area. These were the Santa Monica mountains, San Gabriel mountains, Chino hills, Santa Ana mountains and San Joaquin hills.

For each of these regions, the percent cover for each species was averaged for all sample plots within each vegetation type. This gave an average percent cover by species within the type. The Type maps were then used to gain areal data. Vegetation types from the maps were digitized to provide an acreage for each type within their respective geographical region. For example, 202 km^2 of chamise, 92 km^2 sage, 22 km^2 chaparral and 15 km^2 of woodland were found for the Santa Monica mountains. By multiplying the percent cover for each species (taken from the sample plots), times the area of the type it occurs in (from the maps), an acreage for each species was obtained. The percent cover and area for each of the naturally occurring species reported for the five naturally vegetated regions within the study area are given in Tables IV-4 to IV-8.

The acreage of each individual species was then summed for the five geographical regions to provide a total area covered by each naturally occurring species. These data were then available for use in the leaf mass computations and are given in Table IV-9.

Table IV-4. Percent Cover and Area of Naturally Occurring Species in the Santa Monica Mountain Study Area (a,b,c)

	Percent Cover	Area (sq km)
WOODLAND		
CEANOTHUS SPINOSUS	41.0	6.3
PTERIDIUM AQUILINUM	14.0	2.1
HETEROMELES ARBUTIFOLIA	13.0	2.0
RHAMNUS CROCEA	11.0	1.7
CERCOCARPUS BETULOIDES	8.0	1.2
GRAMINEAE	5.0	0.8
LUPINUS ALBIFRONS	4.0	0.6
ES	2.0	0.3
UMBELLULARIA CALIFORNICA	2.0	0.3
TOTAL	100.0	15.3
CHAMISE CHAPARRAL		
ADENOSTOMA FASCICULATUM	36.8	74.5
CEANOTHUS MEGACARPUS	13.9	28.2
SALVIA MELLIFERA	9.4	19.1
CEANOTHUS SPINOSUS	6.9	13.9
RHUS LAURINA	6.1	12.3
LOTUS SCOPARIUS	5.3	10.6
CERCOCARPUS BETULOIDES	3.8	7.6
ADENOSTOMA SPARSIFOLIUM	2.5	5.1
BARREN	2.0	4.0
HETEROMELES ARBUTIFOLIA	2.0	4.0
ERIOGONUM FASCICULATUM	1.6	3.3
CEANOTHUS CRASSIFOLIUS	1.6	3.3
ARTEMESIA CALIFORNICA	1.2	2.4
YUCCA WHIPPLEI	0.8	1.6
ARCTOSTAPHYLOS GLANDULOSA	0.8	1.5
RHAMNUS CROCEA	0.8	1.5
BD	0.5	1.0
QUERCUS DUMOSA	0.5	1.0
RHUS OVATA	0.3	0.5
ES	0.3	0.5
ERIOGONUM CINERIUM	0.3	0.5
SALVIA LEUCOPHYLLA	0.2	0.4
ERIOPHYLLUM CONFERTIFLORUM	0.2	0.4
RHUS INTEGRIFOLIA	0.1	0.3
RHAMNUS CALIFORNICA	0.1	0.3
PRUNUS ILICIFOLIA	0.1	0.3
CEANOTHUS OLIGANTHUS	0.1	0.3
ARTEMESIA CALIFORNICA	0.1	0.2
SALVIA APIANA	0.1	0.1
HS	0.1	0.1
SAMBUCUS MEXICANA	0.1	0.1
CLA	0.1	0.1
QUERCUS AGRIFOLIA	0.1	0.1
SPHAERALCEA FASCICULATA	0.1	0.1
DA	0.1	0.1
HELIANTHUS GRACILENTUS	0.1	0.1
TOTAL	100.0	202.3
CHAPARRAL		
CEANOTHUS SPINOSUS	24.8	5.5
CEANOTHUS MEGACARPUS	22.8	5.1
QUERCUS DUMOSA	10.2	2.3
PRUNUS ILICIFOLIA	9.2	2.0
ADENOSTOMA SPARSIFOLIUM	7.5	1.7

Table IV-4 (continued) - 2

	Percent Cover	Area (sq km)
CHAPARRAL (continued)		
ARCTOSTAPHYLOS GLANDULOSA	6.7	1.5
HETEROMELES ARBUTIFOLIA	4.0	0.9
ADENOSTOMA FASCICULATUM	2.7	0.6
RHUS OVATA	2.5	0.6
SALVIA MELLIFERA	2.5	0.6
CEANOTHUS SOREDIATUS	2.2	0.5
RHUS LAURINA	1.3	0.3
CERCOCARPUS BETULOIDES	1.3	0.3
HETEROMELES ARBUTIFOLIA	1.0	0.2
LONICERA JOHNSTONII	0.3	0.1
TOXICODENDRON VACCARUM	0.5	0.1
BARREN	0.3	0.1
RHAMNUS CROCEA	0.2	0.0
TOTAL	100.0	22.3
SAGE		
SALVIA MELLIFERA	17.0	15.7
ARTEMESIA CALIFORNICA	15.0	13.8
LOTUS SCOPARIUS	14.8	13.6
RHUS LAURINA	11.0	10.1
SALVIA LEUCOPHYLLA	10.2	9.4
GRAMINEAE	9.2	8.5
ERIOGONUM CINERIUM	4.6	4.2
CERCOCARPUS BETULOIDES	3.8	3.5
RHAMNUS CROCEA	3.4	3.1
ENCELIA CALIFORNICA	3.4	3.1
YUCCA WHIPPLEI	1.8	1.7
CEANOTHUS MEGACARPUS	1.4	1.3
CEANOTHUS SPINOSUS	1.2	1.1
HETEROMELES ARBUTIFOLIA	1.0	0.9
RHUS OVATA	0.8	0.7
LONICERA JOHNSTONII	0.4	0.4
BARREN	0.2	0.2
HS	0.2	0.2
OPUNTIA SPP.	0.2	0.2
TOTAL	100.0	92.2
GRASSLAND		
GRAMINEAE	100.0	6.1
TOTAL	100.0	6.1
TOTAL AREA OF REGION		338.2

a Sum of percent covers and areas may not equal TOTAL due to rounding.

b 0.0 percent cover or area indicates a rounded value <0.05.

c Two and three letter names refer to original abbreviations for which genus and species names were not given in the U.S. Forest Service field plot data cards.

Table IV-5. Percent Cover and Area of Naturally Occurring Species in the San Gabriel Mountain Study Area (a,b,c)

	Percent Cover	Area (sq km)
WOODLAND		
UNSPECIFIED WOODLAND	100.0	24.0
TOTAL	100.0	24.0
CHAMISE CHAPARRAL		
ADENOSTOMA FASCICULATUM	37.3	99.0
BARREN	18.5	49.2
ERIOGONUM FASCICULATUM	9.5	25.2
CEANOTHUS CRASSIFOLIUS	9.5	25.2
SALVIA MELLIFERA	9.0	23.9
RHUS LAURINA	4.0	10.6
CERCOCARPUS BETULOIDES	3.3	8.6
PRUNUS ILICIFOLIA	2.8	7.3
ARTEMESIA CALIFORNICA	1.3	3.3
HETEROMELES ARBUTIFOLIA	1.3	3.3
RHAMNUS ILICIFOLIA	0.8	2.0
ERIODICTYON CALIFORNICUM	0.5	1.3
ARCTOSTAPHYLOS GLAUCA	0.5	1.3
SALVIA APIANA	0.5	1.3
RHUS OVATA	0.5	1.3
QUERCUS DUMOSA	0.3	0.7
YUCCA WHIPPLEI	0.3	0.7
CEANOTHUS LEUCODERMIS	0.3	0.7
DI	0.3	0.7
TOTAL	100.0	265.7
CHAPARRAL		
QUERCUS DUMOSA	17.1	23.4
QUERCUS WISLIZENII	10.1	13.8
CEANOTHUS OLIGANTHUS	9.3	12.7
BARREN	8.4	11.5
CERCOCARPUS BETULOIDES	7.8	10.6
ADENOSTOMA FASCICULATUM	7.4	10.1
CEANOTHUS LEUCODERMIS	7.0	9.6
ARCTOSTAPHYLOS GLANDULOSA	6.4	8.7
HETEROMELES ARBUTIFOLIA	3.9	5.3
GRAMINEAE	3.5	4.8
CEANOTHUS CRASSIFOLIUS	2.9	4.0
PRUNUS ILICIFOLIA	2.5	3.5
ARCTOSTAPHYLOS GLAUCA	2.6	3.5
RHUS OVATA	2.0	2.8
QUERCUS CRYSOLEPIS	1.2	1.7
RHAMNUS CROCEA	1.0	1.4
LOTUS SCOPARIUS	0.9	1.3
RIBES MALVACEUM	0.9	1.2
ERIOGONUM FASCICULATUM	0.9	1.2
SALVIA MELLIFERA	0.8	1.1
RHUS LAURINA	0.8	1.0
RHAMNUS CALIFORNICA	0.6	0.8
SALVIA APIANA	0.5	0.7
NICOTIANA GLAUCA	0.2	0.3
UMBELLULARIA CALIFORNICA	0.1	0.2
ERIODICTYON CALIFORNICUM	0.2	0.2
HS	0.1	0.1
HOLODISCUS DISCOLOR	0.1	0.1
FRAXINUS DIPETALA	0.1	0.1
SC	0.1	0.1
TOTAL	100.0	136.4

Table IV-5 (continued) - 2

TOTAL AREA OF REGION	426.1

a Sum of percent covers and areas may not equal TOTAL due to rounding.
b 0.0 percent cover or area indicates a rounded value <0.05.
c Two and three letter names refer to original abbreviations for which genus and species names were not given in the U.S. Forest Service field plot data cards.

Table IV-6. Percent Cover and Area of Naturally Occurring Species in the Puente and Chino Hills Study Area (a,b,c)

	Percent Cover	Area (sq km)
WOODLAND		
GRAMINEAE	50.0	4.6
ARTEMESIA CALIFORNICA	17.0	1.6
BARREN	15.0	1.4
TOXICODENDRON VACCARUM	10.0	0.9
DPU	5.0	0.5
QUERCUS AGRIFOLIA	2.0	0.2
RHAMNUS CROCEA	1.0	0.1
TOTAL	100.0	9.2
CHAMISE CHAPARRAL		
UNSPECIFIED CHAMISE CHAPARRAL	100.0	13.0
TOTAL	100.0	13.0
CHAPARRAL		
UNSPECIFIED CHAPARRAL	100.0	0.6
TOTAL	100.0	0.6
SAGE		
ARTEMESIA CALIFORNICA	49.7	35.2
SALVIA MELLIFERA	10.9	7.7
GRAMINEAE	10.7	7.6
ADENOSTOMA FASCICULATUM	10.3	7.3
RHUS INTEGRIFOLIA	5.6	3.9
SALVIA APIANA	4.4	3.1
BARREN	3.0	2.1
RHAMNUS CROCEA	2.6	1.8
HETEROMELES ARBUTIFOLIA	1.3	0.9
LOTUS SCOPARIUS	0.6	0.4
QUERCUS DUMOSA	0.1	0.1
JUGLANS CALIFORNICA (1 TREE)	0.0	0.0
TOTAL	100.0	70.8
GRASSLAND		
GRAMINEAE	96.5	159.9
SAMBUCUS MEXICANA	2.5	4.1
JUGLANS CALIFORNICA (2 TREES)	0.0	0.0
QUERCUS AGRIFOLIA (1 TREE)	0.0	0.0
TOTAL	100.0	165.7
TOTAL AREA OF REGION		259.3

a Sum of percent covers and areas may not equal TOTAL due to rounding.

b 0.0 percent cover or area indicates a rounded value <0.05.

c Two and three letter names refer to original abbreviations for which genus and species names were not given in the U.S. Forest Service field plot data cards.

Table IV-7. Percent Cover and Area of Naturally Occurring Species in the Santa Ana Mountain Study Area (a,b,c)

	Percent Cover	Area (sq km)
WOODLAND		
GRAMINEAE	93.0	11.5
ARTEMESIA CALIFORNICA	7.0	0.9
QUERCUS AGRIFOLIA	0.0	0.0
TOTAL	100.0	12.4
CHAMISE CHAPARRAL		
ADENOSTOMA FASCICULATUM	52.4	47.1
CEANOTHUS MEGACARPUS	13.6	12.2
CEANOTHUS OLIGANTHUS	12.5	11.2
CUPRESSUS FORBESII	4.2	3.8
BARREN	3.5	3.1
QUERCUS DUMOSA	3.4	3.1
SALVIA MELLIFERA	2.2	2.0
LOTUS SCOPARIUS	1.5	1.3
CEANOTHUS CRASSIFOLIUS	1.3	1.2
HETEROMELES ARBUTIFOLIA	1.1	1.0
RHAMNUS CROCEA	0.9	0.8
GRAMINEAE	0.8	0.7
RHUS LAURINA	0.8	0.7
ARCTOSTAPHYLOS GLANDULOSA	0.3	0.3
ERIODICTYON CRASSIFOLIUM	0.3	0.3
RHUS OVATA	0.3	0.3
CERCOCARPUS BETULOIDES	0.2	0.2
YUCCA WHIPPLEI	0.1	0.1
SPHAERALCEA FASCICULATA	0.1	0.1
TOTAL	100.0	89.9
CHAPARRAL		
QUERCUS DUMOSA	57.0	16.9
HETEROMELES ARBUTIFOLIA	15.8	4.7
CEANOTHUS OLIGANTHUS	14.0	4.2
CERCOCARPUS BETULOIDES	3.6	1.1
FRAXINUS DIPETALA	3.2	0.9
RHAMNUS CROCEA	1.8	0.5
RHUS OVATA	1.2	0.4
CEANOTHUS CRASSIFOLIUS	0.8	0.2
RHUS INTEGRIFOLIA	0.6	0.2
TOXICODENDRON VACCARUM	0.6	0.2
QUERCUS WISLIZENII	0.2	0.1
RIBES MALVACEUM	0.2	0.1
GRAMINEAE	0.2	0.1
ARCTOSTAPHYLOS GLANDULOSA	0.2	0.1
TOTAL	100.0	29.7
SAGE		
ARTEMESIA CALIFORNICA	41.1	79.9
SALVIA MELLIFERA	28.3	55.0
ERIOGONUM FASCICULATUM	6.1	11.8
SALVIA APIANA	6.0	11.7
GRAMINEAE	1.5	2.8
GAF	1.0	1.9

Table IV-7 (continued) - 2

	Percent Cover	Area (sq km)
SAGE (continued)		
RHUS LAURINA	0.9	1.8
RHUS OVATA	0.8	1.6
RHUS INTEGRIFOLIA	0.7	1.4
ANNUALS	0.7	1.4
RHAMNUS CROCEA	0.5	1.1
PENSTEMON ANTIRRHINOIDES	0.5	0.9
DPU	0.5	0.9
OPUNTIA SPP.	0.3	0.5
HETEROMELES ARBUTIFOLIA	0.3	0.5
BACCHARIS PILULARIS	0.2	0.4
SPHAERALCEA FASCICULATA	0.2	0.4
YUCCA WHIPPLEI	0.2	0.4
BJ	0.1	0.2
TOTAL	100.0	194.4
GRASSLAND		
GRAMINEAE	100.0	6.6
TOTAL	100.0	6.6
TOTAL AREA OF REGION		333.0

a Sum of percent covers and areas may not equal TOTAL due to rounding.

b 0.0 percent cover or area indicates a rounded value <0.05.

c Two and three letter names refer to original abbreviations for which genus and species names were not given in the U.S. Forest Service field plot data cards.

Table IV-8. Percent Cover and Area of Naturally Occurring Species in the San Joaquin Mountain Study Area (a,b,c)

	Percent Cover	Area (sq km)
SAGE		
ARTEMESIA CALIFORNICA	41.2	19.6
ERIOGONUM FASCICULATUM	14.8	7.1
SALVIA MELLIFERA	11.0	5.2
GRAMINEAE	10.5	5.0
LOTUS SCOPARIUS	6.7	3.2
RHUS INTEGRIFOLIA	4.2	2.0
RHUS LAURINA	2.9	1.4
SALVIA APIANA	2.6	1.2
DPU	1.8	0.9
BARREN	1.8	0.9
GAX	1.2	0.6
OPUNTIA SPP.	0.3	0.2
SPHAERALCEA FASCICULATA	0.5	0.2
HAPLOPAPPUS PINIFOLIUS	0.5	0.2
TOTAL	100.0	47.7
GRASSLAND		
GRAMINEAE	100.0	52.6
TOTAL	100.0	52.6
TOTAL AREA OF REGION		100.3

a Sum of percent covers and areas may not equal TOTAL due to rounding.

b 0.0 percent cover or area indicates a rounded value <0.05.

c Two and three letter names refer to original abbreviations for which genus and species names were not given in the U.S. Forest Service field plot data cards.

Table IV-9. Percent Cover and Area of Naturally Occurring Species in All Five Naturally Vegetated Areas (a,b,c)

	Percent Cover	Area (sq km)
WOODLAND		
UNSPECIFIED WOODLAND	39.4	24.0
GRAMINEAE	27.7	16.9
CEANOTHUS SPINOSUS	10.3	6.3
ARTEMESIA CALIFORNICA	4.0	2.4
PTERIDIUM AQUILINUM	3.5	2.1
RHAMNUS CROCEA	2.9	1.8
BARREN	2.3	1.4
CERCOCARPUS BETULOIDES	2.0	1.2
TOXICODENDRON VACCARUM	1.5	0.9
LUPINUS ALBIFRONS	1.0	0.6
DPU	0.8	0.5
ES	0.5	0.3
UMBELLULARIA CALIFORNICA	0.5	0.3
QUERCUS AGRIFOLIA	0.3	0.2
TOTAL	100.0	60.9
CHAMISE CHAPARRAL		
ADENOSTOMA FASCICULATUM	38.6	220.6
BARREN	9.9	56.3
SALVIA MELLIFERA	7.9	45.0
CEANOTHUS MEGACARPUS	7.1	40.4
CEANOTHUS CRASSIFOLIUS	5.2	29.7
ERIOGONUM FASCICULATUM	5.0	28.5
RHUS LAURINA	4.1	23.6
CERCOCARPUS BETULOIDES	2.9	16.4
CEANOTHUS SPINOSUS	2.4	13.9
UNSPECIFIED CHAMISE-CHAPARRAL	2.3	13.0
LOTUS SCOPARIUS	2.1	12.0
CEANOTHUS OLIGANTHUS	2.0	11.5
HETEROMELES ARBUTIFOLIA	1.5	8.4
PRUNUS ILICIFOLIA	1.3	7.6
ARTEMESIA CALIFORNICA	1.0	5.9
ADENOSTOMA SPARSIFOLIUM	0.9	5.1
QUERCUS DUMOSA	0.8	4.7
CUPRESSUS FORBESII	0.7	3.8
YUCCA WHIPPLEI	0.4	2.4
RHAMNUS CROCEA	0.4	2.3
RHUS OVATA	0.4	2.1
RHAMNUS ILICIFOLIA	0.3	2.0
ARCTOSTAPHYLOS GLANDULOSA	0.3	1.8
SALVIA APIANA	0.3	1.5
ERIODICTYON CALIFORNICUM	0.2	1.3
ARCTOSTAPHYLOS GLAUCA	0.2	1.3
BD	0.2	1.0
DI	0.1	0.7
CEANOTHUS LEUCODERMIS	0.1	0.7
GRAMINEAE	0.1	0.7
ES	0.1	0.5
ERIOGONUM CINERIUM	0.1	0.5
SALVIA LEUCOPHYLLA	0.1	0.4
ERIOPHYLLUM CONFERTIFLORUM	0.1	0.4
ERIODICTYON CRASSIFOLIUM	0.0	0.3
RHUS INTEGRIFOLIA	0.0	0.3
RHAMNUS CALIFORNICA	0.0	0.3
SPHAERALCEA FASCICULATA	0.0	0.2
HS	0.0	0.1
DA	0.0	0.1
HELIANTHUS GRACILENTUS	0.0	0.1
SAMBUCUS MEXICANA	0.0	0.1

Table IV-9 (continued) - 2

	Percent Cover	Area (sq km)
CHAMISE CHAPARRAL (continued)		
QUERCUS AGRIFOLIA	0.0	0.1
CLA	0.0	0.1
TOTAL	100.0	570.9
CHAPARRAL		
QUERCUS DUMOSA	22.5	42.6
CEANOTHUS OLIGANTHUS	8.9	16.9
QUERCUS WISLIZENII	7.3	13.8
CERCOCARPUS BETULOIDES	6.3	12.0
BARREN	6.1	11.5
HETEROMELES ARBUTIFOLIA	5.9	11.1
ADENOSTOMA FASCICULATUM	5.7	10.7
ARCTOSTAPHYLOS GLANDULOSA	5.4	10.3
CEANOTHUS LEUCODERMIS	5.1	9.6
PRUNUS ILICIFOLIA	2.9	5.5
CEANOTHUS SPINOSUS	2.9	5.5
CEANOTHUS MEGACARPUS	2.7	5.1
GRAMINEAE	2.6	4.9
CEANOTHUS CRASSIFOLIUS	2.2	4.2
RHUS OVATA	1.9	3.7
ARCTOSTAPHYLOS GLAUCA	1.8	3.5
RHAMNUS CROCEA	1.0	2.0
QUERCUS CRYSOLEPIS	0.9	1.7
ADENOSTOMA SPARSIFOLIUM	0.9	1.7
SALVIA MELLIFERA	0.9	1.7
LOTUS SCOPARIUS	0.7	1.3
RHUS LAURINA	0.7	1.3
RIBES MALVACEUM	0.7	1.3
ERIOGONUM FASCICULATUM	0.6	1.2
FRAXINUS DIPETALA	0.5	1.0
RHAMNUS CALIFORNICA	0.4	0.8
SALVIA APIANA	0.4	0.7
UNSPECIFIED CHAPARRAL	0.3	0.6
CEANOTHUS SOREDIATUS	0.3	0.5
TOXICODENDRON VACCARUM	0.2	0.3
NICOTIANA GLAUCA	0.2	0.3
RHUS INTEGRIFOLIA	0.1	0.2
UMBELLULARIA CALIFORNICA	0.1	0.2
ERIODICTYON CALIFORNICUM	0.1	0.2
SC	0.0	0.1
HS	0.1	0.1
HOLODISCUS DISCOLOR	0.1	0.1
LONICERA JOHNSTONII	0.0	0.1
TOTAL	100.0	189.0
SAGE		
ARTEMESIA CALIFORNICA	36.7	148.5
SALVIA MELLIFERA	20.6	83.6
LOTUS SCOPARIUS	6.1	24.8
GRAMINEAE	5.9	23.9
ERIOGONUM FASCICULATUM	4.7	18.9
SALVIA APIANA	4.0	16.0
RHUS LAURINA	3.3	13.3
BARREN	2.9	11.7
SALVIA LEUCOPHYLLA	2.3	9.4
RHUS INTEGRIFOLIA	1.8	7.3
ADENOSTOMA FASCICULATUM	1.8	7.3

Table IV-9 (continued) - 3

	Percent Cover	Area (sq km)
SAGE (continued)		
RHAMNUS CROCEA	1.5	6.0
ERIOGONUM CINERIUM	1.0	4.2
CERCOCARPUS BETULOIDES	0.9	3.5
ENCELIA CALIFORNICA	0.8	3.1
HETEROMELES ARBUTIFOLIA	0.6	2.4
RHUS OVATA	0.6	2.3
YUCCA WHIPPLEI	0.5	2.0
GAF	0.5	1.9
DPU	0.4	1.8
ANNUALS	0.3	1.4
CEANOTHUS MEGACARPUS	0.3	1.3
CEANOTHUS SPINOSUS	0.3	1.1
OPUNTIA SPP.	0.2	0.9
PENSTEMON ANTIRRHINOIDES	0.2	0.9
GAX	0.1	0.6
SPHAERALCEA FASCICULATA	0.1	0.6
BACCHARIS PILULARIS	0.1	0.4
LONICERA JOHNSTONII	0.1	0.4
HS	0.0	0.2
BJ	0.0	0.2
HAPLOPAPPUS PINIFOLIUS	0.1	0.2
QUERCUS DUMOSA	0.0	0.1
JUGLANS CALIFORNICA (1 TREE)	0.0	0.0
TOTAL	100.0	405.1
GRASSLAND		
GRAMINEAE	97.5	225.2
SAMBUCUS MEXICANA	1.8	4.1
JUGLANS CALIFORNICA (2 TREES)	0.0	0.0
QUERCUS AGRIFOLIA (1 TREE)	0.0	0.0
TOTAL	100.0	231.0
TOTAL AREA OF 5 REGIONS		1456.9

a Sum of percent covers and areas may not equal TOTAL due to rounding.
b 0.0 percent or area indicates a rounded value <0.05.
c Two and three letter names refer to original abbreviations for which genus and species names were not given in the U.S. Forest Service field plot data cards.

V. FIELD SURVEY OF SPECIES COMPOSITION AND GREEN-LEAF MASS IN THE URBAN PORTION OF THE STUDY AREA

A. Introduction

As noted earlier, to our knowledge no detailed, quantitative study of the urban vegetation of Southern California had been carried out prior to the present project. Similarly, previous studies of hydrocarbon emissions from plants have dealt primarily with natural vegetation and agricultural areas (Zimmerman 1979a,c, Hunsaker 1981, Hunsaker and Moreland 1981, Taback et al. 1978) while urban vegetation has typically been ignored or given minor consideration. However, for the present investigation, urban vegetation is the major component on an area basis. Thus, a detailed analysis of the species composition and green-leaf mass in the urban portion of the study area was required as an essential element in determining total emissions of isoprene and the monoterpenes from this area. To obtain the necessary data a field sampling program was designed which constituted the third stage of the stratified random sampling approach described in Figure IV-5. The specific procedures used in this phase of the program are described in detail below.

B. Methods of Approach

The protocol for this study is shown in Figure V-1. The first step involved subdividing the five frame aerial imagery areas for each of the 20 polygons into measurable subunits for ground-based surveillance. As described in detail in Section IV the sample cell in each polygon consisted of a rectangle of approximately 1.8 km^2 (~450 acres), randomly placed within the polygon. The coordinates of each sample cell were supplied to the field botanists by the aerial surveillance team. These rectangles were then superimposed on appropriate Thomas Brothers street maps (as shown for two sample cells in Figures V-2 and V-3) so that they could be subdivided into as many subunits as possible, using city streets as the major reference points for division.

The number of subplots into which these 1.8 km^2 rectangles were divided varied with the density of subdivision defined by streets, ranging from a minimum of 25 in Polygon 11 (Newport Beach), to a maximum of 69 in Polygon 5 (Glendora). A great deal of flexibility was required in this

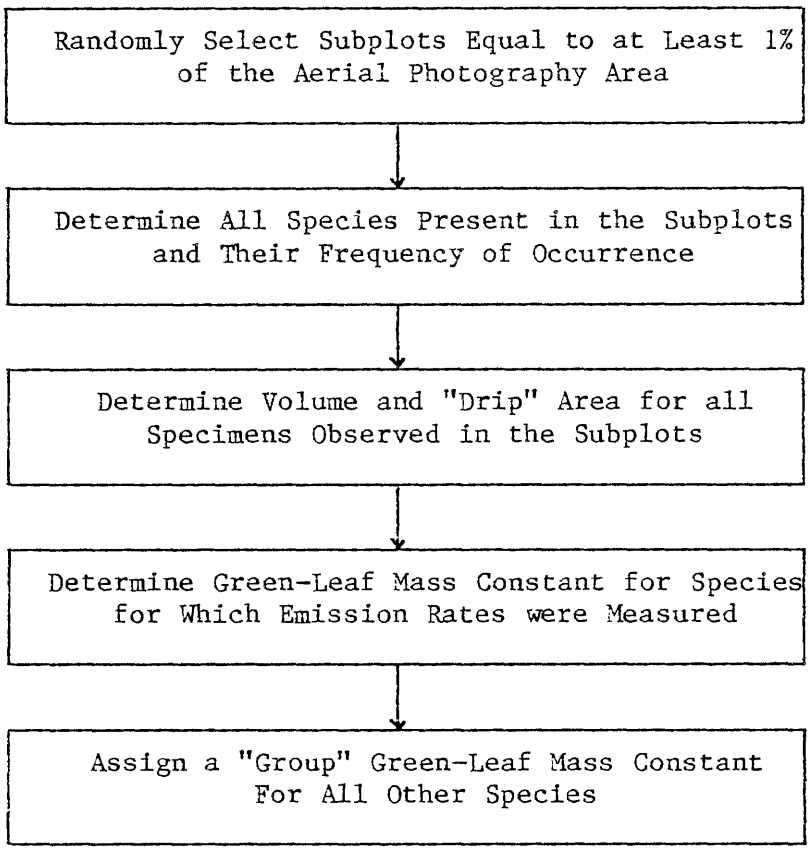

Figure V-1. Protocol for the determination of green-leaf mass by field sampling in the urban portion of the study area.

process. In some cases a continuous length of single city streets were used and in others small city blocks or half-city blocks represented individual subplots. The overriding assumption made was that by subdividing as much as possible, a system of random selection of several subplots would minimize any biases. Once the sample cell for a particular polygon was subdivided, each subplot was assigned a number and those to be sampled were selected by use of a random numbers generator.

A total of approximately 1% of each polygon sample cell was sampled in the field. As each subplot from the randomly selected list was completed its area was added to a running total for the sample and when this total exceeded 215,000 ft^2 the field sampling was terminated for that polygon. The numerical order of subplot selection from the random list was changed only when a subplot was considered by the field team to be too

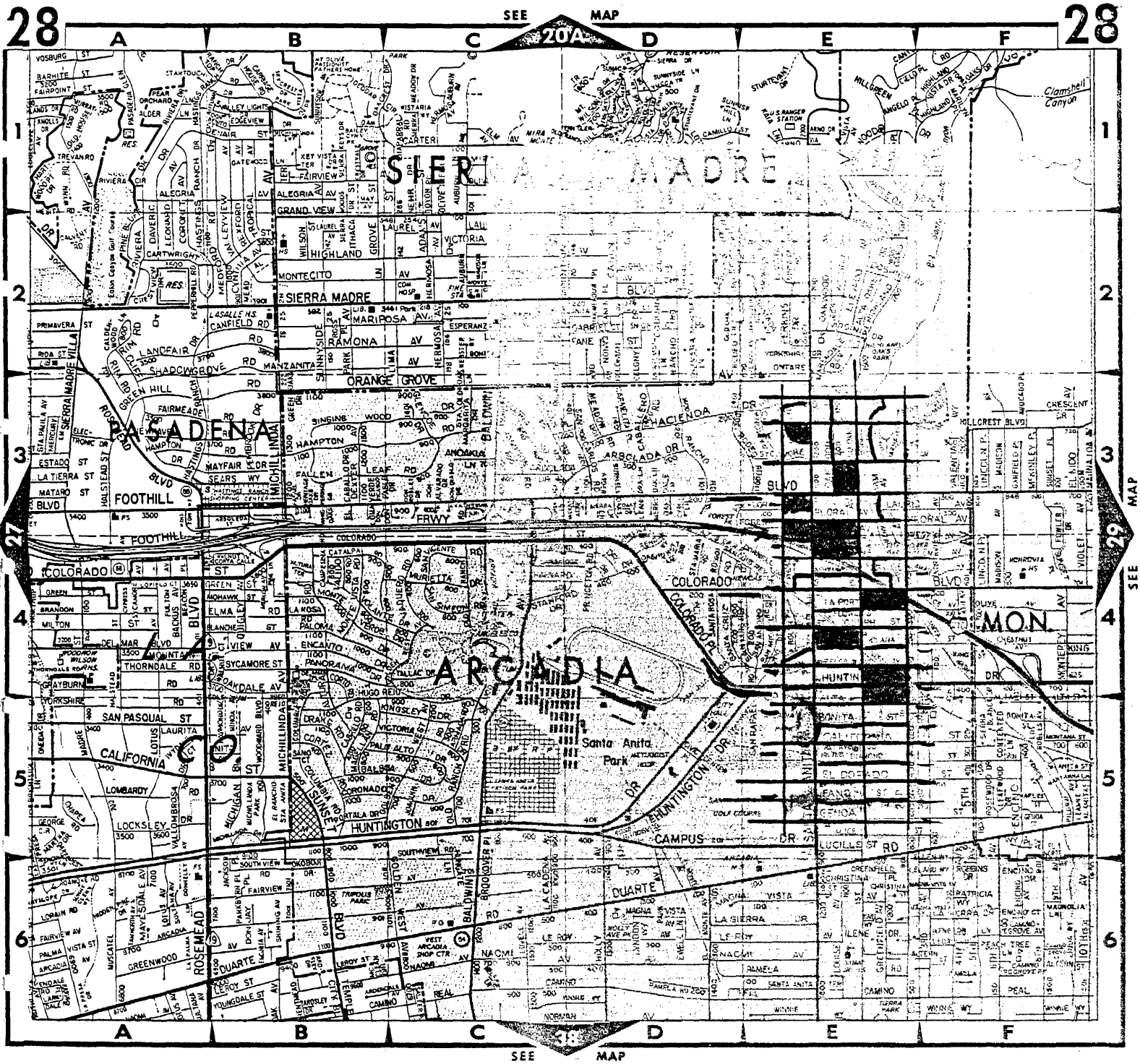

Figure V-2. Overlay of Thomas Brothers street map showing division of sample cell in Polygon 4 into subplots. Darkened subplots were randomly selected as described in text and field surveyed for species composition and green-leaf mass.

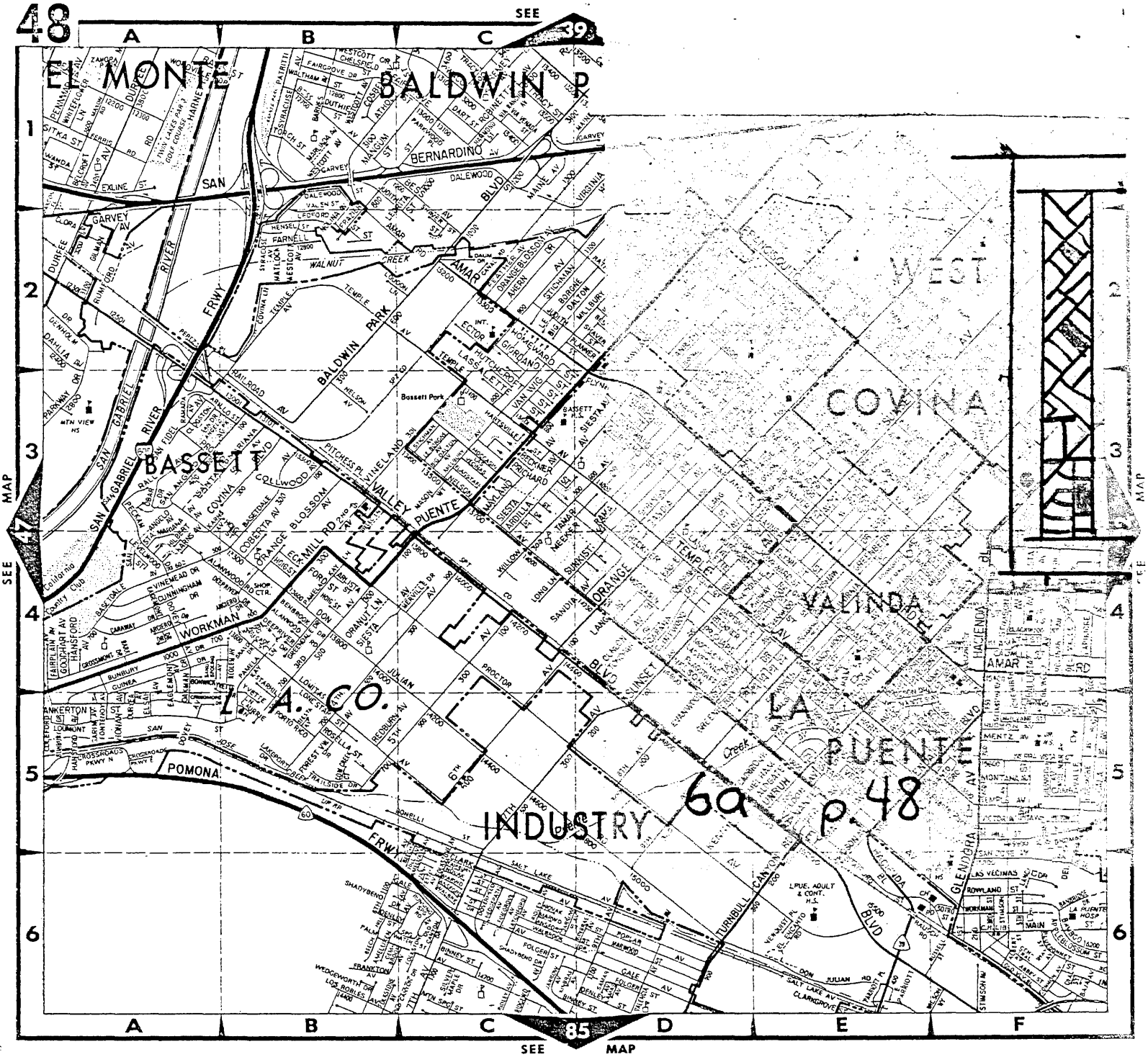

Figure V-3. Overlay of Thomas Brothers street map showing division of sample cell in Polygon 6 into subplots. Darkened subplots were randomly selected as described in text and field surveyed for species composition and green-leaf mass.

difficult for analysis. Typically this was due to an inability to establish the boundary of the subplot either because structures blocked visual reference points, or visual reference points were lacking altogether. In this case the subplot was discarded, and the next one on the list was selected.

In two of the 20 polygons a different sampling method was employed. In Polygon 14 (Long Beach) the sample area fell into a regional park (Eldorado Park) in which there were no readily available reference points for subplot formation. Field surveillance indicated that the vegetation structure of the park was sufficiently consistent so that one large subplot of an appropriate size would give an adequate sampling. This was an ideal situation since the field survey team was able to select essentially the same area in the sample cell which had been selected for mapping by the aerial imagery team (i.e., the center frame of the five frames of imagery obtained). A single 250,000 ft^2 plot was therefore surveyed in the park with the aid of a median level transect. This polygon probably represents the best direct comparison of the ground and aerial surveillance methods. In Polygon 20 (Baldwin Hills) the standard approach to subplot analysis also was not possible due to lack of definable reference points. This area included urban zones with large parcels of land and intermittent natural areas with very few roads. In this sample area sites were selected in the field to represent both the urban and natural zones. Polygon 20 also differed from the usual case in that the field survey area did not overlap the aerial imagery area. The latter had to be changed during the photography overflight due to interference with the flightpath associated with the Los Angeles International Airport. Prior to this, however, the field survey had already been completed in the previously designated area and it could not be repeated.

In the remaining eighteen sample areas the exact dimensions of each subplot were first measured with a Rolatape Corp. measuring wheel (Model No. MN12-III). This was done to keep track of the total area which was being sampled and, in some cases, only a portion of a subplot was used if the area already sampled was nearing the 1% (~215,000 ft^2) cutoff point. In some subplots it was possible to observe the entire area, but in many instances there were portions of the subplots which were not visible

(e.g., closed backyards). In these cases the unobservable areas in each subplot were deleted from the total subplot area.

All visible vegetation was recorded. Individual trees and shrubs were counted, and the dimensions of their leafy crowns or canopies were measured or estimated. A number of geometric shapes were used as models for this purpose, the most common being either spheres or ellipsoids with varying densities. Trees and shrubs with clumped foliage were measured by subtracting the estimated open space found within their general canopy outline. From these data a canopy volume was estimated for each species found in the subplot. Categories listed as unknown trees or shrubs resulted from plants which were in inaccessible places and could not be identified. If a plant could not be identified in the field a small portion was brought back to the laboratory and later identified with the aid of the University herbarium.

In the palm tree group, the number of fronds was reported instead of volume or area dimensions. The fronds were assumed to form a sphere with the radius being the average length of several fronds of the species.

Ground cover was analyzed differently in that only two dimensional data were taken. Only the surface areas of the vegetation were recorded. All grasses (lawns, playground, etc.) were lumped into a general category of "grass" because of their usually highly-mixed nature, which made individual species identification impractical. Other forms of ground cover (dichondra, ice-plant, ivy, flowers, etc.) were recorded under separate specific titles only if large, uniform patches were encountered. Area was computed by measuring the length and width of the ground cover and using a similar or identical geometric shape for an area formula. In many cases, flower beds tended to be made up of several components. In these instances they were designated as "mixed flowerbed." Notes were made as to whether the sampled area was residential, industrial, or commercial to offer the possibility of subsequently assembling species lists for each of these kinds of land use.

C. Green-Leaf Mass Determinations

In order to develop a leaf mass per unit crown volume ($g\ m^{-3}$) constant for each important species, samples of foliage were taken from representatives of those species found in accessible locations. These

foliage samples were taken in discreet multiples of one cubic meter or 1/64 cubic meter units.

Most of the trees and shrubs which were sampled in this fashion were found on the UCR campus, except for the chaparral plants, which were sampled from native stands in Riverside and San Bernardino Counties. Three sampling methods were employed. The smaller shrubs were sampled by placing a 1/64 m^3 frame (0.25 m on a side) constructed out of PVC pipe over the foliage and clipping all of the material inside the frame. Depending on the size of the sampled shrubs, 10-20 such samples were taken, with as many individual plants sampled as possible. Larger shrubs and trees were sampled by clipping out 1 m^3 of foliage, determined visually with meter sticks. In these cases, only five samples were taken, usually from five individual specimens. All samples were individually bagged and transported to the laboratory for the biomass analysis. For palms, which could not be sampled in this manner, whole mature fronds were cut away and brought to the laboratory. Ten fronds were taken for each species of palm, from as many individuals as possible (usually ten).

The bagged leaf and frond material was then sorted to separate green leaves from stems. The leaves were then placed in paper bags, the initial fresh weight was recorded and the bags were placed in a drying oven kept at a constant temperature (~50°C). The samples were checked on a daily basis to record subsequent weight loss during the drying process. When the weight loss stopped the leaves were removed and the final dry weight measured. The palm fronds were cut into small pieces and dried and weighed in the same fashion.

The dry leaf mass per unit volume was computed as the average of all samples for each species of broad-leaf tree, conifer, and shrub (g m^{-3}). Since fronds were counted for each palm, the leaf mass constant was in g $frond^{-1}$. As noted in Section V-B, ground cover and grasses were recorded in two dimensions. Therefore, leaf mass constants for ground cover were in g m^{-2}.

Trees and shrubs were noted as growing in two different morphological forms, either with uniform-to-clumped foliage throughout the canopy volume, or with a dense outer "shell" of foliage surrounding a leafless interior. In the former instance, the biomass constant could be directly applied to the field data. In the latter case, a conversion constant was

derived for each species which compensated for the empty interior portion of the plant by measuring the width of the foliage "shell" and subtracting the leafless internal volume. We found that the depth of the outer foliage shell generally remained fairly consistent, regardless of the overall size of the plant.

Two additional elements entered into the leaf mass estimations for the shrub species found in the coastal sage scrub and chaparral vegetation types which mainly surround the urban area. Leaf mass (gm m^{-3}) was obtained by sampling the ten most frequently encountered species. The volumes of each species were calculated from shapes and size ranges described by Munz and Keck (1968) in "A California Flora." Shapes included spheres, cylinders and inverted cones. The dimensions at the low end of the range for each species is typical of young plants during the early recovery phases following fire and the upper end of the range is typified by older plants in mature shrub stands protected from recent fires. In reality the landscape is covered by a mosaic of size classes. In the case of one species, scrub oak (Quercus dumosa) it was possible to obtain a reliable estimate of leaf mass from the literature. Riggan and Lopez (1981) found that a 35 year old stand of scrub oak had about 18.5 tons ha^{-1} of total above-ground biomass of which 14.4 percent or 2.67 tons (91 gm m^{-2}) was leaf mass. During the early recovery phases after fire, leaf mass was 37 gm m^{-2}.

D. Properties of Urban Vegetation in CSCAB Study Area

The field studies described resulted in the identification of a total of 184 plant species. These included 64 species of broad-leaf trees, 8 of conifers, 35 of ground cover, 4 of palms, 2 of lawns or grasses and 71 of shrubs. An additional 8 species could not be identified, for a total of 192 observed species. These species are listed in Table V-1 by alphabetical order of common names with the corresponding Latin binomial included for each.

The detailed data for the dominant species in each of the five vegetation groups for all 20 polygons are given in Appendix B. These include the total number of times a given species was observed in the field and the total area and volume. The experimentally determined leaf mass constants for urban species and for natural species are given in

Table V-1. Vegetation Species Observed in Urban Study Area

GENUS SPECIES	COMMON NAME
ABELIA SPECIES	ABELIA
ABELIA GRANDIFLORA	ABELIA
ACACIA SPECIES	ACACIA
ACACIA BAILEYANA	ACACIA TREE
OSTEOSPERMUM FRUTICOSUM	AFRICAN DAISY
AGAPANTHUS AFRICANUS	AFRICAN LILY
AGAVE SPECIES	AGAVE
ALNUS SPECIES	ALDER
ALOE SPECIES	ALOE
ULMUS AMERICANA	AMERICAN ELM
MALUS PUMILA	APPLE
PRUNUS ARMENIACA	APRICOT
ARALIA SPECIES	ARALIA
ARAUCARIA SPECIES	ARAUCARIA
THUJA SPECIES	ARBOR-VITAE
SALIX LASIOLEPIS	ARROYO WILLOW
FRAXINUS SPECIES	ASH
ASPARAGUS PLUMOSUS	ASPARAGUS FERN
DICKSONIA ANTARTICA	AUSTRALIAN TREE FERN
PERSEA AMERICANA	AVOCADO
RHODODENDRON SPECIES	AZALEA
CENTAUREA CYANUS	BACHELOR BUTTON
BAMBUSA VULGARIS	BAMBOO
MUSA PARADISIACA	BANANA
FAGUS GRANDIFLORA	BEECH
BEGONIA SPECIES	BEGONIA
CAMPANULA SPECIES	BELLFLOWER
RUBUS SPECIES	BERRIES
BETULA SPECIES	BIRCH
STRELITZIA REGINAE	BIRD OF PARADISE
ROBINIA PSEUDOACACIA	BLACK LOCUST
JUGLANS NIGRA	BLACK WALNUT
CALLISTEMON SPECIES	BOTTLEBRUSH
BOUGAINVILLEA	BOUGAINVILLEA
PTERIS SPECIES	BRACKEN FERN
SCHINUS TEREBINTHIFOLIUS	BRAZILIAN PEPPER
TRISTANIA CONFERTA	BRISBANE BOX
EUONYMUS JAPONICUS	BURNING-BUSH
BRASSICA OLERACEA	CABBAGE
WASHINGTONIA FILIFERA	CALIFORNIA FAN PALM
QUERCUS AGRIFOLIA	CALIFORNIA LIVE OAK
ARTEMESIA CALIFORNICA	CALIFORNIA SAGEBRUS
PLATANUS RACEMOSA	CALIFORNIA SYCAMORE
ZONTEDESCHIA AETHIOPICA	CALLA LILY
CAMELLIA SPECIES	CAMELLIA
CINNAMONUM CAMPHORA	CAMPHOR
PHOENIX CANARIENSIS	CANARY ISLAND PALM
PINUS CANARIENSIS	CANARY ISLAND PINE
TECOMARIA CAPENSIS	CAPE-HONEYSUCKLE
CERATONIA SILIQUA	CAROB
CUPANIOPSIS ANACARDIOIDES	CARROTWOOD
CASUARINA EQUISETIFOLIA	CASUARINA
PRUNUS LYONII	CATALINA CHERRY
CEANOTHUS SPECIES	CEANOTHUS
BETA VULGARIS	CHARD
PRUNUS CAROLINIANA	CHERRY LAUREL
ULMUS PARVIFOLIA	CHINESE ELM
JUNIPERUS CHINENSIS	CHINESE JUNIPER
CHRYSANTHEMUM SPECIES	CHRYSANTHEMUM
BELOPERONE CALIFORNICA	CHUPAROSA
CITRUS SPECIES	CITRUS
ARECASTRUM ROMANZOFFIANUM	COCOS PALM
MYRTUS COMMUNIS	COMMON MYRTLE
ERYTHRINA ARBOREA	CORAL TREE
QUERCUS SUBER	CORK OAK
COTONEASTER SPECIES	COTONEASTER
BACCHARIS PILULARIS	COYOTE BUSH

Table V-1 (continued) - 2

GENUS SPECIES	COMMON NAME
LAGERSTROEMIA INDICA	CRAPE MYRTLE
LYSIMACHIA NUMMULARIA	CREEPING CHARLIE
PHOENIX DACTYLIFERA	DATE PALM
CEDRUS DEODARA	DEODAR CEDAR
DICHONDRA REPENS	DICHONDRA
SAMBUCUS MEXICANA	ELDERBERRY
ESCALLONIA SPECIES	ESCALLONIA
EUCALYPTUS SPECIES	EUCALYPTUS
PYRUS KAWAKAMI	EVERGREEN PEAR
FICUS SPECIES	FICUS
FICUS CARICA	FIG
POTENTILLA SPECIES	FIVE FINGERS
FUCHSIA SPECIES	FUCHSIA
GARDENIA SPECIES	GARDENIA
PELARGONIUM GRAVEOLENS	GERANIUM
GLADIOLUS SPECIES	GLADIOLUS
LIGUSTRUM LUCIDUM	GLOSSY PRIVET
VITIS SPECIES	GRAPE
LONICERA JAPONICA	HALL'S HONEYSUCKLE
CRATAEGUS SPECIES	HAWTHORN
NANDINA DOMESTICA	HEAVENLY BAMBOO
HEBE VENUSTULA	HEBE
HIBISCUS SPECIES	HIBISCUS
MARRUBIUM VULGARE	HOARHOUND
ILEX SPECIES	HOLLY
LAMPRANTHUS SPECIES	ICE PLANT
CARPOBROTUS SPECIES	ICE PLANT
RAPHIOLEPIS INDICA	INDIA-HAWTHORN
IRIS SPECIES	IRIS
CUPRESSUS SEMPERVIRENS	ITALIAN CYPRESS
HEDERA SPECIES	IVY
JACARANDA MIMOSAFOLIA	JACARANDA
CRASSULA SPECIES	JADE PLANT
PITTOSPORUM TOBIRA	JAPANESE PITTOSPORUM
JASMINUM SPECIES	JASMINUM
JUNIPERUS SPECIES	JUNIPER
LANTANA MONTEVIDENSIS	LANTANA
PLUMBAGO CAPENSIS	LEADWORT
AMARYLLIS SPECIES	LILY
LIGUSTRUM SEMPERVIRENS	LINGLESH
LIQUIDAMBAR STYRACIFLUA	LIQUIDAMBAR
PLATANUS ACERIFOLIA	LONDON PLANE
MAGNOLIA GRANDIFLORA	MAGNOLIA
MAHONIA SPECIES	MAHONIA
GINKGO BILOBA	MAIDENHAIR
ACER SPECIES	MAPLE
TAGETES SPECIES	MARIGOLD
MIMOSA SPECIES	MIMOSA
MENTHA SPECIES	MINT
	MIXED FLOWERS
PINUS RADIATA	MONTEREY PINE
BACCHARIS VIMINEA	MULE FAT
FORTUNELLA MARGARITA	NAGAMI KUMQUAT
SOLANUM SPECIES	NIGHTSHADE
GREVELLIA NOELLII	NOEL GREVILLEA
NERIUM OLEANDER	OLEANDER
OLEA EUROPAEA	OLIVE
PINUS MONOPHYLLA	ONE-LEAVED PINYON
MURRAYA PANICULATA	ORANGE JESSAMINE
BAUHINIA VARIEGATA	ORCHID TREE
CORTADERIA SELLOANA	PAMPAS GRASS
PRUNUS PERSICA	PEACH
CARYA ILLINOENSIS	PECAN
VINCA MAJOR	PERIWINKLE
SCHINUS MOLLE	PERUVIAN PEPPER
PETUNIA SPECIES	PETUNIA
PHILODENDRON SPECIES	PHILODENDRON

Table V-1 (continued) - 3

GENUS SPECIES	COMMON NAME
PODOCARPUS SPECIES	PODOCARPUS
EUPHORBIA PULCHERRIMA	POINSETTIA
POLYPODIUM FERN SPECIES	POLYPODY FERN
PUNICA GRATANUM	POMAGRANATE
PORTULACA SPECIES	PORTULACA
OPUNTIA FICUS-INDICA	PRICKLY PEAR
PRIMULA SPECIES	PRIMROSE
PRUNUS SPECIES	PRUNUS
PRUNUS CERASIFERA	PURPLELEAF PLUM
PYRACANTHA COCCINEA	PYRACANTHA
POPULUS TREMULOIDES	QUAKING ASPEN
SEQUOIA SEMPERVIRENS	REDWOOD
EUCALYPTUS VIMINALIS	RIBBON GUM
HOMALOCLADIUM PLATYCLADUM	RIBBON PLANT
ROSA SPECIES	ROSE
CYCAS REVOLUTA	SAGO PALM
EQUISETUM HYEMALE	SCOURING RUSH
SEDUM SPECIES	SEDUM
XYLOSMA CONGESTUM	SHINY XYLOSMA
GREVILLEA ROBUSTA	SILK OAK
EUCALYPTUS POLYANTHEMOS	SILVER DOLLAR GUM
ANTIRRHINUM MAJUS	SNAPDRAGON
YUCCA GLORIOSA	SOFT-TIPPED YUCCA
TRACHELOSPERMUM JASMINOIDES	STAR JASMINE
RHUS SPECIES	SUMAC
HELIANTHUS ANNUUS	SUNFLOWER
ACACIA LONGIFOLIA	SYDNEY GOLDEN WATTLE
EUCALYPTUS GLOBULUS	TASMANIAN BLUE GUM
TERNSTROEMIA GYMNANTHERA	TERNSTROEMIA
LYCOPERSICON ESCULENTUM	TOMATO
HETEROMELES ARBUTIFOLIA	TOYON
NICOTIANA GLAUCA	TREE TOBACCO
SCIRPUS CERNUUS	TULE
LIRODENDREN TULIPIFERA	TULIP TREE
SALSOLA KALI	TUMBLEWEED
CARISSA GRANDIFLORA	TUTTLE NATAL PLUM
ASTER SPECIES	UNIDENTIFIED ASTER
	UNIDENTIFIED FERN
	UNIDENTIFIED GRASS
	UNIDENTIFIED SUCCULENTS
VIBURNUM SPECIES	VIBURNUM
PITTOSPORUM UNDULATUM	VICTORIAN BOX
JUGLANS SPECIES	WALNUT
TRADESCANTIA SPECIES	WANDERING JEW
SALIX BABYLONICA	WEEPING WILLOW
SALIX GOODDINGII	WILLOW
SALIX LAEVIGATA	WILLOW
SALIX SPECIES	WILLOW

Tables V-2 and V-3, respectively, in alphabetical order by common name. The leaf mass constants and the leaf mass of the plants observed for species in the urban study area are also given in the tables in Appendix B.

A summary of the field survey data for all subplots and of the leaf mass determinations for the individual species for all 20 polygons is provided in Table V-4. The subtotals for the number of specimens, areas, volumes and leaf mass for the less dominant species of broad-leaf trees, shrubs and ground covers observed, and the grand totals for each vegetation group are also given in Table V-4. For convenience, the grand totals for each vegetation class are given in Table V-5 as well.

Table V-2. Experimentally Determined Leaf Mass Constants For Urban Species

COMMON NAME	GENUS SPECIES	LEAF MASS CONSTANT g/cu m
ABELIA	ABELIA GRANDIFLORA	1400
AMERICAN ELM	ULMUS AMERICANA	28
AVOCADO	PERSEA AMERICANA	59
BLACK LOCUST	ROBINIA PSEUDOACACIA	19
BRAZILIAN PEPPER	SCHINUS TEREBINTHIFOLIUS	70
CALIFORNIA FAN PALM	WASHINGTONIA FILIFERA	520a
CALIFORNIA LIVE OAK	QUERCUS AGRIFOLIA	310
CALIFORNIA SAGE BRUSH	ARTEMESIA CALIFORNICA	52
CALIFORNIA SYCAMORE	PLATANUS RACEMOSA	86
CAMELLIA	CAMELLIA SASANQUA	1600
CAMPHOR	CINNAMONUM CAMPHORA	75
CANARY ISLAND PALM	PHOENIX CANARIENSIS	550a
CANARY ISLAND PINE	PINUS CANARIENSIS	470
CAPE-HONEYSUCKLE	TECOMARIA CAPENSIS	630
CEANOTHUS	CEANOTHUS CRASSIFOLIUS LIM	280
CHINESE ELM	ULMUS PARVIFOLIA	25
CHINESE JUNIPER	JUNIPERUS CHINENSIS	3700
COMMON MYRTLE	MYRTUS COMMUNIS	50
COTONEASTER	COTONEASTER PANNOSA	260
CRAPE MYRTLE	LAGERSTROEMIA INDICA	950
DEODAR CEDAR	CEDRUS DEODARA	920
EVERGREEN ASH	FRAXINUS UHDEI	170
EVERGREEN PEAR	PYRUS KAWAKAMI	180b
FERN PINE	PODOCARPUS GRACILIOR	240
GLOSSY PRIVET	LIGUSTRUM LUCIDIUM	230b
HALL'S HONEYSUCKLE	LONICERA JAPONICA	390
HEAVENLY BAMBOO	NANDINA DOMESTICA	550
HIBISCUS	HIBISCUS SPECIES	400b
INDIA-HAWTHORN	RAPHIOLEPIS INDICA	550
ITALIAN CYPRESS	CUPRESSUS SEMPERVIRENS	5100
JACARANDA	JACARANDA OVALIFOLIA	90
JAPAN. PITTOSPORUM	PITTOSPORUM TOBIRA	2700
LEADWORT	PLUMBAGO CAPENSIS	650
LEMON	CITRUS LIMON BURM	280
LEMON BOTTLEBRUSH	CALLISTEMON CITRUNUS	470
MAGNOLIA	MAGNOLIA GRANDIFLORA	350
MONTEREY PINE	PINUS RADIATA	390
OLEANDER	NERIUM OLEANDER	230
OLIVE	OLEA EUROPAEA	500
PERUVIAN PEPPER	SCHINUS MOLLE	150
PYRACANTHA	PYRACANTHA COCCINEA	290
RIBBON GUM	EUCALYPTUS VIMINALIS	340
ROSE	ROSA SPECIES	360
SHINY XYLOSMA	XYLOSMA CONGESTUM	470
SILVER DOLLAR GUM	EUCALYPTUS POLYANTHEMOS	270
SILVER MAPLE	ACER FLORIDANUM	44
SUGAR BUSH	RHUS OVATA	200
SYDNEY GOLDEN WATTLE	ACACIA LONGIFOLIA	150
TUTTLE NATAL PLUM	CARISSA GRANDIFLORA	160b
VICTORIAN BOX	PITTOSPORUM UNDULATUM	2700
WEEPING WILLOW	SALIX BABYLONICA	110

a g/frond
b Estimate

Table V-3. Experimentally Determined Leaf Mass Constants For Natural Species

COMMON NAME	GENUS SPECIES	LEAF MASS CONSTANT g/cu m
BLACK SAGE	SALVIA MELLIFERA	310
BUCKTHORN	RHAMNUS CROCEA	150
BUCKWHEAT	ERIOGONUM FASCICULATUM	340
CALIFORNIA SAGE BRUSH	ARTEMESIA CALIFORNICA	52
CEANOTHUS	CEANOTHUS CRASSIFOLIUS	280
CHAMISE	ADENOSTOMA FASCICULATUM	140
ENCELIA	ENCELIA FARINOSA	180
MANZANITA	ARCTOSTAPHYLOS GLANDULOSA	2500
SHRUB OAK	QUERCUS DUMOSA	200
SUGAR BUSH	RHUS OVATA	200

Table V-4. Summary of Field Survey Data for All Subplots and Leaf Mass Determinations

COMMON NAME	NUMBER OF SPECIMENS	AREA[a] sq m	VOL[a] cu m	LEAF MASS CONSTANT[b] g/cu m	LEAF MASS[a] kg
CONIFERS					
MONTEREY PINE	219	3400	8200	390	3200
CANARY ISLAND PINE	145	1100	2400	470	1100
ITALIAN CYPRESS	325	600	1000	5100	5100
DEODAR CEDAR	10	440	870	920	800
ARAUCARIA	18	100	200	--	--
REDWOOD	3	47	130	--	--
SAGO PALM	6	8	8	--	--
OTHERS	2	4	1	NA	--
TOTAL	728	5700	13000	NA	10000
BROAD-LEAF TREES					
RIBBON GUM	457	9800	14000	340	4800
ASH	145	4100	18000	170	3100
CALIFORNIA LIVE OAK	58	2200	8700	310	2700
CHINESE ELM	75	2200	11000	25	280
AMERICAN ELM	99	1800	10000	28	280
MAPLE	66	1600	11000	44	480
CALIFORNIA SYCAMORE	101	1400	5600	86	480
PERUVIAN PEPPER	41	1300	3100	150	470
JACARANDA	43	1200	3800	90	340
VICTORIAN BOX	66	840	770	2700	2100
BLACK LOCUST	40	760	2000	19	38
CRAPE MYRTLE	117	700	1600	950	1500
AVOCADO	39	650	2300	59	140
CAMPHOR	40	590	1200	75	90
MAGNOLIA	55	540	1700	350	600
OTHERS	852	9200	25000	NA	1300
TOTAL	2294	39000	120000	NA	18000
PALMS					
COCOS PALM	38	970	350	--	--
CALIFORNIA FAN PALM	82	830	2500c	520d	1300
CANARY ISLAND PALM	17	430	1600c	550d	880
DATE PALM	2	51	180c	--	--
TOTAL	139	2300	4700c	NA	2200
SHRUBS					
CALIF. SAGE BRUSH	640	2000	2600	52	140
SYDNEY GOLDEN WATTLE	7	1700	7600	150	1100
JUNIPER	389	1400	1300	3700	4800
GLOSSY PRIVET	176	1100	2300	230	530
BOTTLEBRUSH	219	1100	1800	470	850
CHINESE JUNIPER	556	890	580	3700	2100
CAMELLIA	365	770	970	1600	1600
OLEANDER	106	720	1300	230	300
HIBISCUS	184	710	1400	400	560
ROSE	762	700	650	360	230
SHINY XYLOSMA	282	560	700	470	330
COYOTE BUSH	173	540	710	--	--
JAPAN. PITTOSPORUM	394	510	400	2700	1100
TOYON	35	460	1300	--	--
OTHERS	3579	6300	7900	NA	790
TOTAL	7867	19000	32000	NA	15000

Table V-4 (continued) - 2

COMMON NAME	NUMBER OF SPECIMENS	AREA sq m	VOL cu m	LEAF MASS CONSTANT g/cu m	LEAF MASS kg
LAWNS & GRASSES					
GRASS (unid.)	NA	120000	NA	NA	NA
DICHONDRA	NA	3000	NA	NA	NA
TOTAL	NA	130000	NA	NA	NA
GROUND COVER					
IVY	NA	11000	NA	NA	NA
AFRICAN DAISY	NA	3300	NA	NA	NA
ICE PLANT	NA	1800	NA	NA	NA
FIVE FINGER	NA	180	NA	NA	NA
PERIWINKLE	NA	170	NA	NA	NA
GERANIUM	NA	160	NA	NA	NA
LILY	NA	130	NA	NA	NA
JADE PLANT	NA	120	NA	NA	NA
AFRICAN LILY	NA	55	NA	NA	NA
BELLFLOWER	NA	37	NA	NA	NA
BACHELOR BUTTON	NA	37	NA	NA	NA
WANDERING JEW	NA	33	NA	NA	NA
IRIS	NA	32	NA	NA	NA
TULE	NA	25	NA	NA	NA
OTHERS	NA	1600	NA	NA	NA
TOTAL	NA	18000	NA	NA	NA

a Area, volume and leaf mass rounded to 2 significant digits
b Dry weight of green tissue per unit volume
c Number of fronds -- Not measured
d g/frond NA Not applicable

Table V-5. Grand Totals of Data from Field Surveys for All Subplots and Leaf Mass Determinations

STRUCTURAL CLASS	NUMBER OF SPECIMENS	AREA sq m	VOL cu m	LEAF MASS kg
CONIFERS	728	5700	13000	10000
BROAD-LEAF TREES	2294	39000	120000	18000
PALMS	139	2300	4700a	2200
SHRUBS	7867	19000	32000	15000
LAWNS AND GRASSES	NA	130000	NA	NA
GROUND COVERS	NA	18000	NA	NA

a Number of fronds

NA Not applicable

VI. EMISSION INVENTORY FOR ISOPRENE AND SELECTED MONOTERPENES IN THE STUDY AREA

A. Introduction

Emission inventories for isoprene and selected monoterpenes were developed for (a) urban vegetation based on cover areas analyzed from aerial imagery (Section IV-E) and field survey data (Section V), and (b) naturally occurring vegetation using the available field plot data of the U. S. Forest Service (Section IV-F). To do this, it was first necessary to calculate leaf masses from the above data by incorporating leaf mass constants from the determinations described in Section V-C. Isoprene and monoterpene emissions were then calculated by multiplying the leaf masses by the emission rates reported in Section III.

B. Methods of Approach for Calculation of Urban Emission Inventory

1. Approximations Used for Determining Leaf Mass

The following approximations and subjective measurements were necessary in order to calculate the emissions in the urban region of the study area.

a. Each broad-leaf tree, conifer and shrub had to be categorized as an idealized geometric shape in order to estimate volume (used for leaf mass calculations) and maximum cross section area (used as the cover area that would be seen from aerial imagery). The shapes used were solid spheres, cones, cylinders, ellipsoids and rectangular boxes. However, for most species the leaf mass density was considered to be uniform throughout the solid shape. For some species the leaf mass was considered to cover only the outer shell of one of the above shapes. For example, juniper, abelia, Cape-honeysuckle and pittosporum species were assigned a shell thickness of 30.5 cm (1 ft) if their measurements exceeded 30.5 cm in all three dimensions. Italian cypress and oleander were assigned a shell thickness of 45.7 cm (1.5 ft) and 61 cm (2 ft) respectively.

b. Some very small plants, reported only as an approximate volume with no dimensions, were arbitrarily considered to be spheres of the reported volume. The radius of the sphere was used to calculate a cover area.

c. All data for palm trees were reported as the number of fronds. Again, some estimate of dimensions was needed for calculation of cover areas. Palms were assumed to be of spherical shape. The cover area was simply the area of a circle whose radius was equal to the average frond length of that species. The average frond lengths used were 2.85 m, 1.8 m and 2.85 m for Phoenix spp., Washingtonia filifera and Arecastrum romanzoffianum, respectively.

d. The Rolling Hills polygon (No. 18) was sampled in December after the leaves of deciduous trees had dropped. Data for evergreens were accepted as reported. Deciduous plants were estimated to have had the entire dimensions of the specimen filled with leaf matter.

e. Only the genus of some plants was recorded since it was not always possible to identify plants found in the field by both genus and species. However, species used for leaf mass constant determinations and emission rate measurements were identified by both genus and species names. In some cases these constants for a particular species were used for all plants observed in the field of the same genus. For example, the leaf mass constant and emissions rates were measured for evergreen ash, and all ash trees found were assigned these constants.

f. Structural classes were defined as conifers, broad-leaf trees, palms, shrubs, lawns/grasses and ground cover. Classification of some plants into one of these structural classes sometimes required subjective decisions, e.g., tree versus shrub, or shrub versus ground cover. Podocarpus, Ficus, and Prunus species were recorded under two structural classes: broad-leaf trees and shrubs. If the class was not reported, plants with a diameter of greater than 4 meters were classified as a broad-leaf tree instead of shrub. [Trachelospermum jasminoides (Star jasmine) was categorized as a shrub and ground cover].

g. Sago palms are neither true conifers nor palms. They were placed into the conifer structural class, however, since very few specimens were found, their classification did not influence the results.

h. Some broad common names were used for species found in the field, such as unidentified fern, succulents, aster (daisy) and mixed flowers. Lawns and grasses had two entries - unidentified grass and dichondra. The emission rates for four grass species (Cynodon dactylon, Poa pratensis, Lolium perenne, Festuca eliator) were measured and all were

non-emitters (or emitted below the detection limit of the gas chromatographs).

i. Leaf mass constants were estimated based on analogies to related species for four species for which the emission rates were measured but for which the leaf mass constants were unknown. These were evergreen pear, natal plum, glossy privet and hibiscus.

j. The number of subplots sampled per cell and the ground area sampled per cell varied from polygon to polygon. However, enough subplots were surveyed to account for at least 1% of the area in each sample cell.

2. Approximations Used for Estimating Emission Rates

Emission rate measurements were made under varying conditions of light intensity and temperature. Each measurement was corrected to a standard temperature, and the arithmetic mean of these corrected rates were used as the emission rate for that species.

All experimental emission rates were corrected to a constant temperature, 30°C for daylight hours (Tingey et al. 1980). Isoprene emission determinations ($\mu g\ g^{-1}\ hr^{-1}$) were corrected as follows:

$$\text{Emis}_{30^\circ C} = \frac{\text{measured emission rate} \times 34.194}{\exp\left[\frac{4.88}{1 + \exp[-0.18 \times (\text{temp in } ^\circ C - 25.26)]} + 0.11\right]}$$

The corrected rates for the same species were then averaged. Isoprene emission for all plants was assumed to cease during the nighttime hours.

Similarly, the average emission rates for the sum of selected monoterpenes were corrected to 30°C for daylight hours and to 25°C for nighttime hours.

$$\text{Emis}_{30^\circ C} = \frac{\text{measured emission rate} \times 6.392}{\exp\,[-0.332 + 0.0727\ (\text{temp in } ^\circ C)]}$$

$$\text{Emis}_{25^\circ C} = \frac{\text{measured emission rate} \times 4.44}{\exp\,[-0.332 + 0.0727\ (\text{temp in } ^\circ C)]}$$

3. Calculations

Although the polygons were outlined as homogeneous regions (Section IV) on the basis of the NASA U-2 imagery, on a much finer scale, individual field subplots within the same sample cell of a polygon contained differing distributions of vegetation. The small number of samples at each stage (i.e., one sample cell per polygon and as few as 1 or 2 subplots per sample cell) did not permit the calculation of variances at each stage, or the accumulation of variances from several stages. Given these inherent limitations, it was decided to calculate the emission inventory by a number of different methods to assess the sensitivity of the calculated total emissions to various statistical techniques, and to obtain an estimate of the range of possible uncertainties in the final inventory values.

Leaf masses for each structural class, namely, broad-leaf tree, conifer and shrub were calculated as the product of the volume of the plant (m^3) and its leaf mass constant (g m^{-3}). Palm leaf masses were the product of the number of fronds and the palm leaf mass constant (g $frond^{-1}$). Only species with known or estimated leaf mass constants and emission rates were used in leaf mass calculations and subsequent emission calculations.

For simplicity of notation, species with experimentally measured emission rates or leaf mass constants are referred to as "knowns" (Tables III-18, V-2 and V-3). Species that were found in the field but for which leaf mass constants or emission rates were not determined are referred to as "unknowns."

Leaf mass (g) and the temperature-corrected emission rates ($\mu g\ g^{-1}\ hr^{-1}$) were multiplied to give emissions rates in $\mu g\ hr^{-1}$ for each species measured. The cover area (a maximum cross section area of a given plant as seen from overhead) was calculated for each specimen from the field data dimensions to be analogous to imagery cover data from aerial photographs. In all the calculations described below, each structural class was treated separately. In some methods subplots were calculated separately. Isoprene emission was kept independent of monoterpenes emission. They were summed in the final steps of the various methods to yield a polygon emission ($kg\ hr^{-1}$).

Thirteen calculation methods were used. These were devised in order to estimate total emissions in a variety of ways so that the range of values possible from this data base could be determined. These methods are described in flow chart format in Appendix C. For each method an individual flow chart shows the specific subset of variables entering into that calculation and the operations (e.g., multiplication, division, summation, etc.) used. The reader may wish to refer to the flow charts in Appendix C in conjunction with the equations given below for each method.

Emission calculations were divided into four cases. Case I includes calculation Methods 1 through 3. In Case I the total hydrocarbon emissions for each polygon were based on imagery cover areas, emission rates and field survey cover areas of "knowns." This was the only Case involving imagery data. Case II polygon emissions were calculated by extrapolating the emission rates of "knowns" from the subplots to the entire polygon on the basis of subplot areas and polygon areas (Methods 4 and 5). Case I and II are thus based on only the "knowns." Polygon emissions were calculated from the rate of emissions of "knowns" and the ratio of the mapped area to the polygon area.

Case III and IV calculated polygon emissions based on "knowns" and "unknowns." In Case III (Methods 6, 7, 10 and 11) we calculated the emissions of "knowns" (product of leaf mass and emission rate). In addition, for each structural class, we took an average product of "known" emission rates and leaf mass constants for that structural class (broad-leaf trees, conifers and shrubs). The procedure for the class average is described below. The average was multiplied by the volume of "unknowns" in the class. Since palm leaf mass constants are measured in g frond^{-1}, the average emission rate-leaf mass constant product was multiplied by the number of fronds of unknown palms. An average emission rate-leaf mass constant product for ground cover and for lawn classes were multiplied by the areas attributed to "unknowns" in those two classes. The emissions of the "unknowns" were added to the emissions of the "knowns" as emission rate (μg hr^{-1}) for each class observed in the polygon.

Case IV (Methods 8, 9, 12 and 13) is similar to Case III. Average emission rate - leaf mass constant products were again used for each class based on the values of "knowns." However, in this case, these averages

are multiplied by the volume of all species in the class in the subplot; i.e., the total volume of "knowns" and "unknowns" was multiplied by the class average emission rate - leaf mass value.

In summary, 13 different methods of calculating total emissions were used; these consisted of several methods based on each of Cases I through IV. In six of the methods (1, 4, 6, 8, 10 and 12) field data from the same sample cell (different subplots) were combined as if there was only one large subplot per sample cell. In the other seven methods (2, 3, 5, 7, 9, 11 and 13) each subplot was calculated separately and the sample cell emission rate was the average of subplot emissions in that cell. A discussion of the detailed calculations employed for each of the 13 methods are given below.

Case I. Broad-leaf trees and conifers could not be differentiated by imagery. Thus, only five structural classes were reported (Table IV-3). To be consistent with the imagery areal cover data, field data for broad-leaf trees and conifers were combined into one class for analysis by the three methods of Case I.

Method #1. All field data for the structural classes in all subplots in the same cell were combined. Leaf masses (g) were multiplied by the appropriate isoprene emission rates ($\mu g\ g^{-1}\ hr^{-1}$) to give isoprene emissions ($\mu g\ hr^{-1}$) for each species found in the field. Emissions and cover area for each structural class were summed. The ratio of the total isoprene emissions ($g\ hr^{-1}$) to the corresponding cover area (m^2) was calculated for each structural class. This ratio ($g\ hr^{-1}\ m^{-2}$) was multiplied by the imagery cover area for the class to yield the emission for the mapped area. The sum of the five classes was then multiplied by the ratio of the polygon area to the mapped area to extrapolate the isoprene emission to the entire polygon. Monoterpene emissions were calculated in exactly the same manner.

$$\begin{array}{c}\text{Isoprene}\\ \text{or}\\ \text{monoterpene}\\ \text{emissions}\\ \text{for each}\\ \text{polygon}\\ (\mu g\ hr^{-1})\end{array} = \sum_{\text{Structural classes}} \left(\frac{\sum_{\text{Knowns}} \begin{array}{c}\text{HC}(\mu g\ hr^{-1})\\ \text{For each}\\ \text{class}\end{array}}{\sum_{\text{Knowns}} \begin{array}{c}\text{Cover area}\\ \text{for each}\\ \text{class } (m^2)\end{array}} \times \begin{array}{c}\text{Imagery}\\ \text{cover}\\ \text{area } (m^2)\\ \text{for each}\\ \text{class}\end{array} \right) \times \frac{\begin{array}{c}\text{Polygon}\\ \text{area}\\ (km^2)\end{array}}{\begin{array}{c}\text{Area of}\\ \text{photo}\\ \text{frame } (km^2)\end{array}}$$

Method #2. The data from individual subplots were not combined. The ratio of hydrocarbon emission rate (g hr^{-1}) to the cover area for subplots in the same polygon were averaged class by class and multiplied by the class imagery cover area. The classes were then summed and extrapolated to the polygon by multiplying by the ratio of the polygon area to the mapped area.

$$\begin{pmatrix}\text{Isoprene or monoterpene emissions per polygon } (\mu g\ hr^{-1})\end{pmatrix} = \sum_{\text{Structural classes}} \left[\frac{\sum_{\text{Subplot}} \left(\frac{\sum_{\text{Knowns}} \text{HC } (\mu g\ hr^{-1})}{\sum_{\text{Knowns}} \text{Cover area for each class } (m^2)} \right)}{\text{Number of subplots}} \times \begin{pmatrix}\text{Imagery cover area } (m^2) \\ \text{for each class}\end{pmatrix} \right] \times \frac{\text{Polygon area } (km^2)}{\text{Area of photo frame } (km^2)}$$

Method #3. The subplots varied in size, therefore the emissions were weighted by the subplot areas.

$$\begin{pmatrix}\text{Isoprene or monoterpene emissions per polygon } (\mu g\ hr^{-1})\end{pmatrix} = \sum_{\text{Structural classes}} \left[\frac{\sum_{\text{Subplot}} \left(\frac{\sum_{\text{Knowns}} \text{HC } (\mu g\ hr^{-1}) \times \text{subplot area } (m^2)}{\sum_{\text{Knowns}} \text{Cover area for each class } (m^2)} \right)}{\sum_{\text{Subplot}} \text{Subplot area } (m^2)} \times \begin{pmatrix}\text{Imagery cover area } (m^2) \\ \text{for each class}\end{pmatrix} \right] \times \frac{\text{Polygon area } (km^2)}{\text{Area of photo frame } (km^2)}$$

Case II. For these methods ground field observations were used instead of imagery data. Therefore all six structural classes were used.

Method #4. As in Method #1, all subplot data in the same sample cell were combined. The emissions for each class was extrapolated to the entire polygon by the ratio of the polygon area to the field survey area.

$$\begin{pmatrix}\text{Isoprene or monoterpene emissions per polygon } (\mu g\ hr^{-1})\end{pmatrix} = \sum_{\text{Structural classes}} \left[\left(\sum_{\text{Knowns}} \text{HC} (\mu g\ hr^{-1}) \right) \times \frac{\text{Polygon area } (km^2)}{\sum_{\text{Subplot}} \text{Subplot area } (km^2)} \right]$$

Method #5. Instead of combining data for all subplots, emissions were calculated individually for each subplot, and the ratios of emissions to subplot area were averaged. Again the emissions were extrapolated by multiplying by the polygon area.

$$\begin{matrix}\text{Isoprene or monoterpene emissions per polygon } (\mu g\ hr^{-1})\end{matrix} = \sum_{\text{Structural classes}} \left[\frac{\sum_{\text{Subplot}} \left(\frac{\sum \text{HC Knowns } (\mu g\ hr^{-1})}{\text{Subplot area } (m^2)} \right)}{\text{Number of subplots}} \right] \times \text{Polygon area } (km^2)$$

Case III. An attempt was made to estimate the contribution to emissions made by "unknowns" actually observed in the field survey instead of basing everything on the emissions calculated from the "knowns." First, the emissions due to "knowns" was calculated as before. The known emissions could then be added to the estimated emissions of the "unknowns."

For Methods 6, 7, 10 and 11, the average emission rate-leaf mass constant was calculated as the average of the products of (emission rate) x (leaf mass constant); e.g., the emission rate for evergreen ash was multiplied by the leaf mass constant for evergreen ash. These products were summed and divided by the number of species with emission rate measurements in the class.

$$\text{Ave. class emis} = \frac{\text{Known } \sum_{\text{species}} [\text{Emis}(\mu g\ g^{-1}\ hr^{-1}) \times \text{leaf mass constants}]}{\text{Number of species}}$$

In Methods 8, 9, 12 and 13, the average emission rate-leaf mass constant product for a class was calculated as the average emission rate multiplied by the average leaf mass constant for "knowns" in that class. All emission rates in a class were averaged; all leaf mass constants were averaged. Thus, for these methods the product of the two averages was used.

$$\text{Ave. class emis} = \frac{\sum_{\text{Knowns}} \text{Emis}}{\text{Number of species}} \times \frac{\sum_{\text{Knowns}} \text{Leaf mass constants}}{\text{Number of species}}$$

Method #6. All data from subplots in the same cell were combined.

$$\begin{pmatrix}\text{Isoprene or monoterpene emissions per polygon} \\ (\mu g\ hr^{-1})\end{pmatrix} = \sum_{\text{Structural class}} \left(\sum_{\text{Knowns}} \text{HC}\ (\mu g\ hr^{-1}) + \sum_{\text{Unknowns}} \text{HC}\ (\mu g\ hr^{-1}) \right) \times \frac{\text{Polygon area } (km^2)}{\sum \text{Subplot areas } (km^2)}$$

$$\text{where} \quad \sum_{\text{Unknowns}} \text{HC}\ (\mu g\ hr^{-1}) = \begin{pmatrix}\text{Volume of foliage } (m^3) \\ \text{or} \\ \text{Area of ground cover } (m^2) \\ \text{or} \\ \text{Number of fronds}\end{pmatrix} \times \begin{pmatrix}\text{Average of (leaf mass) x (emission rate)} \\ (\mu g\ hr^{-1}\ m^{-3}) \text{ or} \\ (\mu g\ hr^{-1}\ m^{-2}) \text{ or} \\ (\mu g\ hr^{-1}\ \text{frond}^{-1})\end{pmatrix}$$

Method #7. The emissions for each subplot were calculated separately and averaged.

$$\begin{pmatrix}\text{Isoprene or monoterpene emissions per polygon} \\ (\mu g\ hr^{-1})\end{pmatrix} = \sum_{\text{Structural class}} \left[\frac{\sum_{\text{Subplots}} \left(\frac{\sum_{\text{Knowns}} \text{HC}\ (\mu g\ hr^{-1}) + \sum_{\text{Unknowns}} \text{HC}\ (\mu g\ hr^{-1})}{\text{Subplot areas } (km^2)} \right)}{\text{Number of subplots}} \right] \times \text{Polygon area } (km^2)$$

where $\sum_{\text{Unknowns}} \text{HC}\ (\mu g\ hr^{-1})$ is as defined for Method #6.

Method #8. This is the same as Method #6 except that the average (emission rate) x (average leaf mass constant) product was used for each class.

$$\begin{pmatrix}\text{Isoprene or monoterpene emissions per polygon} \\ (\mu g\ hr^{-1})\end{pmatrix} = \sum_{\text{Structural classes}} \left(\sum_{\text{Knowns}} HC\ (\mu g\ hr^{-1}) + \sum_{\text{Unknowns}} HC\ (\mu g\ hr^{-1}) \right) \times \frac{\text{Polygon area } (km^2)}{\sum \text{Subplot area } (km^2)}$$

where $\sum_{\text{Unknowns}} HC\ (\mu g\ hr^{-1})$ is as defined for Method #6.

Method #9. This is the same as Method #7 except that the average (emission rate) x (average leaf mass constant) product was used instead of the average (emission rate) x (leaf mass constant) product.

$$\begin{pmatrix}\text{Isoprene or monoterpene emissions per polygon} \\ (\mu g\ hr^{-1})\end{pmatrix} = \sum_{\text{Structural classes}} \left[\frac{\sum_{\text{Subplots}} \left(\frac{\sum_{\text{Knowns}} HC\ (\mu g\ hr^{-1}) + \sum_{\text{Unknowns}} HC\ (\mu g\ hr^{-1})}{\text{Subplot areas } (km^2)} \right)}{\text{Number of subplots}} \right] \times \text{Polygon area } (km^2)$$

where $\sum_{\text{Unknowns}} HC\ (\mu g\ hr^{-1})$ is as defined for Method #6.

The comparison of Case IV to Case III gave some indication of the validity of the class average emission rate-leaf mass constant products used in Case III. Rather than calculating the "known" emission and adding it to some estimate for "unknowns," the volume of "knowns" and "unknowns" were combined and multiplied by the average emission rate-leaf mass constant product ($\mu g\ hr^{-1}\ m^{-3}$ for trees, conifers and shrubs) to yield emission in ($\mu g\ hr^{-1}$). The units for the average emission rate-leaf mass constant product is ($\mu g\ hr^{-1}$ frond^{-1}) for palms and ($\mu g\ hr^{-1}\ m^{-2}$) for ground cover or grasses.

Method #10. All data from subplots in the same cell were combined.

$$\begin{pmatrix}\text{Isoprene}\\ \text{or}\\ \text{monoterpene}\\ \text{emissions}\\ \text{per}\\ \text{polygon}\\ (\mu g\ hr^{-1})\end{pmatrix} = \sum_{\text{Structural classes}} \left[\text{Knowns + Unknowns}\right] \times \frac{\text{Polygon}_2\ \text{Area}\ (km^2)}{\sum \text{Subplot}_2\ \text{areas}\ (km^2)}$$

Where [Knowns + Unknowns] =

$$\left[\begin{pmatrix}\text{Total vol. knowns } (m^3)\\ \text{or}\\ \text{Area of ground}_2\ \text{cover}\\ \text{knowns } (m^2)\\ \text{or}\\ \text{Number of fronds}\\ \text{knowns}\end{pmatrix} + \begin{pmatrix}\text{Total vol. unknowns } (m^3)\\ \text{or}\\ \text{Area of ground cover}\\ \text{unknowns } (m^2)\\ \text{or}\\ \text{Number of fronds}\\ \text{unknowns}\end{pmatrix} \times \begin{pmatrix}\text{Average emission}\\ \text{of a structural}\\ \text{class}\\ (\mu g\ hr^{-1}\ m^{-3})\ \text{or}\\ (\mu g\ hr^{-1}\ m^{-2})\ \text{or}\\ (\mu g\ hr^{-1}\ \text{frond}^{-1})\end{pmatrix}\right]$$

Area or number of fronds may be substituted for volume.

Method #11. The emissions of subplots were calculated individually and averaged.

$$\begin{pmatrix}\text{Isoprene}\\ \text{or}\\ \text{monoterpene}\\ \text{emissions}\\ \text{per}\\ \text{polygon}\\ (\mu g\ hr^{-1})\end{pmatrix} = \sum_{\text{Structural classes}} \left[\frac{\sum_{\text{Subplot}} \left(\frac{\text{Total volume } (m^3)\ \text{or Area of ground cover } (m^2)\ \text{or No. of fronds}}{\text{Subplot area } (km^2)}\right) \times \begin{pmatrix}\text{Average emission}\\ \text{of a class}\\ (\mu g\ hr^{-1}\ m^{-3})\ \text{or}\\ (\mu g\ hr^{-1}\ m^{-2})\ \text{or}\\ (\mu g\ hr^{-1}\ \text{frond}^{-1})\end{pmatrix}}{\text{Number of subplots}}\right] \times \begin{pmatrix}\text{Polygon}\\ \text{area}\\ (km^2)\end{pmatrix}$$

Area or number of fronds may be substituted for volume.

Methods #12 and #13. These are analogous to Methods 10 and 11 except that the average emission rate-leaf mass constant product for a class in Methods 12 and 13 were the (average emission rate) x (average leaf mass constant) and the average emission rate-leaf mass constant products for Methods 10 and 11 were the average (emission rate x leaf mass constant).

$$\begin{pmatrix}\text{Isoprene}\\ \text{or}\\ \text{monoterpene}\\ \text{emissions}\\ \text{per}\\ \text{polygon}\\ (\mu g\ hr^{-1})\end{pmatrix} = \sum_{\text{Structural classes}} \left[\text{Knowns + Unknowns}\right] \times \frac{\text{Polygon}_2\ \text{area}\ (km^2)}{\sum \text{Subplot}_2\ \text{areas}\ (km^2)}$$

Where [Knowns + Unknowns] =

$$\left[\begin{pmatrix}\text{Total vol. knowns } (m^3)\\ \text{or}\\ \text{Area of ground cover knowns } (m^2)\\ \text{or}\\ \text{Number of fronds knowns}\end{pmatrix} + \begin{pmatrix}\text{Total vol. unknowns } (m^3)\\ \text{or}\\ \text{Area of ground cover unknowns } (m^2)\\ \text{or}\\ \text{Number of fronds unknowns}\end{pmatrix}\right] \times \begin{pmatrix}\text{Average}\\ \text{emission}\\ \text{rate of}\\ \text{a class}\end{pmatrix} \times \begin{pmatrix}\text{Average}\\ \text{leaf mass}\\ \text{constant}\\ \text{of a class}\end{pmatrix}$$

$(\mu g\ hr^{-1}\ m^{-3})$ or $(\mu g\ hr^{-1}\ m^{-2})$ or $(\mu g\ hr^{-1}\ frond^{-1})$

$$\begin{pmatrix}\text{Isoprene}\\ \text{or}\\ \text{monoterpene}\\ \text{emissions}\\ \text{per}\\ \text{polygon}\\ (\mu g\ hr^{-1})\end{pmatrix} = \sum_{\text{Structural classes}} \left[\frac{\sum_{\text{Subplot}} \left(\frac{\text{Total Volume } (m^3) \text{ or Area of ground cover } (m^2) \text{ or No. of fronds}}{\text{Subplot area } (km^2)}\right)}{\text{Number of subplots}} \times \begin{pmatrix}\text{Average}\\ \text{emission}\\ \text{rate of}\\ \text{a class}\end{pmatrix} \times \begin{pmatrix}\text{Average}\\ \text{leaf mass}\\ \text{constant}\\ \text{of a class}\end{pmatrix}\right] \times \begin{pmatrix}\text{Polygon}\\ \text{area}\\ (km^2)\end{pmatrix}$$

$(\mu g\ hr^{-1}\ m^{-3})$ or $(\mu g\ hr^{-1}\ m^{-2})$ or $(\mu g\ hr^{-1}\ frond^{-1})$

4. Results

According to our stratified model, the emissions for the subplots were extrapolated to the sample cell, the cell emissions extrapolated to the polygon and the polygon emissions summed to give the total emissions in the urban region of the study area. An emission rate in $\mu g\ hr^{-1}$ (and $kg\ hr^{-1}$) for isoprene and for the sum of selected monoterpenes was calculated for each polygon by each of the 13 methods described earlier.

The results reported in Table VI-1 represent the hydrocarbon emission inventory for isoprene and the monoterpenes for the urban regions of the study area. All 13 calculations were repeated in order to estimate an "upper limit" emission inventory. In this case, all initial emission rates measured as zero (below detection) were considered to be equal to the detection limit. The results of this second set of 13 calculations are given in Table VI-2.

Table VI-1. Emission Inventory for 20 Polygons by 13 Methods (kg hr^{-1}) [a]

POLYGON NO.	METHOD 1			METHOD 2			METHOD 3			METHOD 4		
	ISO [b]	MONO [c]		ISO	MONO		ISO	MONO		ISO	MONO	
	DAY	DAY	NIGHT	DAY	DAY	NIGHT	DAY	DAY	NIGHT	DAY	DAY	NIGHT
1	16.3	10.7	7.4	11.0	12.8	8.9	12.8	13.3	9.1	5.8	5.7	3.9
2	0.4	6.6	4.6	0.4	6.6	4.6	0.4	6.6	4.6	0.1	0.6	0.4
3	14.4	12.9	8.9	14.6	12.1	8.3	13.2	10.2	7.0	11.0	3.9	2.7
4	52.5	1.2	0.8	49.8	1.4	1.0	50.1	1.2	0.8	52.5	1.3	0.9
5	31.5	2.6	1.8	25.7	2.6	1.8	31.0	3.2	2.2	22.4	1.0	0.7
6	60.9	18.9	13.1	80.6	26.2	18.1	59.0	21.7	15.0	40.4	14.4	9.9
7	11.1	4.8	3.3	10.1	5.2	3.6	10.2	5.1	3.5	19.7	5.8	4.0
8	0.0	0.1	0.1	0.0	0.0	0.0	0.0	0.1	0.0	0.0	0.0	0.0
9	4.1	8.3	5.7	2.1	5.5	3.8	1.5	5.3	3.6	2.4	6.5	4.5
10	38.9	0.0	0.0	31.8	0.0	0.0	41.6	0.0	0.0	47.1	0.1	0.0
11	4.0	1.1	0.8	2.3	1.3	0.9	0.5	1.8	1.3	0.8	0.2	0.1
12	9.5	4.1	2.8	8.4	2.9	2.0	8.4	2.4	1.7	14.7	4.5	3.1
13	52.8	23.1	15.9	46.4	29.1	20.1	62.6	13.1	9.0	32.5	11.3	7.8
14	20.8	1.4	1.0	20.8	1.4	1.0	20.8	1.4	1.0	7.2	0.5	0.3
15	45.8	5.7	3.9	28.9	8.7	6.0	41.1	13.0	9.0	39.9	3.6	2.5
16	1.0	0.2	0.2	0.6	0.1	0.1	0.6	0.1	0.1	4.9	0.5	0.3
17	19.2	5.1	3.5	20.1	4.5	3.1	20.6	4.7	3.3	25.8	1.7	1.2
18	22.5	3.1	2.2	21.3	3.9	2.7	19.3	4.3	2.9	24.8	4.4	3.1
19	36.5	0.8	0.6	17.4	1.5	1.0	14.1	1.1	0.8	5.2	0.4	0.3
20	52.6	42.7	29.5	62.8	35.7	24.6	98.4	16.5	11.4	5.4	4.2	2.9
TOTAL	495	154	106	455	162	112	506	125	86	363	71	49

Table VI-1 (continued) - 2

POLYGON NO.	METHOD 5			METHOD 6			METHOD 7			METHOD 8		
	ISO	MONO		ISO	MONO		ISO	MONO		ISO	MONO	
	DAY	DAY	NIGHT	DAY	DAY	NIGHT	DAY	DAY	NIGHT	DAY	DAY	NIGHT
1	8.1	13.0	9.0	8.4	5.9	4.1	12.8	13.5	9.3	9.6	6.1	4.2
2	0.1	0.6	0.4	8.7	1.1	0.8	8.7	1.1	0.8	5.8	0.9	0.7
3	11.2	4.3	3.0	29.7	5.2	3.6	23.4	5.2	3.6	19.5	4.5	3.1
4	77.6	2.1	1.5	62.1	1.8	1.3	87.1	2.8	1.9	57.6	1.6	1.1
5	19.4	1.1	0.7	23.6	1.0	0.7	21.0	1.2	0.8	23.1	1.0	0.7
6	54.0	17.2	11.9	65.8	16.5	11.4	87.3	20.1	13.9	57.9	16.4	11.3
7	19.7	5.8	4.0	38.6	7.1	4.9	38.5	7.1	4.9	37.0	7.2	5.0
8	0.0	0.0	0.0	1.1	0.1	0.1	1.1	0.1	0.1	0.8	0.1	0.1
9	3.5	7.4	5.1	12.4	7.1	4.9	17.1	8.3	5.7	6.4	6.7	4.7
10	36.9	0.1	0.0	50.1	0.3	0.2	39.9	0.3	0.2	51.6	0.5	0.3
11	3.1	0.5	0.3	1.6	0.2	0.2	6.8	0.8	0.6	1.6	0.2	0.2
12	17.5	5.4	3.7	33.2	5.6	3.8	33.5	6.2	4.3	23.4	4.9	3.4
13	25.8	26.2	18.1	61.3	13.6	9.4	82.9	30.8	21.3	43.1	12.8	8.8
14	7.2	0.5	0.3	8.6	0.6	0.4	8.6	0.6	0.4	7.5	0.5	0.4
15	27.2	3.3	2.3	58.7	5.0	3.5	47.3	4.9	3.4	50.8	4.6	3.2
16	5.0	0.5	0.3	7.5	0.7	0.5	7.8	0.7	0.5	9.8	0.9	0.6
17	25.0	1.7	1.1	38.2	2.0	1.4	37.7	2.0	1.4	38.2	2.1	1.4
18	14.8	20.5	14.2	33.7	5.4	3.7	55.2	25.6	17.7	39.1	5.9	4.1
19	7.0	0.4	0.3	23.0	1.1	0.7	24.6	1.1	0.8	25.2	1.4	0.9
20	10.8	13.5	9.3	6.1	4.3	2.9	12.4	13.7	9.4	7.1	4.4	3.0
TOTAL	374	124	86	572	85	59	654	146	101	515	83	57

Table VI-1 (continued) - 3

POLYGON NO.	METHOD 9			METHOD 10			METHOD 11			METHOD 12		
	ISO	MONO		ISO	MONO		ISO	MONO		ISO	MONO	
	DAY	DAY	NIGHT	DAY	DAY	NIGHT	DAY	DAY	NIGHT	DAY	DAY	NIGHT
1	13.4	13.6	9.4	33.7	3.6	2.5	52.4	4.8	3.3	41.8	5.2	3.6
2	5.8	0.9	0.7	12.3	1.5	1.0	12.3	1.5	1.0	10.5	2.0	1.4
3	18.1	4.9	3.4	107.5	12.9	8.9	74.3	13.5	9.3	44.9	14.8	10.2
4	82.3	2.6	1.8	40.0	3.2	2.2	52.5	4.4	3.0	27.7	3.0	2.1
5	20.7	1.2	0.8	21.7	1.8	1.2	24.4	1.8	1.2	7.1	1.1	0.8
6	78.9	20.1	13.9	215.3	16.6	11.4	206.2	16.5	11.4	82.6	9.4	6.5
7	37.0	7.3	5.0	132.9	11.5	8.0	128.6	11.3	7.8	64.7	9.7	6.7
8	0.9	0.1	0.1	1.1	0.1	0.1	1.1	0.1	0.1	0.9	0.1	0.1
9	9.4	7.8	5.4	22.7	11.9	8.2	29.2	9.9	6.8	12.2	21.5	14.8
10	42.0	0.5	0.4	56.0	3.9	2.7	50.7	3.6	2.5	23.7	1.8	1.2
11	6.7	0.8	0.6	2.5	0.3	0.2	10.3	1.1	0.8	1.4	0.3	0.2
12	25.8	5.7	3.9	72.6	12.5	8.6	80.5	14.3	9.9	36.8	18.0	12.5
13	46.8	29.2	20.1	103.4	14.0	9.6	156.5	25.9	17.9	49.4	17.2	11.8
14	7.5	0.5	0.4	3.7	0.8	0.6	3.7	0.8	0.6	0.9	1.1	0.8
15	38.7	4.4	3.0	101.3	6.8	4.7	113.1	8.0	5.5	56.0	4.5	3.1
16	10.2	1.0	0.7	10.1	0.7	0.5	10.4	0.7	0.5	12.7	1.1	0.8
17	37.7	2.0	1.4	53.4	3.2	2.2	53.3	3.2	2.2	40.8	3.7	2.5
18	113.2	31.2	21.5	46.4	4.3	2.9	117.5	14.8	10.2	41.9	4.8	3.3
19	26.9	1.4	1.0	34.7	1.9	1.3	34.9	1.8	1.3	33.0	2.3	1.6
20	13.7	13.8	9.5	9.1	1.2	0.8	29.2	3.7	2.6	6.8	1.7	1.1
TOTAL	636	149	103	1080	113	78	1241	142	98	596	123	85

Table VI-1 (continued) - 4

POLYGON NO.	METHOD 13		
	ISO	MONO	
	DAY	DAY	NIGHT
1	50.1	5.7	3.9
2	10.5	2.0	1.4
3	34.0	19.5	13.4
4	29.4	3.7	2.6
5	9.9	1.1	0.8
6	91.0	11.0	7.6
7	63.6	9.6	6.7
8	1.0	0.1	0.1
9	17.9	16.9	11.7
10	24.0	1.9	1.3
11	5.5	1.2	0.8
12	41.8	21.0	14.5
13	64.9	34.9	24.1
14	0.9	1.1	0.8
15	53.5	4.8	3.3
16	13.3	1.2	0.8
17	39.8	3.6	2.5
18	252.5	29.1	20.1
19	34.7	2.4	1.6
20	19.9	5.1	3.5
TOTAL	958	176	122

a Species with isoprene and sum of monoterpenes emission rates below the detection limit were considered to be non-emitters.
b Isoprene
c Sum of selected monoterpenes

Table VI-2. Emission Inventory for 20 Polygons by 13 Methods: Detection Limit Case (kg hr^{-1})[a]

POLYGON NO.	METHOD 1			METHOD 2			METHOD 3			METHOD 4		
	ISO[b]	MONO[c]		ISO	MONO		ISO	MONO		ISO	MONO	
	DAY	DAY	NIGHT	DAY	DAY	NIGHT	DAY	DAY	NIGHT	DAY	DAY	NIGHT
1	28.1	17.9	11.3	23.4	18.9	12.0	25.2	19.6	12.5	14.0	9.4	6.1
2	18.9	11.9	8.1	18.9	11.9	8.1	18.9	11.9	8.1	5.0	2.1	1.3
3	87.0	41.7	27.4	69.0	30.6	20.2	76.3	37.2	24.5	39.4	15.6	9.6
4	58.3	4.7	3.2	56.3	5.0	3.4	56.1	4.8	3.3	61.0	5.9	3.9
5	37.8	6.7	4.1	31.9	6.4	4.0	36.5	6.8	4.2	26.2	4.2	2.1
6	99.0	47.7	31.9	119.2	48.5	32.5	95.2	46.4	31.1	78.8	43.9	23.7
7	30.5	16.0	9.5	31.7	16.5	9.8	31.7	16.5	9.8	48.5	20.6	12.3
8	7.8	2.4	1.3	4.1	1.4	0.7	3.6	1.3	0.6	0.5	0.3	0.1
9	19.8	12.2	7.0	14.3	9.8	5.3	14.7	9.1	4.9	19.7	14.1	5.4
10	45.9	5.9	3.7	38.6	5.3	3.3	48.4	6.1	3.9	56.6	7.5	4.9
11	5.4	1.8	1.0	3.6	1.7	1.1	2.0	1.9	1.3	1.0	0.3	0.2
12	27.6	12.4	7.3	21.7	9.3	5.1	20.1	8.3	4.4	35.0	14.7	8.5
13	104.4	41.1	25.8	100.3	45.5	28.8	104.6	32.5	19.8	64.4	23.0	14.4
14	23.1	2.9	2.0	23.1	2.9	2.0	23.1	2.9	2.0	8.0	1.0	0.7
15	56.6	16.0	8.7	45.2	18.6	10.6	54.3	22.3	13.1	50.3	13.7	6.2
16	4.2	1.2	0.8	3.0	0.9	0.6	3.0	0.9	0.6	10.7	3.1	1.6
17	43.9	14.8	9.9	43.7	13.6	9.2	44.9	14.0	9.5	38.9	9.1	6.0
18	31.9	7.9	5.4	37.8	11.0	7.6	41.1	13.0	8.9	37.8	11.9	6.8
19	66.7	17.1	11.3	44.9	13.7	9.0	39.6	12.3	8.0	22.0	7.9	4.3
20	80.0	54.9	36.7	91.0	49.3	32.8	131.5	35.0	22.9	8.5	6.0	3.8
TOTAL	877	337	217	822	321	206	871	303	193	626	214	122

Table VI-2 (continued) - 2

POLYGON NO.	METHOD 5			METHOD 6			METHOD 7			METHOD 8		
	ISO	MONO		ISO	MONO		ISO	MONO		ISO	MONO	
	DAY	DAY	NIGHT	DAY	DAY	NIGHT	DAY	DAY	NIGHT	DAY	DAY	NIGHT
1	22.2	18.2	11.8	18.9	10.6	6.9	30.5	20.2	13.1	19.3	10.5	6.9
2	5.0	2.1	1.3	17.1	4.6	3.0	17.1	4.6	3.0	12.2	3.4	2.2
3	33.4	12.5	7.7	65.0	20.9	13.3	50.8	16.3	10.3	49.8	17.5	10.9
4	87.8	7.9	5.1	73.0	8.1	5.4	100.1	10.3	6.8	66.7	6.8	4.5
5	24.0	4.5	2.4	28.0	4.6	2.3	26.6	5.1	2.8	27.1	4.3	2.2
6	91.5	41.5	24.1	117.1	52.5	29.7	142.6	53.2	32.1	102.7	49.0	27.3
7	48.1	20.4	12.2	76.8	26.6	16.4	76.4	26.3	16.3	71.2	24.9	15.3
8	0.5	0.3	0.1	2.1	0.7	0.3	2.2	0.7	0.3	1.5	0.5	0.2
9	18.5	13.8	6.2	33.3	16.9	7.4	37.0	17.7	8.9	24.7	14.9	6.0
10	48.1	7.2	4.7	62.1	8.7	5.8	53.9	8.6	5.7	62.8	8.7	5.8
11	3.7	0.9	0.5	2.4	0.6	0.4	10.1	2.4	1.5	2.1	0.5	0.3
12	41.4	17.4	10.0	58.6	19.1	11.5	61.8	21.2	12.6	44.7	16.1	9.4
13	71.0	37.5	23.9	103.3	31.4	20.1	148.1	54.0	35.3	78.0	26.1	16.5
14	8.0	1.0	0.7	9.8	1.4	1.0	9.8	1.4	1.0	8.4	1.1	0.7
15	39.2	14.1	6.3	78.1	19.9	10.5	69.0	20.6	10.7	64.8	16.7	8.3
16	11.1	3.2	1.7	15.7	4.2	2.4	16.3	4.4	2.5	17.5	4.4	2.6
17	38.2	8.9	5.9	53.7	11.0	7.3	53.3	10.8	7.2	52.8	10.7	7.1
18	31.3	27.3	17.9	55.9	16.5	9.9	131.5	54.4	36.6	58.7	16.5	9.9
19	23.0	7.7	4.2	45.5	11.6	6.8	46.8	11.6	6.8	45.8	11.3	6.6
20	17.9	17.7	10.9	10.3	6.5	4.2	21.5	18.7	11.5	11.0	6.6	4.2
TOTAL	664	264	158	927	276	165	1105	362	225	822	251	147

Table VI-2 (continued) - 3

POLYGON NO.	METHOD 9			METHOD 10			METHOD 11			METHOD 12		
	ISO	MONO		ISO	MONO		ISO	MONO		ISO	MONO	
	DAY	DAY	NIGHT	DAY	DAY	NIGHT	DAY	DAY	NIGHT	DAY	DAY	NIGHT
1	29.7	19.8	12.9	61.2	15.2	10.5	87.7	20.9	14.4	60.7	13.8	9.5
2	12.2	3.4	2.2	19.4	4.7	3.3	19.4	4.7	3.3	15.6	4.0	2.8
3	42.3	14.2	8.9	146.5	34.5	23.8	105.5	28.7	19.8	69.2	22.3	15.4
4	93.5	9.0	5.9	58.9	12.9	8.9	74.8	16.4	11.3	37.2	7.8	5.4
5	25.8	4.8	2.6	28.6	6.0	4.2	32.1	6.6	4.6	8.9	2.1	1.4
6	125.9	49.1	29.3	294.4	63.2	43.6	287.6	62.6	43.2	105.7	22.6	15.6
7	70.8	24.7	15.1	185.5	40.8	28.1	180.2	39.7	27.4	87.4	20.4	14.1
8	1.7	0.5	0.2	1.8	0.4	0.3	1.9	0.4	0.3	1.3	0.3	0.2
9	25.8	15.2	7.2	39.1	17.0	11.7	47.0	16.5	11.4	43.6	26.0	17.9
10	55.3	8.7	5.8	77.2	16.3	11.3	71.3	15.2	10.5	29.6	5.6	3.9
11	8.9	2.0	1.3	3.6	0.9	0.6	15.1	3.6	2.5	2.1	0.6	0.4
12	50.7	18.7	10.9	102.4	27.0	18.6	114.1	30.4	21.0	65.5	25.0	17.2
13	98.2	43.7	28.2	149.2	37.3	25.7	224.0	59.6	41.1	80.7	26.9	18.5
14	8.4	1.1	0.7	5.2	1.5	1.1	5.2	1.5	1.1	2.5	1.4	1.0
15	54.7	17.2	8.4	136.9	27.5	19.0	153.0	31.5	21.7	69.0	12.5	8.6
16	18.2	4.6	2.7	15.8	3.2	2.2	16.3	3.4	2.3	16.8	3.2	2.2
17	52.3	10.5	7.0	65.8	11.1	7.6	65.7	11.1	7.7	48.5	8.1	5.6
18	176.5	59.3	40.0	76.9	18.3	12.6	273.8	73.5	50.7	59.5	13.2	9.1
19	47.1	11.3	6.6	47.5	8.7	6.0	47.4	8.4	5.8	40.9	6.9	4.7
20	22.3	18.7	11.6	13.8	3.4	2.3	41.9	10.0	6.9	10.3	2.9	2.0
TOTAL	1020	336	207	1530	350	241	1864	445	307	855	226	156

Table VI-2 (continued) - 4

POLYGON NO.	METHOD 13		
	ISO	MONO	
	DAY	DAY	NIGHT
1	71.2	15.7	10.8
2	15.6	4.0	2.8
3	64.3	26.4	18.2
4	39.4	8.7	6.0
5	12.1	2.5	1.7
6	119.8	26.3	18.1
7	86.4	20.3	14.0
8	1.4	0.3	0.2
9	44.2	21.7	15.0
10	30.6	5.9	4.1
11	8.2	2.3	1.6
12	75.3	29.0	20.0
13	120.9	48.5	33.5
14	2.5	1.4	1.0
15	66.5	12.7	8.7
16	17.6	3.3	2.3
17	47.2	7.9	5.4
18	373.6	83.7	57.7
19	42.7	7.0	4.8
20	29.9	8.5	5.9
TOTAL	1270	336	232

a Species with isoprene and sum of monoterpenes emission rates below the detection limit were considered to emit at the detection limit.
b Isoprene
c Sum of selected monoterpenes

C. Methods of Approach for Calculation of Emission Inventory for Naturally Vegetated Region

Cover areas for five vegetative groups (woodland, chamise chaparral, chaparral, sage and grassland) in five naturally vegetated regions in the study area are reported in Tables IV-4 through IV-8 and are the basis for the emission inventory for naturally vegetated regions. The raw data were obtained from the U. S. Forest Service (Section IV-F-1). Emission rates for isoprene and selected monoterpenes and leaf mass constants for the major naturally occurring species were reported in Sections III-D, and V above.

1. Approximations

In this study the dry leaf mass constants were measured in g m^{-3}, based on volume. However, the U. S. Forest Service survey data (see Section IV-F-1) were reported in square kilometers of areal cover, and not volume. To resolve this difference of units, the major naturally occurring species were assigned geometric shapes and size ranges (Table VI-3) gathered from Munz and Keck (1968). Using both upper and lower size limits, two sets of volume to cover area ratios (m^3 m^{-2}) were calculated. These ratios were used to convert leaf mass constants from g m^{-3} to g m^{-2}.

Again the emission rates used in our calculations were corrected to 30°C for day and 25°C for night by the same method used in the urban inventory calculations. Each measurement was corrected for temperature and measurements for the same species were then averaged.

2. Calculations

The main objective was to estimate an upper and lower limit emission inventory. Towards this end, the two sets of adjusted leaf mass constants were associated with two sets of emission rates (μg g^{-1} hr^{-1}). The leaf mass constants based on the lower dimensions of the size range were used, with emission rates of non-emitters (i.e., those species whose emission rates were below the detection limit of the gas chromatographs) being set to zero. The leaf mass constants adjusted by using the upper end of the size range were associated with emission rates where any species emitting below the detection limit was considered to emit at the detection limit.

Table VI-3. Leaf Mass Per Unit Volume to Leaf Mass Per Unit Cover Area Conversion Summary[a]

Species	Leaf Mass Constant g m^{-3}	Shape	Diameter m	Height m	Lower Mass Constant g m^{-2}	Upper Mass Constant g m^{-2}
Adenostoma fasciculatum	140	inverted cone	0.4-3.0	0.5-3.5	23	160
Arctostaphylos glandulosa	2500	cylinder	2.3-4.5	1.5-2.5	3800	6300
Artemesia californica	50	inverted cone	0.4-1.0	0.6-1.5	10	26
Ceanothus crassifolia	280	cylinder	1.4-2.5	2.0-3.5	560	980
Encelia farinosa	180	sphere	0.3-0.8	0.3-0.8	35	93
Eriognum fasciculatum	340	hemisphere	1.2-2.4	0.6-1.2	140	270
Quercus dumosa	200	sphere	1.0-3.0	1.0-3.0	37[a]	91[b]
Rhamnus crocea	150	cylinder	0.8-1.5	1.0-2.0	150	300
Rhus ovata	200	sphere	1.5-3.0	1.5-3.0	200	400
Salvia mellifera	300	sphere	1.0-2.0	1.0-2.0	200	410

[a]Shapes, diameters and heights were obtained from Munz and Keck (1968).
[b]Riggan and Lopez (1981).

The leaf mass attributed to each species was taken as the product of cover area and the converted leaf mass constants ($\mu g\ m^{-2}$). The emission of these major species ($g\ hr^{-1}$) was the product of the leaf mass and emission rate ($\mu g\ g^{-1}\ hr^{-1}$). Emissions from species in the same vegetative group were added together. As with the calculations of the urban region, the observed species were divided into "knowns" for which both experimentally measured emission rates and leaf mass constants were known along with cover areas, and "unknowns" for which only cover areas were known. The cover areas of our known species accounted for most of the natural study area. To normalize the emissions of "knowns" to the complete natural vegetation study area, the emissions of each vegetative group were multiplied by the ratio of the imagery cover area of the group (Section IV) to the cover area of the knowns in the group. The results are listed in Tables VI-4 and VI-5.

D. Total Emission Inventory for the Entire Study Area

In the final step, an estimate for the emission in the entire study area was obtained for a summer day. For the purposes of this inventory, $30^{o}C$ was chosen as a daytime temperature and applied to emissions of both isoprene and the monoterpenes. The nighttime temperature was taken as $25^{o}C$ for emission of selected monoterpenes only. We considered a day with 15 hours of light and 9 hours of darkness (which is appropriate for the summer solstice at 34^{o} N).

Daytime isoprene and monoterpene emissions ($kg\ hr^{-1}$) were multiplied by 15 hours and summed with the nighttime monoterpene emissions multiplied by 9 hours. This was done for all 13 of the methods described above. The results are kg of hydrocarbons per day. For purposes of comparison with anthropogenic ROG emissions these data were also converted to tons. Table VI-6 summarizes the total emissions of isoprene and monoterpenes from the urban study area in tons per day for each of the calculation methods. Note that the emissions labeled 1 to 13 are for the urban region, and Naturals refers to the naturally vegetated region.

The values listed in Table VI-6 were obtained by assuming that the emission rates were zero when no emissions were observed above the detection limit of the gas chromatographs. The values listed for Naturals were based on the lower limit for dimensions in the leaf mass constant

Table VI-4. Emission Inventory for Naturally Vegetated Regions: Lower Limits (kg hr^{-1})[a,b]

Vegetation Group	Isoprene Day	Sum of Monoterpenes Day	Sum of Monoterpenes Night
Chaparral	200	6	4
Woodland	22	0	0
Sage	41	263	182
Chamise Chaparral	29	127	88
Grassland	0	0	0
Total	292	396	274

[a]Species emitting below detection limits were considered non-emitters.
[b]15 hour daylight at 30°C, 9 hour dark at 25°C.

Table VI-5. Emission Inventory for Naturally Vegetated Regions: Upper Limits (kg hr^{-1})[a,b]

Vegetation Type	Isoprene Day	Sum of Monoterpenes Day	Sum of Monoterpenes Night
Chaparral	456	194	134
Woodland	72	32	22
Sage	289	559	386
Chamise Chaparral	426	540	373
Grassland	16	16	11
Total	1259	1341	926

[a]Species emitting below detection limits were considered to emit at the detection limit.
[b]15 hour daylight at 30°C, 9 hour dark at 25°C.

adjustment. Combining the lowest estimate for the urban region with the estimate for the naturally vegetated region yields a total of 22 tons day^{-1}. The highest estimate for the urban region, when combined with the estimate for the natural region yields, a grand total of 38 tons day^{-1}.

A simple average of the highest and lowest values is 30 tons day^{-1} with a range of ±8 tons day^{-1}. A better total emissions value is probably obtained by adding the average of the totals for Methods 1-3 to the

Table VI-6. Summary of Emission Inventory for Study Area in Tons Per Day: Lower Limits[a,b]

Method	Isoprene	Monoterpenes[c] (tons per day)	Total
Based on Aerial Imagery and Ground Survey Data			
1	8.2	3.6	11.8
2	7.5	3.8	11.3
3	8.4	2.9	11.3
Based on Ground Survey Data Only			
4	6.0	1.7	7.7
5	6.2	2.9	9.1
6	9.4	1.9	11.4
7	10.8	3.4	14.2
8	8.5	1.9	10.4
9	10.5	3.5	14.0
10	17.8	2.7	20.5
11	20.5	3.3	23.8
12	9.8	2.9	12.7
13	14.2	4.1	18.3
Naturals	4.8	9.3	14.1

[a]Species with emission rates below the detection limit were considered to be non-emitters.
[b]15 hour daylight at 30°C, 9 hour dark at 25°C.
[c]Sum of selected monoterpenes.

Naturals total; this gives 26 tons day^{-1}. Methods 1-3 were based only on aerial imagery data, which covered a much larger sample of urban vegetation than the field survey data used in the remaining calculations, and the good agreement for the three different methods suggests that a higher level of confidence may be placed on this result.

Table VI-7 gives results from calculations where those species showing no measurable emissions were considered to emit at the detection limit of the gas chromatographic analyses (rather than zero), and the values for Naturals were based on the upper limit of size dimensions. Again, combining the lowest estimate for the urban region with the estimate for the naturally vegetated region yields a total of 67 tons day^{-1}. When the highest estimate for the urban region is combined with the total for

Table VI-7. Summary of Emission Inventory for Study Area in Tons Per Day: Upper Limits[a,b]

Method	Isoprene	Monoterpenes[c]	Total
Based on Aerial Imagery and Ground Survey Data			
1	14.5	7.7	22.2
2	13.6	7.3	20.9
3	14.4	6.9	21.3
Based on Ground Survey Data Only			
4	10.3	4.8	15.1
5	10.9	5.9	16.8
6	15.3	6.2	21.5
7	18.3	8.2	26.5
8	13.6	5.6	19.1
9	16.8	7.6	24.4
10	25.3	8.2	33.4
11	30.8	10.4	41.2
12	14.1	5.3	19.4
13	20.9	7.8	28.7
Naturals	20.8	31.3	52.1

[a]Species with emission rates below the detection limit were considered to emit at the detection limit.
[b]15 hour daylight at 30°C, 9 hour dark at 25°C.
[c]Sum of selected monoterpenes.

Naturals, a value of 93 tons day^{-1} is obtained. A simple average of the upper and lower values results in emissions of 80 tons day^{-1} with a range of ±13 tons day^{-1}. Taking the averge of Methods 1-3 (as above) and adding it to the total for Naturals yields a value of 74 tons day^{-1}.

In summary, the results from this study suggest that total daily emissions of isoprene and the monoterpenes in the study area are in the range of ~25 to ~80 tons. This can be compared to the total daily (i.e., average summer weekday) emissions of ROG from anthropogenic sources in the study area of ~1200 tons (SCAQMD/SCAG 1982a). It is recommended that those interested in modeling the impacts of isoprene and monoterpene emissions from vegetation on photochemical air pollution in the CSCAB investigate the effects of such emissions over the range from 25 to 80 tons day^{-1}.

VII. MEASUREMENTS OF AMBIENT CONCENTRATIONS OF ISOPRENE AND SELECTED MONOTERPENES

A. Introduction and Background

As discussed in Section II, isoprene and the monoterpenes, as well as oxygenated organics, have been observed in a variety of locations and above a variety of vegetative canopies, generally at very low concentrations. Average isoprene concentrations have ranged from 0.1 ppbC for a pine forest to 10 ppbC for an oak forest, while average monoterpene concentrations have ranged from below detection limits in many locations to as high as 24 ppbC in a coniferous forest in Norway (Tingey and Burns 1980).

Lonneman et al. (1978) conducted a three-day study in the St. Petersburg/Tampa, Everglades and Miami areas and collected samples within inches of citrus trees as well as in remote areas. No significant natural hydrocarbon contribution was observed in any of the collected samples and the monoterpene concentrations were below the limit of detectability (1 ppbC). Holdren and co-workers (1979) carried out a study over a period of ten months using gas chromatography/mass spectrometric analysis of monoterpenes collected by either cryogenic or solid adsorbent-Tenax techniques in a rural forested site in north central Idaho. Concentrations of the monoterpenes varied considerably depending upon location within the forest canopy, but the concentration of individual species never exceeded 10 ppbC during the 10-month sampling period, and total monoterpene concentrations for all samples fell in the range of 0.5-16 ppbC.

A summary of measurements of biogenic hydrocarbon concentrations in ambient air has been given by Arnts and Meeks (1980). They concluded that non-methane hydrocarbons in rural and remote areas consist mainly of anthropogenic species and that biogenically related compounds (i.e., monoterpenes and isoprene) generally constitute less than 10% of the total concentration.

Tingey and co-workers have investigated the dependence of ambient concentrations of natural organics on emission rates, mixing height and reaction conditions (i.e., dark vs light). Peterson and Tingey (1980) used a box model to estimate ambient air concentrations of isoprene and monoterpenes. The predicted isoprene concentrations increased during the

daylight hours, reached a maximum at midafternoon and then decreased to zero during the early evening when isoprene emissions ceased. Despite the fact that monoterpene emissions were at a maximum during midday, predicted ambient monoterpene concentrations were lowest because of atmospheric dilution, photooxidation and ozonolysis. In contrast, monoterpene concentrations were the highest during the evening and early morning hours because monoterpenes are emitted at night when atmospheric mixing is low and hydrocarbon reactions are slow. This predicted monoterpene profile has been verified by field measurements (Arnts and Gay 1979).

In summary, most investigators have reported very low ambient concentrations of natural organics, whether in rural/remote vegetative canopies or suburban/urban areas. Values observed typically range from below the detection limits (~0.1-1 ppbC) to ~5-10 ppbC. Only rarely have values as high as several tens of ppbC been reported. Dimitriades (1981) and others (Bufalini and Arnts 1981) have discussed the apparent conflict between the low ambient concentrations observed in such studies and the substantial emission rates estimated for the natural hydrocarbons over vegetative canopies (see Section II).

In the present study, our objective was to obtain a limited amount of data concerning the ambient concentrations of isoprene and the monoterpenes in the study area. These data were intended to complement the determinations of the source strength of emissions of these compounds from vegetation and to provide further information relevant to the apparent discrepancies in many previous studies between estimated emissions and ambient concentrations of naturally emitted hydrocarbons.

In order to accomplish this, ambient concentrations of isoprene and selected monoterpenes were measured at three representative urban locations in the study area. Ambient air samples were taken near dawn, before emissions from the morning traffic peak would adversely impact hydrocarbon analyses. Samples collected simultaneously were sent to Environmental Design Consultants (EDC) of Pullman Washington (headed by Dr. Dagmar Cronn) for independent analysis.

B. Methods of Approach

The capillary-column gas chromatograph used for the emission rate studies was employed for these analyses. This system is described in

detail in Section III. The detection limit was dependent on the background chromatograms obtained with ultra-pure air, which generally showed small but variable traces of contamination. Normally, any response greater than several ppbC could be construed as a meaningful measurement. A 100 mℓ all-glass syringe was used for sampling to facilitate transfer to the loop. A Varian 1400 gas chromatograph with an OV-101 packed column was also utilized in this study (as described in Section III).

Three sampling canisters were purchased from D & S Instrument (DSI) Ltd. of Pullman, WA. These were stainless steel electro-polished (Summa polished) vessels (6 ℓ) specifically developed for the collection and storage of trace atmospheric gases. The vessels were first tested for hydrocarbon contamination by filling them with zero air and obtaining a chromatographic sample. The canisters were then spiked with a 25 hydrocarbon stock mixture to a nominal level of 25 ppbC. Concentrations were measured immediately and then again several hours later. The results are shown in Table VII-1. Losses of the monoterpenes over periods of less than 6 hours were generally no more than 30% and may well be within the analytical uncertainties at the low concentrations employed. Thus, provided analyses were carried out within ~6 hrs or less, reliable data could be obtained for isoprene and the monoterpenes.

Interlaboratory assessments of accuracy and precision were made on two of the sampling dates by quantitatively dosing EDC canisters with hydrocarbons and backfilling with ultra-zero grade air. Preparation of these samples was done on a "blind" basis by SAPRC technicians not affiliated with this study. These dosed canisters were then analyzed out in the field by the SAPRC personnel working on this program, and then immediately shipped to the EDC group.

The "blind" samples were prepared as follows. The hydrocarbons were added in two steps. First, aliquots were injected into a 46.15 ℓ glass bottle and allowed to mix for 1 hr. Then a portion of this (100 mℓ) was added to a DSI canister and pressurized to ~18 psi. The "high" concentration (ppm levels) in the 46.15 ℓ glass bulb was measured by gas chromatography. Thus, the final concentrations could be derived strictly from the magnitude of each dilution step or from the concentrations measured in the

Table VII-1. Stability of Hydrocarbons in Dosed Stainless Steel Canisters

Compound	Canister 1			Canister 2[a]			Canister 3		
	Conc T=0 hr ppbC	Conc T=4 ppbC	Conc T=4 hr / Conc T=0 hr	Area Units T=0 hr	Area Units T=6 hr	Area Units T=6 hr / Area Units T=0 hr	Conc T=0 hr ppbC	Conc T=3 hr ppbC	Conc T=3 hr / Conc T=0 hr
Isoprene	18.8	23.5	1.25	276	261	0.95	-	-	-
α-Pinene	24.5	21.5	0.88	377	351	0.93	27.8	23.5	0.84
β-Pinene	25.1	20.0	0.80	418	345	0.83	26.9	20.0	0.75
Myrcene	24.0	13.3	0.55	264	186	0.71	19.1	13.1	0.69
Δ^3-Carene	26.4	20.5	0.78	295	299	1.01	29.7	22.1	0.74
p-Cymene	29.4	20.3	0.69	456	367	0.81	27.9	19.0	0.68
d-Limonene	27.6	21.2	0.77	478	384	0.80	27.2	21.9	0.81
N-Hexane	19.2	18.8	0.98	284	288	1.01	25.1	20.7	0.83
Benzene	21.9	24.4	1.12	243	314	1.29	28.7	26.8	0.93
N-Heptane	46.0	39.5	0.86	264	262	0.99	51.1	39.9	0.78
Methylcyclohexane	22.6	24.8	1.10	299	286	0.96	30.3	25.1	0.83
Toluene	86.0	65.9	0.77	427	475	1.11	83.5	75.1	0.90
N-Octane	17.1	19.7	1.15	285	268	0.94	23.0	20.8	0.90
Ethylbenzene	23.1	21.0	0.91	314	290	0.92	26.4	20.7	0.79
m-Xylene	26.6	23.8	0.89	412	410	1.00	29.3	25.9	0.88
o-Xylene	22.2	21.9	0.99	397	402	1.01	26.2	22.5	0.86
N-Nonane	18.6	18.1	0.98	297	295	0.99	21.9	18.7	0.85
Isopropylbenzene	24.2	21.8	0.90	404	355	0.88	27.1	22.5	0.83
N-Propylbenzene	24.4	20.8	0.85	373	324	0.87	25.7	21.3	0.83
1,2,4-Trimethylbenzene	28.3	23.6	0.84	439	545	1.24	27.9	24.9	0.89
N-Decane	24.2	18.4	0.76	382	365	0.96	23.8	19.0	0.80
N-Undecane	31.4	20.4	0.65	644	455	0.71	28.5	19.4	0.68
N-Dodecane	26.4	19.4	0.73	992	654	0.66	26.3	17.6	0.67
N-Tridecane	27.9	24.9	0.89	986	462	0.47	29.6	20.3	0.68
N-Tetradecane	27.0	23.4	0.87	272	166	0.61	30.4	24.5	0.81
N-Pentadecane	11.8	12.5	1.06	b	b	b	7.1	15.3	2.15

[a]Instrument was not calibrated, initial concentrations are approximately 25 ppbC.
[b]Not reported.
(-) Not observed at detection limit (1-5 ppbC).

first step and the final dilution ratio. Both calculations resulted in similar values, and those reported are the average of the two.

The results of two of these intercomparisons are shown in Tables VII-2 and VII-3. The second experiment also included another independent analysis at UCR by the SAPRC personnel who prepared the samples. In both cases, the UCR measurements were made the day the canisters were prepared while those of EDC were made several days later, due to delays in either shipping or analyses.

In addition to a substantial scatter in the data, the intercomparisons indicated that the EDC canisters did not store certain hydrocarbons at the ppbC level over the timescale of collection and analysis at EDC.

Table VII-2. Results of Interlaboratory Analyses of Hydrocarbon Dosed Canister #293 (Concentrations in ppbC)

Compound	Calculated Concentration[a]	SAPRC[b]	EDC[c]
Isoprene	250	210	202.7
Cyclohexane	37	-	6.6
n-Heptane	46	64	21.6
Methylcyclohexane	28	20	6.5
Toluene	71	93	43.2
n-Octane	31	23	21.1
p- and m-Xylene	53	50	35.1
n-Nonane	49	33	36.0
α-Pinene	82[d]	8	27.3
Isopropylbenzene	e	-	5.3
Myrcene	e	-	23.5
n-Decane	41	21	f
d-Limonene	65	40	f
Unknown			1.6
Unknown			4.1
Unknown			5.3
o-Xylene	e		1.0

[a]Average value, see text.
[b]Analyses done by the field personnel on this program.
[c]Analyzed four days later (9/28/81).
[d]Dilution calculation only.
[e]Not added.
[f]Not reported.
(-) Not observed at detection limit (1-5 ppbC).

Table VII-3. Results of Interlaboratory Analyses of Hydrocarbon-Dosed Canister #264 (Concentrations in ppbC)

Compound	Calculated Concentration[a]	SAPRC (In Field)	EDC[b]	SAPRC (At UCR)
Isoprene	36	36	24.3	47
n-Heptane	27	29	22.3	38
Methylcyclohexane	23	28	15.3	26
Toluene	42	23	18.1	53
n-Octane	32	25	17.3	47
o-Xylene	35	9	3.2	27
n-Nonane	37	13	4.5	42
α-Pinene	28	-	0.4	6
β-Pinene	36	-	c	-
Myrcene	d	-	0.4	
n-Decane	34	-		32
d-Limonene	d	e	c	e
Unknown		113	2.7	
Unknown		3.8		
Unknown		1069		

[a]Average value, see text.
[b]Analyzed three days later (10/8/81).
[c]Not reported.
[d]Not added.
[e]Peak at correct retention times.

This was particularly true of the monoterpenes associated with vegetative emissions. There were also problems in peak identifications (EDC saw a substantial level of myrcene when none was added or observed by UCR) as well as large unknown peaks which did not correspond to hydrocarbons added or substantiated by the other analyses. It was concluded that the stainless steel storage canisters were useful for a number of the monoterpenes only if analyses could be performed within a few hours.

Samples were taken simultaneously at the three locations using the stainless steel canisters. A metal bellows pump, which had previously been cleaned with dichloromethane and thoroughly dried, was used to fill the sampling canisters. A canister was attached to the pump and purged for 10 min, at which time the outlet valve was closed for the next 5 min to pressurize the canister. The inlet valve was then closed to seal the canister. Samples were obtained for analysis using a 100 mℓ all-glass

syringe attached to the outlet. Canisters supplied by the EDC group were purged and filled in the same manner. At each site, UCR and EDC canisters were filled with ambient air, one immediately after the other. The contents of all canisters were analyzed at UCR, and then the EDC vessels were shipped via air freight for same-day delivery.

The sampling locations were chosen to be representative of the urban portion of the study area and in close proximity to both a field sample plot (employed as described in Sections IV and V) and a South Coast Air Quality Management District (SCAQMD) air monitoring station. The three locations and the rationale behind their choice are listed below:

La Habra Heights (Near Intersection of Solejar and West Roads). This was a mid-airshed location reasonably distant from vehicular emissions. The immediate vicinity consisted of low density residential housing and open, grassy fields. This site was expected to exhibit "maximum" vegetative hydrocarbon emissions for this particular area. The SCAQMD air quality monitoring station was located several kilometers away.

Beverly Hills (Near Intersection of Canon and Lamita Avenues). This site was located at Will Rogers Memorial Park in the midst of low density housing with very heavy ornamental vegetation. This site was in close proximity to canyons in the Santa Monica mountains, from which drainage occurs at night (possibly carrying accumulated emissions from natural vegetation).

Azusa (Near Intersection of Dalton and Sierra Madre Avenues). This site, located at Laura Jones Park, was chosen because it is at the base of a large canyon extending far into the San Gabriel mountains. Again, nocturnal drainage, carrying vegetative hydrocarbons from the mountains, was possible. In addition, there was a substantial amount of medium-density housing with associated ornamental plants typical of the CSCAB.

C. Results From Simultaneous Ambient Air Collections at Selected CSCAB Sites

A trial collection of simultaneous ambient air samples was conducted on August 7, 1981, using the protocol described above. The EDC canisters were analyzed at UCR within four hours, then air-freighted to Washington and analyzed by the EDC group within 33 hours of collection. The UCR canisters were analyzed four to eight hours after the collection. Results

from the UCR analyses showed large and variable background peaks due to difficulties with the gas chromatograph used during this experiment. No isoprene or monoterpenes were found in the EDC analyses. This indicated either loss of these compounds in the EDC canisters or their absence in the collected air samples. Based on the results of the dosed-canister studies described earlier neither possibility can be ruled out.

Another sampling episode was conducted on September 24, 1981 after installation of a new GC column. Early morning samples were obtained using the same protocol as for the previous episode. Due to circumstances beyond their control, the EDC group was unable to start their analyses for several days after the arrival of the canisters; therefore the decision was made not to do the analyses. The UCR analyses were conducted within 8 hours of the time the samples were collected. Specifically, the EDC and UCR canisters for La Habra Heights, Beverly Hills and Azusa were analyzed at 1, 2 and 3 hours and 6, 7 and 8 hours elapsed time, respectively. Prior to injection, 70 mℓ samples from the UCR canisters were syringe-diluted with 30 mℓ of ultra-zero air to minimize the possibility of water freezing at the head of the column.

The results obtained by the UCR group are shown in Table VII-4. Since isoprene was observed at comparable concentrations using two independent gas chromatographs and sample syringes, the measurements are considered to be reliable. No myrcene was detected, but ~9 ppbC d-limonene was observed in each of the UCR canisters while only 1 ppbC was observed in the EDC canisters. This may have been due to previous stability experiments involving d-limonene in the UCR canisters. Agreement between the UCR and EDC canisters was fair to good for most anthropogenic compounds, considering the interval between sample collection.

This study was repeated on October 6, 1981. The resulting data are shown in Table VII-5. Only one UCR canister was analyzed since it was felt that duplicate consecutive samples were not generating any additional useful information. The three EDC canisters collected at La Habra Heights, Beverly Hills and Azusa were analyzed at UCR within 3 hours of collection. They were then air-freighted to Washington where they were analyzed 50-55 hours after collection. The UCR canister filled at Azusa was analyzed 4 hours after sample collection.

Table VII-4. Hydrocarbon Analyses of Ambient Air Simultaneously Collected at Three Selected CSCAB Sites, September 24, 1981 (Concentrations are in ppbC)

Compound	La Habra Heights		Beverly Hills		Azusa	
	EDC Canister UCR	UCR Canister UCR	EDC Canister UCR	UCR Canister UCR	EDC Canister UCR	UCR Canister UCR
Isoprene[a]	11	12	7	10	11	14
α-Pinene	-	-	-	-	-	2
β-Pinene	-	-	-	-	-	-
Myrcene	-	-	-	-	-	-
Δ^3-Carene	-	-	-	-	-	-
p-Cymene	-	-	-	-	-	-
d-Limonene	1	9	1	9	1	10
N-Hexane	10	10	9	8	10	7
Benzene	18	13	9	12	14	74
N-Heptane	11	6	9	6	2	3
Methylcyclohexane	10	14	5	23	7	23
Toluene	26	29	22	30	27	28
N-Octane	2	1	1	2	16	< >
Ethylbenzene	2	6	2	3	4	4
m- and p-Xylene	6	16	7	7	12	6
o-Xylene	2	2	2	< >	3	1
N-Nonane	2	4	1	3	2	3
Isopropylbenzene	-	-	-	-	-	-
N-Propylbenzene	-	3	1	2	2	1
1,2,4-Trimethylbenzene	2	3	1	0	3	1
N-Decane	0	4	1	2	6	1
N-Undecane	1	10	1	7	1	7
N-Dodecane	< >	1	0	0	< >	1
N-Tridecane	< >	< >	< >	< >	0	0
N-Tetradecane	1	9	2	10	< >	8.4
N-Pentadecane	< >	< >	< >	< >	< >	< >
Unknown	18	62	8			
Unknown			25			

[a]The value was an average from two separate GC instruments.
(-) Not observed at detection limit (1-5 ppbC).
< > Values were negative after subtracting the blank.

Table VII-5. Hydrocarbon Analyses of Ambient Air Simultaneously Collected at Three Selected CSCAB Sites, October 6, 1981 (Concentrations are in ppbC)

Compound	La Habra Heights		Beverly Hills		Azusa		
	EDC Canister		EDC Canister		EDC Canister		UCR Canister
	EDC	UCR	EDC	UCR	EDC	UCR	UCR
Isoprene[a]	0.4	28	0.8	15	-	4	-
α-Pinene	8.1	-	1.8	2.5	-	-	-
β-Pinene	-	-	-	-	-	-	-
Myrcene	-	-	-	-	-	-	-
Δ^3-Carene	-	-	-	-	-	-	-
p-Cymene	-	-	-	-	-	-	-
d-Limonene	-	3	-	< >	-	< >	< >
N-Hexane	9.6	26	6.6	12	1.6	3	3
Benzene	20.3	44	11.8	19	3.0	3	4
N-Heptane	5.9	12	4.0	3	0.9	< >	< >
Methylcyclohexane	7.6	< >	4.8	17	1.0	8	< >
Toluene	37.7	67	31.3	42	5.9	2	6
N-Octane	2.8	1	1.7	2	0.2	0	< >
Ethylbenzene	29.1	6	5.5	5	1.0	1	0
m- and p-Xylene	25.1	24	19.3	20	2.7	2	2
o-Xylene	9.2	8	8.0	8	1.2	1	1
N-Nonane	2.0	3	0.9	2	-	2	-
Isopropylbenzene	-	-	-	-	-	-	-
N-Propylbenzene	-	3	-	2	-	-	-
1,2,4-Trimethylbenzene	16	5	7.3	6	-	1	0
N-Decane	-	< >	-	< >	-	< >	< >
N-Undecane	-	< >	-	< >	-	< >	< >
N-Dodecane	-	0	-	0	-	1	0
N-Tridecane	-	0	-	2	-	< >	2
N-Tetradecane	-	< >	-	0	-	< >	< >
N-Pentadecane	-	< >	-	< >	-	3	< >
Unknown	141[b]	16	30.2[b]	6	59.1[b]		
Unknown		23		21			
Unknown		74		7			

[a]At UCR the value was the average from two separate GC instruments.
[b]Total of unidentified compounds.
(-) Not observed at detection limit (1-5 ppbC).
< > Values were negative after subtracting the blank.

Significant amounts of isoprene were again observed by UCR, but only traces were found by the EDC group. This may be due to isoprene decomposition in the sampling vessels since the EDC analyses were done 50 to 55 hours after collection. Small amounts of α-pinene were seen by both laboratories in the Beverly Hills sample; this represented the only corroborated monoterpene appearance during two sampling episodes. The small amount of d-limonene detected by UCR in the La Habra Heights canister was probably an artifact. Agreement between the two laboratories on other hydrocarbons was better than in the first comparison but differences above 50% were still observed. Some of these differences may also be attributed to hydrocarbon loss in the EDC canisters (particularly for the aromatics).

From these ambient measurements we conclude that while measurable amounts of isoprene can be observed (a significant contribution from anthropogenic sources cannot be ruled out), ambient concentrations of the monoterpenes are usually less than 1 ppbC. We further conclude that ambient measurements in additional CSCAB sites would probably not show higher concentrations, since the widely separated sites used in this study were chosen to maximize these concentrations.

The present data were consistent with measurements by previous workers showing that, at least for the monoterpenes, ambient concentrations are low. Our experimental ambient measurements for the monoterpenes are also consistent with the ambient concentrations of monoterpenes ($\lesssim$1 ppbC) predicted by simplified computer model simulations and for isoprene our experimental data were somewhat higher, but in the range of the model simulations ($\sim$1-3 ppbC) (Carter 1982).

VIII. IMPLICATIONS FOR PHOTOCHEMICAL OZONE FORMATION IN THE CALIFORNIA SOUTH COAST AIR BASIN

A. Introduction

The isoprene and monoterpene emissions data obtained in this study will be made available in a format consistent with the UTM grid system used for the ARB/SCAQMD anthropogenic ROG emission inventory prepared for the 1982 AQMP revision. Thus, they can be used as input data for urban airshed model calculations (see Appendix D) designed to estimate the extent to which ROG emissions from vegetation contribute to the photochemical oxidant problem in the California South Coast Air Basin. Such models have varying degrees of complexity. These include (a) airshed grid models such as those developed by Systems Applications Incorporated (Reynolds et al. 1979) and researchers at the California Institute of Technology (McCrae et al. 1982), which require basin-wide time-dependent emissions and meteorological data as well as large computing resources; (b) trajectory models (Lloyd et al. 1979, Chock et al. 1981); (c) more approximate "EKMA" (Empirical Kinetic Modeling Approach) type trajectory or box models (U.S. EPA 1977, 1978); and (d) simplistic box or linear rollback models. Although a comprehensive grid or trajectory modeling study was clearly beyond the scope of this program, estimates of the magnitude of the contribution of vegetative emissions were made using a more approximate approach. This is briefly discussed in this section.

B. Methods of Approach and Results

The simplest approach currently employed which incorporates effects of chemistry in estimates of the effects of hydrocarbon emissions on O_3 formation is the "EKMA" technique. This involves analyses of O_3 isopleth plots produced by floating "box"-type photochemical model calculations, and is discussed in more detail elsewhere (U.S. EPA 1977, 1978, Dodge 1977a,b, Dimitriades 1977, Whitten and Hogo 1978). Briefly this approach involves the following steps: (1) A photochemical hydrocarbon-NO_x-air mechanism is "validated" by comparing its predictions of O_3 yields against those observed for hydrocarbon-NO_x-air mixtures irradiated in environmental chambers (where the hydrocarbons in such experiments are chosen to represent as closely as possible, in both reactivity and chemical

composition, those emitted in urban atmospheres). (2) This mechanism is modified by removing provisions for chamber effects and incorporating mixing height variations and diurnally varying photolysis rates appropriate for the latitude and season for the airshed of interest (in this case, Los Angeles on the summer solstice). (3) Isopleth plots of maximum one-day O_3 yields as a function of varying initial NO_x and hydrocarbon levels are calculated (see Figure VIII-1 for an example of such a plot). (4) Using a hydrocarbon/NO_x ratio and an O_3 level considered representative of pollution episodes in the airshed, a point on the plot considered to be characteristic of the airshed at the present time is obtained (that point being the intersection of the line defined by the assumed hydrocarbon/NO_x ratio and the isopleth curve for the representative O_3 level). (5) The effects of relative changes of hydrocarbon and/or NO_x emissions are estimated by determining that O_3 level predicted on the isopleth plot if the hydrocarbon and/or NO_x levels are changed by a corresponding (relative) amount from the point assumed to represent the current situation.

As an example of this approach, Figure VIII-1 shows the point corresponding to an O_3 level of 0.3 ppm (typical of many CSCAB air pollution episodes) and an assumed (arbitrarily chosen) HC/NO_x ratio of 8. This point corresponds to an initial hydrocarbon level of ~1.1 ppmC and an initial NO_x level of ~0.13 ppm. Thus if one wanted to calculate the effect of a 10% increase in hydrocarbon concentration one would calculate the O_3 level predicted with the hydrocarbon level increased from ~1.1 ppmC to 1.2 ppmC. In this case an O_3 yield of 0.33 ppm is obtained - an approximate 10% increase.

If we restrict our consideration to relatively small percentage increases ($\lesssim$~20%) in total hydrocarbon emissions (as is the case when considering the effect of adding isoprene and monoterpene emissions to total anthropogenic ROG emissions in the study area), then it can be shown that the change in O_3 predicted by this type of EKMA analysis is approximately proportional to the increases in hydrocarbon levels. The specific proportionality constant depends on the HC/NO_x ratio and the O_3 level assumed to be characteristic of the particular airshed in question.

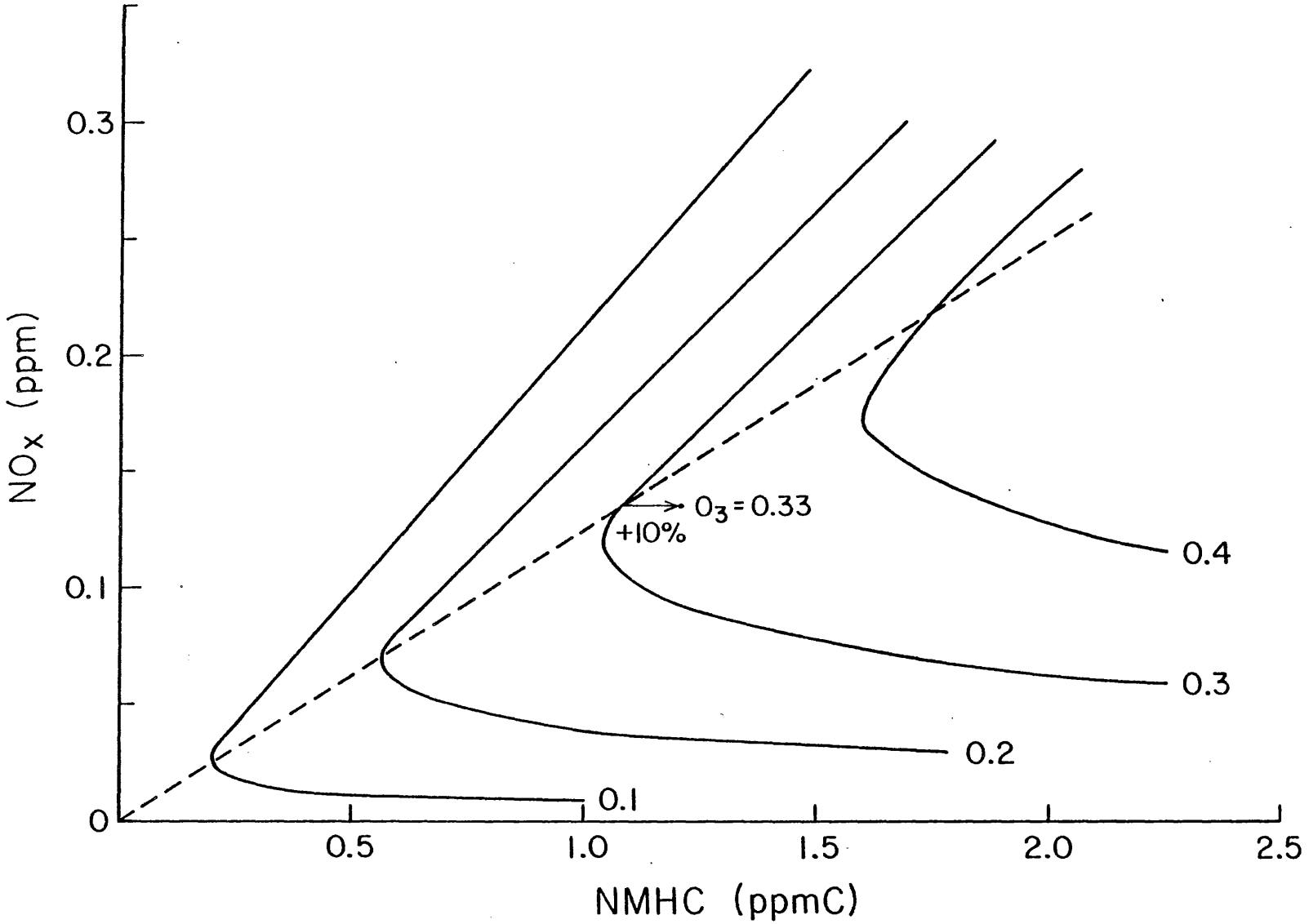

Figure VIII-1. Isopleth plots for O_3 = 0.1, 0.2, 0.3 and 0.4 ppm calculated using the SAPRC EKMA model. ---- line for $NMHC/NO_x$ = 8.

This can be expressed by the following formula,

$$\frac{\Delta O_3}{O_3} = f(HC/NO_x,\ O_3)\ \frac{\Delta HC}{HC} \qquad (I)$$

where $(\Delta O_3/O_3)$ is the fractional change in O_3 levels resulting from a fractional change of hydrocarbon levels given by $(\Delta HC/HC)$. This approach ignores chemical differences between biogenic and anthropogenic organics, as well as meteorological, topographical and spatial factors. Thus, in this case, $(\Delta HC/HC)$ represents the fraction of total hydrocarbon emissions which come from vegetation and $\Delta O_3/O_3$ is the fraction of the O_3 formed which results from those emissions.

Based on the emissions inventory compiled by the South Coast Air Quality Management District and by the California Air Resources Board for use in detailed airshed calculations for the CSCAB (SCAQMD/SCAG 1982a), total emissions of all classes of reactive organics from anthropogenic sources (on an average summer day) in our study area amount to ~1200 tons day^{-1} (i.e., 69.4% of 1693 tons day^{-1} = 1175 tons day^{-1}). In comparison, for the summer solstice, assuming the average temperature is 30°C during the day and 25°C at night, the best estimate of hydrocarbon emissions from vegetation obtained in this study amounted to ~30 tons day^{-1} of isoprene and monoterpenes (i.e., about 2.5% of total ROG emissions), and the best estimate of the upper limit (or "detection level" limit - see Chapter VI) for emissions for the same day are ~80 tons day^{-1}, or ~6% of the total ROG emissions. The "worst case" upper limit value obtained was 93 tons day^{-1}, or ~7% of total (i.e., anthropogenic plus vegetation) ROG in the study area. Thus with a knowledge of the proportionality factor, f, the effect of increased hydrocarbon emissions, or the impact of emissions from a particular source (such as vegetation) on O_3 formation can be estimated.

Two different kinetic mechanisms and representations of reactive organics, designated models "E" and "S" in the subsequent discussion, were used to derive the proportionality factor for equation (I). Model "E" is the standard EPA propene-butane model (Dodge 1977a,b) which was tested with irradiated auto exhaust smog chamber data (Dimitriades 1970, 1972). This model is of interest because until recently it has been the basis of

essentially all EKMA analyses conducted by the EPA. It is still incorporated in the lowest level of the current EKMA modeling option available to regulatory officials concerned with developing air quality management plans and state implementation plans for achieving federally-mandated air quality standards. The major disadvantage of this Level III EKMA approach is that it is based on an outdated chemical mechanism which is known to be inaccurate in a number of significant details (Pitts et al. 1980, Carter et al. 1982, Hov and Derwent 1981).

Model "S" incorporates a propene-butane mechanism similar to, but updated (Atkinson and Lloyd 1983) from, that developed by Carter et al. (1979). This mechanism is consistent with current laboratory data concerning the propene/butane/NO_x photooxidation mechanism (Atkinson and Lloyd 1983). The propene-butane levels were chosen such that the model could simulate O_3 formation observed in SAPRC glass-chamber NO_x-photooxidation experiments, which employed a hydrocarbon mix designed as a "surrogate" for the Los Angeles atmospheric hydrocarbon mix (Pitts et al. 1975, 1976). The original mechanism of Carter et al. (1979) was validated against SAPRC "surrogate" hydrocarbon chamber data (Carter et al. 1982) and has been used as a basis for our studies of the effects on EKMA predictions of varying kinetic mechanisms and hydrocarbon representations (Carter et al. 1982). With minor corrections in certain rate constants, this mechanism was also used to investigate the effects on EKMA predictions of initially-present HONO (Harris et al. 1982). In a further study, portions of the propene photooxidation mechanism dealing with reactions subsequent to the OH-propene and O_3-propene reactions were updated (Atkinson et al. 1982a). This model was then used to investigate the effects of other atmospheric radical sources on EKMA predictions (Carter 1981). It should be noted that this most recent version of the propene-butane model, which was used to calculate the O_3 isopleths shown in Figure VIII-1, yields essentially identical predictions to the original propene-butane mechanism of Carter et al. (1979).

The differences between the two models, "E" and "S", used in the present analysis are summarized in Table VIII-1. Other than the kinetic mechanism and the hydrocarbon representation, the conditions employed in the EKMA simulations with the two models were the same: calculations were performed using diurnally varying photolysis rates with known chamber

Table VIII-1. Differences between Models used for EKMA Simulations

	Model "E"	Model "S"
CHEMICAL MECHANISM	Durbin et al. (1975); Dodge (1977a), not updated. "1974 chemistry"	Carter et al. (1979) Updated based on Atkinson and Lloyd (1983) "1982 chemistry"
HYDROCARBON REPRESENTATION (ppb/ppmC NMHC, nominal)		
n-Butane	188	172
Propene	83	60
Formaldehyde	20	26
Acetaldehyde	15	0
CO	0	2200
VALIDATION DATA BASE	Bureau of Mines data from irradiation of auto exhaust (Dimitriades 1970, 1972)	SAPRC data from irradiation of "surrogate" HC-NO_x-air mixtures in all-glass chamber (Pitts et al. 1975, 1976)

effects removed. The photolysis rates were calculated using the actinic irradiations as derived as a function of zenith angle by Peterson (1976), using his "best estimate" surface albedos. Except for the kinetic mechanism and the hydrocarbon representation, the conditions employed in all ambient air simulations were those used in standard EPA isopleth calculations (Dodge 1977a,b, Whitten and Hogo 1978). In particular, full pollutant loading was assumed to occur at 7:00 a.m. local standard time, with the simulation terminating at 6:00 p.m. A constant dilution rate of 3% h^{-1} was used. Initial NO_x was assumed to consist of 25% NO_2, and all calculations were done for a latitude of 34.1°N and a solar declination of 23.5° (which is appropriate for Los Angeles in the summer).

A comparison of the O_3 isopleths calculated with the two models is shown in Figure VIII-2. As discussed previously (Carter et al. 1982), the models indeed give significantly different predictions. Plots of the

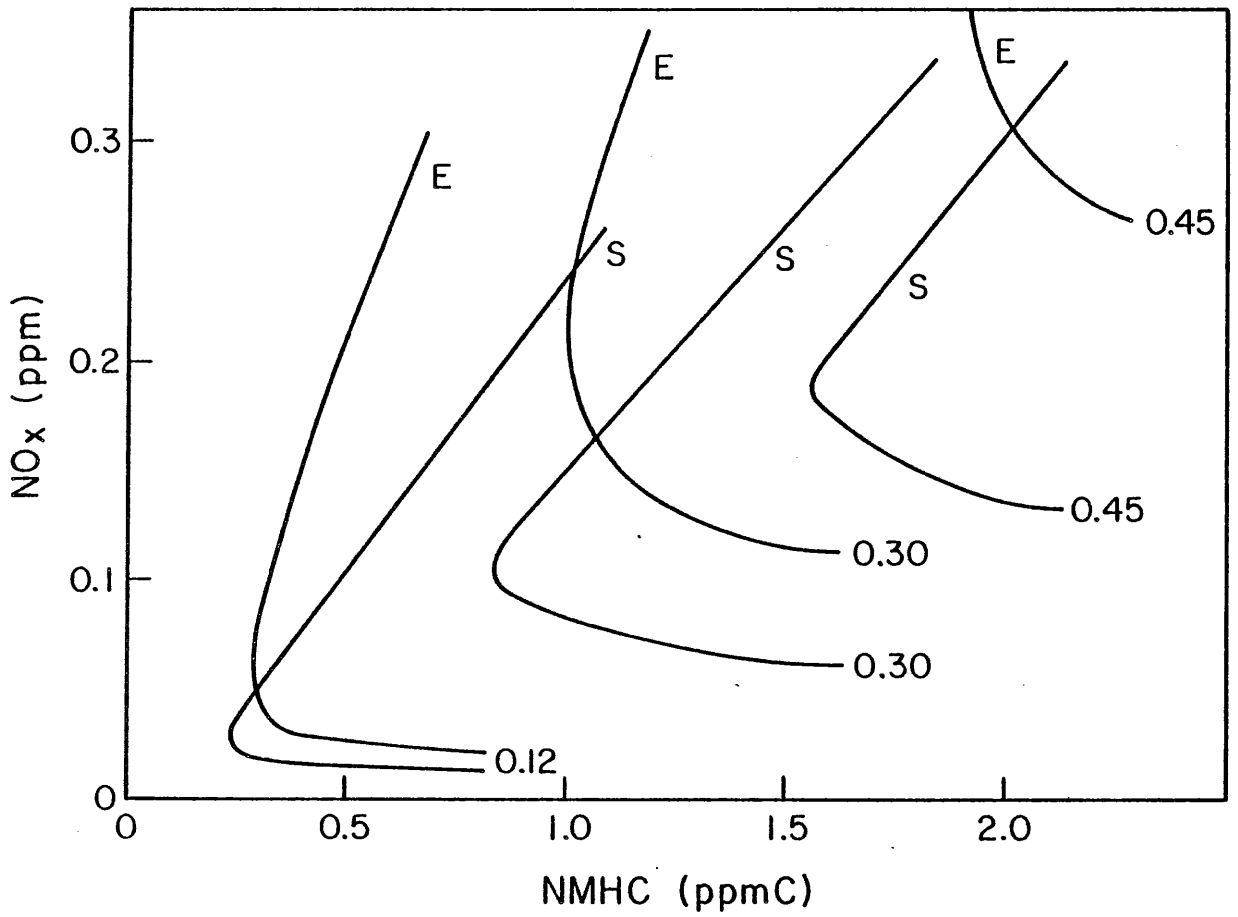

Figure VIII-2. Isopleth plots for O_3 = 0.12, 0.3 and 0.4 ppm calculated using the standard EPA EKMA model (E) and the SAPRC EKMA model (S). Note that axis labels refer to molar quantities.

proportionality factor, f, for equation (I) against the $NMHC/NO_x$ ratio calculated using the two models for assumed ambient O_3 levels of 0.2, 0.3, and 0.4 ppm are shown in Figure VIII-3. It can be seen that the proportionality factor is not particularly sensitive to the base O_3 level assumed (indeed, for model "E" it is almost completely insensitive - only a single curve is shown), but both models predict a significant dependence on the $NMHC/NO_x$ ratio, with the f-values approaching ~3 at low HC/NO_x ratios, and leveling off at ~0.3-0.4 at high HC/NO_x conditions. However, since model "S" predicts that NO_x is significantly more efficient in inhibiting O_3 formation than does model "E" (see Figure VIII-2), the models differ considerably in the $NMHC/NO_x$ levels below which the proportionality factor starts to increase rapidly. In addition, model "S" predict that no significant O_3 formation will occur at HC/NO_x ratios below ~6, and thus the analysis based on that model breaks down if ratios of 6 or lower are assumed. On the other hand, model "E" predicts significant O_3 can be formed at ratios as low as 3. Thus, except at HC/NO_x ratios above ~9, the calculated proportionality factors for equation (I) must also be considered to be highly sensitive to the kinetic mechanism and hydrocarbon representation employed in the EKMA analysis.

Although the HC/NO_x ratio most appropriate for use in EKMA analyses of the CSCAB is still uncertain (EQL 1980), it is generally believed to be in the range of 8-12, based on data for 6:00-9:00 a.m. NMHC and NO_x ambient air concentrations (EQL 1980). Within this range, model "E" predicts $f \cong 0.3\text{-}0.4$, which is independent of the HC/NO_x ratio assumed, while model "S" predicts that f may be as high as ~1.7 if the ratio at the low end of this range is assumed. However, it should be noted that if model "S" is used and HC/NO_x ratios less than ~9 are assumed, then the results indicate that signficiant NO_x levels remain at the end of the day. This is not observed during high O_3 episodes in the CSCAB. Therefore, if we restrict ourselves to HC/NO_x ratios and models which give detailed predictions reasonably consistent with what is actually observed in the basin, it is reasonable to conclude that f is less than 1.

Based on the above considerations concerning the probable range of values for the proportionality factor, f, equation (I) can then be used to estimate the contribution of the biogenic emissions to the maximum O_3 levels observed in the CSCAB. Since our "lower limit" for ROG emissions

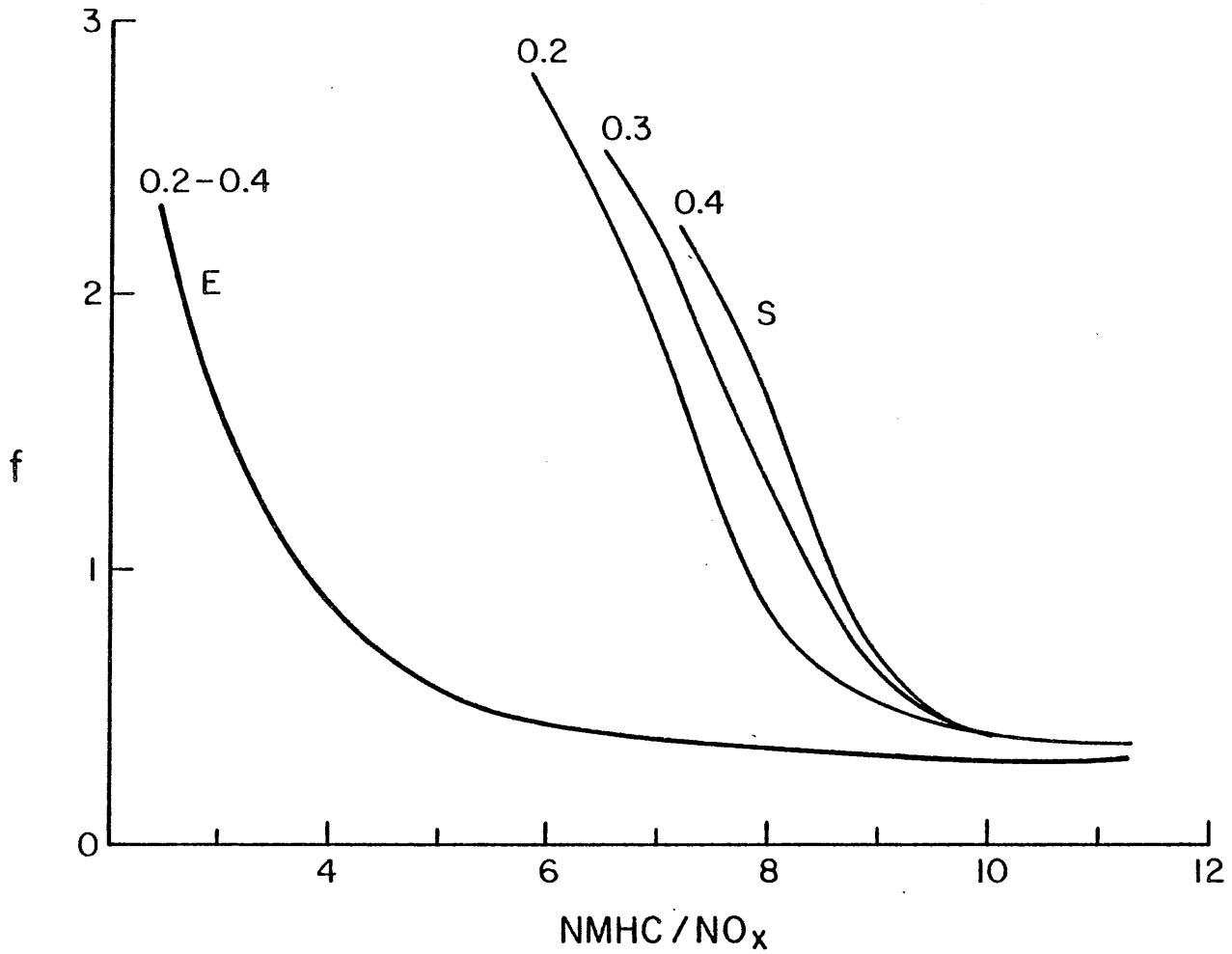

Figure VIII-3. Proportionality factor, f, for equation II plotted against HC/NO_x ratio for O_3 = 0.2, 0.3 and 0.4 ppm calculated using the standard EPA EKMA model (E) and the SAPRC EKMA model (S). Note that the abscissa units refer to mole ratios (ppmC/ppm) which must be divided by ~3.5 to give weight ratios.

from vegetation corresponds to ~2-3% of the total ROG emitted from anthropogenic sources in the study area (see Section VI), this means that the isoprene and monoterpene emissions could contribute from <1% to ~3% of the O_3 formed, depending on which model and specific HC/NO_x ratio (within the limits specified above) is assumed. Likewise, if the "worst case" upper limit emission rate of 93 tons day^{-1} of ROG from vegetation is assumed (corresponding to to ~8% of the total anthropogenic organic emissions in the study area), the isoprene and the monoterpenes could contribute to between ~2% to ~8% of the O_3 formed. Thus, an absolute "worst case" EKMA analysis predicts that the ROG emissions from vegetation in the "source" area will contribute less than 10% of the O_3 formed in the CSCAB.

C. Discussion and Conclusions

It should be re-emphasized that the analyses discussed above do not account for spatial or temporal effects of emissions, factors relating to meteorology or transport of pollutants, or considerations relating to differing reactivities of isoprene and the monoterpenes relative to anthropogenic hydrocarbons. Thus these calculations must be considered highly approximate at best. However, the comparatively low emission inventory determined for isoprene and the monoterpenes from vegetation is consistent with the very low ambient levels observed for these compounds. Further, outdoor chamber experiments have shown that replacing up to ~20% of an urban-like hydrocarbon mixture with a corresponding amount of α-pinene results in no significant change in O_3 formation (Kamens 1981), and that isoprene is less reactive, in terms of O_3 formation, than propene (Arnts and Gay 1979). Thus reactivity considerations may be unimportant. On the other hand, temporal and spatial variations in vegetation and anthropogenic emissions may be such that vegetative emissions could have a non-negligible effect on O_3 levels in localized areas, even if their effects on average O_3 levels throughout the basin are small.

Clearly, more sophisticated model calculations are required to fully elucidate the effects of emissions of hydrocarbons from vegetation on the formation of photochemical smog in the CSCAB. However, the available evidence indicates that hydrocarbon emissions from vegetation in the study area are unimportant relative to reactive organic compounds emitted from

anthropogenic sources in producing the high levels of photochemical oxidant observed in the CSCAB.

In view of this, any further efforts should be focused on refining and improving the anthropogenic ROG and NO_x emission inventories. The apparent discrepancy between the NMHC/NO_x ratio for the anthropogenic emissions inventory (SCAQMD/SCAG 1982a) vs observed ambient 6:00-9:00 a.m. concentrations (EQL 1980) suggests that the anthropogenic ROG inventory may be significantly low. If this is the case, then hydrocarbons emitted by vegetation would make an even smaller contribution to the photochemical oxidant problem in the CSCAB than these results would indicate.

IX. REFERENCES

Arnts, R. R., Seila, R. L., Kuntz, R. L., Mowry, F. L., Knoerr, K. R. and Dudgeon, A. C. (1978): Measurement of α-pinene fluxes from a loblolly pine forest. In: Proceedings, 4th Joint Conference on Sensing of Environmental Pollutants, New Orleans, LA, November 6-11, p. 829.

Arnts, R. R. and Gay, B. W., Jr. (1979): Photochemistry of some naturally emitted hydrocarbons. EPA 600/3-79-081.

Arnts, R. R. and Meeks, S. A. (1980): Biogenic hydrocarbon contribution to the ambient air of selected areas: Tulsa, Great Smoky Mountain, Rio Blanco County, CO. EPA 600/3-80-023.

Arnts, R. R. and Meeks, S. A. (1981): Biogenic hydrocarbon contribution to the ambient air of selected areas. Atmos. Environ., 15, 1643.

Arnts, R. R., Petersen, W. B., Seila, R. L. and Gay, B. W., Jr. (1982): Estimates of α-pinene emissions from a loblolly pine forest using an atmospheric diffusion model. Atmos. Environ., 16, 2127.

Atkinson, R., Lloyd, A. C. and Winges, L. (1982a): An updated chemical mechanism for hydrocarbon/NO_x/SO_2 photooxidations suitable for inclusion in atmospheric simulation models. Atmos. Environ., 16, 1341.

Atkinson, R., Winer, A. M. and Pitts, J. N., Jr. (1982b): Rate constants for the gas phase reactions of O_3 with the natural hydrocarbons isoprene and α- and β-pinene. Atmos. Environ., 16, 1017.

Atkinson, R., Aschmann, S. M., Winer, A. M. and Pitts, J. N., Jr. (1983): Kinetics of the gas phase reactions of NO_3 radicals with a series of dialkenes, cycloalkenes and monoterpenes at 295 ± 1 K. Environ. Sci. Technol., submitted for publication.

Atkinson, R. and Lloyd, A. C. (1983): Evaluation of kinetic and mechanistic data for modeling photochemical smog. J. Phys. Chem. Ref. Data, in press.

Bonner, J. and Varner, J. E., Eds. (1965): Plant Biochemistry. Academic Press, NY.

Bufalini, J. J. (1979): Technical comment on factors in summer ozone production in San Francisco Air Basin. Science, 203, 82.

Bufalini, J. J. and Arnts, R. R. (1981): Atmospheric Biogenic Hydrocarbons. Vols. 1 and 2, Ann Arbor Science, Ann Arbor, MI.

Carter, W. P. L., Lloyd, A. C., Sprung, J. L. and Pitts, J. N., Jr. (1979): Computer modeling of smog chamber data: progress in validation of a detailed mechanism for the photooxidation of propene and n-butane in photochemical smog. Int. J. Chem. Kinet., 11, 45.

Carter, W. P. L. (1981): Effect of radical initiators on EKMA predictions and validation. Presented at the EKMA workshop, Research Triangle Park, NC, December 15-16.

Carter, W. P. L. (1982): Private communication.

Carter, W. P. L., Winer, A. M. and Pitts, J. N., Jr. (1982): Effects of kinetic mechanisms and hydrocarbon composition on oxidant-precursor relationships predicted by the EKMA isopleth technique. Atmos. Environ., 16, 113.

Chatfield, R. B., Rasmussen, R. A. and Holdren, M. W. (1979): Hydrocarbon species in rural Missouri air. J. Geophys. Res., accepted for publication.

Chock, D. P., Dunker, A. M., Kumar, S. and Sloane, C. S. (1981): Effect of NO_x emission rates on smog formation in the California South Coast Air Basin. Environ. Sci. Technol., 15, 933.

Coffey, P. E. (1977): Analysis of evidence and viewpoints. Part IV. The issue of natural organic emissions. International Conference on Oxidants, 1976. EPA 600/3-77-116, October 1977.

Davis, M. and Trijonis, J. (1981): Historial emission and ozone trends in the Houston area. Santa Fe Research Corporation. EPA Contract No. 68-02-2976.

DeMarrais, G. A., Holzworth, G. C. and Husler, C. R. (1965): Meteorological summaries pertinent to atmospheric transport and dispersion over Southern California. Technical Paper No. 54, U. S. Weather Bureau.

Dement, W. A., Tyson, B. J. and Mooney, H. A. (1975): Mechanism of monoterpene volatilization in Salvia mellifera. Phytochem., 14, 2555.

Derwent, R. G. and Hov, O. (1980): The contribution from natural hydrocarbons to photochemical air pollution formation in the United Kingdom. In: Proceedings, First European Symposium on Physico-Chemical Behavior of Atmospheric Pollutants, B. Versino and H. Ott, Eds., Ispra, Italy, Oct. 16-18, 1979, p. 367.

Dimitriades, B. (1970): On the function of hydrocarbon and nitrogen oxides in photochemical smog formation. U. S. Bureau of Mines Report of Investigations, RI 7433, September.

Dimitriades, B. (1972): Effects of hydrocarbon and nitrogen oxides on photochemical smog formation. Environ. Sci. Technol., 6, 253.

Dimitriades, B. (1977): An alternative to the Appendix J method for calculating oxidant and NO_2-related control requirements. In: Proceedings of the International Conference on Photochemical Oxidant Pollution and its Control, U.S. Environmental Protection Agency, Research Triangle Park, NC. EPA-600/3-77-001.

Dimitriades, B. (1981): The role of natural organics in photochemical air pollution: issues and research needs. JAPCA, 31, 229.

Dodge, M. C. (1977a): Combined use of modeling techniques and smog chamber data to derive ozone-precursor relationships. In: Proceedings, International Conference on Photochemical Oxidant Pollution and its Control, U. S. Environmental Protection Agency, Research Triangle Park, NC. EPA-600/3-77-001.

Dodge, M. C. (1977b): Effect of selected parameters on predictions of a photochemical model. U. S. Environmental Protection Agency, Research Triangle Park, NC. EPA-600/3-77-048.

Duce, R. A. (1978): Speculations on the budget of particulate and vapor phase non-methane organic carbon in the global troposphere. Pure Appl. Geophys., 116, 244.

Durbin, R. A., Hecht, T. A. and Whitten, G. Z. (1975): Mathematical modeling of simulated photochemical smog. EPA-650/4-75-026, June.

Environmental Quality Laboratory (1980): Conference on Air Quality Trends in the South Coast Air Basin, California Institute of Technology, February 21-22.

Evans, R. C., Tingey, D. T., Gumpertz, M. L. and Burns, W. F. (1982): Estimates of isoprene and monoterpene emission rates in plants. Bot. Gaz., 143, 304.

Fitz, D. R., Dodd, M. C. and Winer, A. M. (1981): Photooxidation of α-pinene at near-ambient concentrations under simulated atmospheric conditions. Paper No. 81-27.3, presented at the 74th Annual Meeting, Air Pollution Control Association, Philadelphia, PA, June 21-26.

Flyckt, D. L. (1979): Seasonal variation in the volatile hydrocarbon emissions from ponderosa pine and red oak. Masters Thesis. Washington State University, Pullman.

Flyckt, D. L., Westberg, H. H. and Holdren, M. W. (1980): Natural organic emissions and their impact on air quality. Presented at the 73rd Annual Meeting, Air Pollution Control Association, Montreal, Canada, June 22-27.

Gerhold, H. D. and Plank, G. H. (1970): Monoterpene variations in vapors from white pines and hybrids. Phytochem., 9, 1393.

Graedel, T. E. (1979): Terpenoids in the atmosphere. Rev. Geophys. Space Phys., 17, 937.

Grimsrud, E. P., Westberg, H. H. and Rasmussen, R. A. (1975): Atmospheric reactivity of monoterpene hydrocarbons, NO_x photooxidation and ozonolysis. In: Int. J. Chem. Kinet., Symposium 1 (Chemical Kinetics Data for the Lower and Upper Atmosphere), p. 183.

Hanes, T. L. (1977): Chaparral. In: Terrestrial Vegetation of California, M. G. Barbour and J. Major, Eds., John Wiley and Sons, NY.

Harris, G. W., Carter, W. P. L., Winer, A. M. and Pitts, J. N., Jr. (1982): Observations of nitrous acid in the Los Angeles atmosphere and implications for predictions of ozone-precursor relationships. Environ. Sci. Technol., 16, 414.

Holdren, M. W., Westberg, H. H. and Zimmerman, P. R. (1979): Analysis of monoterpene hydrocarbons in rural atmospheres. J. Geophys. Res., 84, 5083.

Holzer, G., Shanfield, H., Zlatkis, A., Bertsch, W., Juarez, P., Mayfield, H. and Liebich, H. M. (1977): Collection and analysis of trace organic emissions from natural sources. J. Chromatog., 142, 755.

Hov, O. and Derwent, R. G. (1981): Sensitivity studies of the effects of model formulation on the evaluation of control strategies for photochemical air pollution formation in the United Kingdom. JAPCA, 31, 1260.

Hunsaker, D. (1981): Selection of biogenic hydrocarbon emission factors for land cover classes found in the San Francisco Bay Area. Air Quality Tech. Memo 31, Association of Bay Area Governments, January.

Hunsaker, D. and Moreland, R. (1981): Compilation of a biogenic hydrocarbon emissions inventory for the evaluation of ozone control strategies in the San Francisco Bay Area. Air Quality Tech. Memo 35, Association of Bay Area Governments, March.

Jones, C. A. and Rasmussen, R. A. (1975): Production of isoprene by leaf tissue. Plant Physiol., 55, 982.

Kamens, R. M. (1981): The impact of alpha-pinene on urban smog formation: an outdoor smog chamber study. In: Atmospheric Biogenic Hydrocarbons, J. J. Bufalini and R. R. Arnts, Eds., Ann Arbor Science, Ann Arbor, MI, Vol. 2, p. 187.

Kamiyama, K., Takai, T. and Yamanaka, Y. (1978): Correlation between volatile substances released from plants and meteorological conditions. In: Proceedings, International Clean Air Conference, E. T. White, P. Hetherington, B. R. Thiele, Eds., Brisbane, Australia, p. 365.

Kleindienst, T. E., Harris, G. W. and Pitts, J. N., Jr. (1982): Rates and temperature dependences of the reaction of OH with isoprene, its oxidation products, and selected terpenes. Environ. Sci. Technol., 16, 844.

Lloyd, A. C., Lurmann, F. W., Godden, D. K., Hutchins, J. F., Eschenroeder, A. E. and Nordsieck, R. A. (1979): Development of the ELSTAR photochemical air quality simulation model and its evaluation relative to the LARPP data base. Environmental Research and Technology, document P-5287-500, July.

Lloyd, A. C., Atkinson, R., Lurmann, F. W. and Nitta, B. (1983): Modeling potential ozone impacts from natural hydrocarbons. Part I: Development and testing of a chemical mechanism for the NO_x-air photooxidations of isoprene and α-pinene under ambient conditions. Atmos. Environ., in press.

Lonneman, W. A., Seila, R. L. and Bufalini, J. J. (1978): Ambient air hydrocarbon concentrations in Florida. Environ. Sci. Technol., 12, 459.

Ludlum, K. H. and Bailey, B. S. (1979): Correspondence to the editor, Environ. Sci. Technol., 13, 235.

Lurmann, F. W., Lloyd, A. C. and Nitta, B. (1983a): Modeling potential ozone impacts from natural hydrocarbons. Part II: Hypothetical biogenic HC emission scenario modeling. Atmos. Environ., in press.

Lurmann, F. W., Nitta, B., Ganesen, K. and Lloyd, A. C. (1983b): Modeling potential ozone impacts from natural sources. Part III: Ozone modeling in Tampa/St. Petersburg, Florida. Atmos. Environ., submitted November 1982.

McCrae, G. J., Goodin, W. R. and Seinfeld, J. H. (1982): Mathematical modeling of photochemical air pollution. EQL Report No. 18, California Institute of Technology. Final Report, California Air Resources Board, ARB Contract Nos. A5-046-87 and A7-187-30, April.

Meigh, D. F. (1955): Volatile alcohols, aldehydes, ketones and ester. In Modern Methods of Plant Analysis. K. Paech and M. V. Tracey, Eds., Springer-Verlag, Berlin, Vol. 2, p. 403.

Mendenhall, W., Lyman, G. H. and Scheaffer, R. L. (1971): Elementary Survey Sampling. Wadsworth Publishing Co., Belmont, CA.

Miller, P. R., Pitts, J. N., Jr. and Winer, A. M. (1979): Technical comment on factors in summer ozone production in the San Francisco Air Basin. Science, 203, 81.

Minnich, R. A., Bowden, L. W. and Pease, R. W. (1969): Mapping montaine vegetation in Southern California from color infrared imagery. In: Studies in Remote Sensing of Southern California Environments, University of California at Riverside, Department of Geography, Technical Report 111, 54 pp.

Mooney, H. A. (1977): Southern coastal scrub. In: Terrestrial Vegetation of California, M. G. Barbour and J. Major, Eds., John Wiley and Sons, NY.

Munz, P. A. and Keck, D. D. (1968): A California Flora. University of California Press, Berkeley and Los Angeles, CA.

Orme, A. R., Bowden, L. W. and Minnich, R. A. (1971): Remote sensing of disturbed insular vegetation from color infrared imagery. In: Proceedings, Seventh Symposium on Remote Sensing of the Environment, University of Michigan, Ann Arbor, p. 1235.

Pacific Coast Nurserymen and Gardener's Journal (1982): Private communication.

Paysen, T. E. (1978): Sampling wildland vegetation. Ph.D. Thesis, University of California, Riverside, 185 pp.

Peterson, E. W. and Tingey, D. T. (1980): An estimate of the possible contributions of biogenic sources to airborne hydrocarbon concentrations. Atmos. Environ., 14, 79.

Peterson, J. T. (1976): Calculated actinic fluxes (290-700 nm) for air pollution photochemistry application. EPA-600/4-76-025.

Pitts, J. N., Jr., Winer, A. M., Darnall, K. R., Doyle, G. J. and McAfee, J. M. (1975): Chemical consequences of air quality standard and of control implementation programs: roles of hydrocarbons, oxides of nitrogen, and aged smog in the production of photochemical oxidant. Final Report, California Air Resources Board Contract No. 3-017, July.

Pitts, J. N., Jr., Winer, A. M., Darnall, K. R., Doyle, G. J. and McAfee, J. M. (1976): Chemical consequences of air quality standards and of control implementation programs: roles of hydrocarbons, oxides of nitrogen and aged smog in the production of photochemical oxidant. California Air Resources Board Contract No. 4-214, Final Report, May.

Pitts, J. N., Jr., Winer, A. M., Carter, W. P. L., Doyle, G. J., Graham, R. A. and Tuazon, E. C. (1980): Chemical consequences of air quality standards and control implementation programs. Final Report, California Air Resources Board.

Platt, U., Perner, D., Winer, A. M., Harris, G. W. and Pitts, J. N., Jr. (1980): Detection of NO_3 in the polluted troposphere by differential optical absorption. Geophys. Res. Letts., 7, 89.

Platt, U., Winer, A. M., Biermann, H. W., Atkinson, R. and Pitts, J. N., Jr. (1983): Measurement of nitrate radical concentrations in continental air. Environ. Sci. Technol., submitted for publication.

Rand Corporation, (1955): A Million Random Digits with 100,000 Normal Deviates, Free Press, Glencoe, IL.

Rasmussen, R. A. and Went, F. W. (1965): Volatile organic material of plant origin in the atmosphere. Proc. Nat. Acad. Sci., 53, 215.

Rasmussen, R. A. (1970): Isoprene: identified as a forest-type emission to the atmosphere. Environ. Sci. Technol., 4, 667.

Rasmussen, R. A. (1972): What do the hydrocarbons from trees contribute to air pollution? JAPCA, 22, 537.

Rasmussen, R. A. and Jones, C. A. (1973): Emission isoprene from leaf discs of Hamamelis. Phytochem., 12, 15.

Reynolds, S. D., Tesche, T. W. and Reid, L. E. (1979): An introduction to the SAI airshed model and its usage. Systems Applications, Incorporated, San Rafael, CA. EF78-53R4 - EF79-31, March.

Riggan, P. J. and Lopez, E. (1981): Nitrogen relations in a Quercus dumosa community. In: Dynamics and Management of Mediterranean-Type Ecosystems, USDA Forest Service, PSW General Technical Report PSW-58, p. 631.

Robinson, E. (1978): Hydrocarbons in the atmosphere. Pageoph., 116, 372.

Sanadze, G. A. and Kalandze, A. N. (1966): Evolution of the diene C_5H_8 by poplar leaves under various conditions of illumination. Dokl. Bot. Sci. 168, 95.

Sandberg, J. S., Basso, M. J. and Okin, B. A. (1978): Winter rain and summer ozone: a predictive relationship. Science, 200, 1051.

Schulting, F. L., Meyer, G. M. and van Aalst, R. M. (1980): Emission of hydrocarbons by vegetation and its contribution to air pollution in the Netherlands. TNO Report No. CMP 80/16, November 1.

Sculley, R. D. (1979): Correspondence to the editor. Environ. Sci. Technol., 13, 234.

South Coast Air Quality Management District/Southern California Association of Governments (1982a): Draft, Air Quality Management Plan, 1982 Revision, Appendix No. IV-A: Final 1979 emissions inventory for the South Coast Air Basin, July.

South Coast Air Quality Management District/Southern California Association of Governments (1982b): Draft, Air Quality Management Plan, 1982 Revision, August.

Taback, H. J., Sonnichsen, T. W., Brunetz, N. and Stredler, J. L. (1978): Control of hydrocarbon emissions from stationary sources in the California South Coast Air Basin. Final Report, Vol. I, California Air Resources Board, Contract No. 5-1323, June.

Tingey, D. T., Ratsch, H. C., Manning, M., Grothaus, L. C., Burns, W. F. and Peterson, E. W. (1978): Isoprene emission rates from live oak. EPA-CERL Report No. 40, May.

Tingey, D. T., Manning, M., Grothaus, L. C. and Burns, W. F. (1979): The influence of light and temperature on isoprene emission rates from live oak. Physiol. Plant., 47, 112.

Tingey, D. T. and Burns, W. F. (1980): Hydrocarbon emissions from vegetation. In: Proceedings, Symposium on Effects of Air Pollutants on Mediterranean and Temperate Forest Ecosystems, Riverside, CA, June 22-27, and references therein.

Tingey, D. T., Manning, M., Grothaus, L. C. and Burns, W. F. (1980): The influence of light and temperature on monoterpene emission rates from slash pine. Plant Physiol., 65, 797.

Tingey, D. T. (1981): The effect of environmental factors on the emission of biogenic hydrocarbons from live oak and slash pine. In: Atmospheric Biogenic Hydrocarbons, J. J. Bufalini and R. R. Arnts, Eds., Ann Arbor Science, Ann Arbor, MI, Vol. 1, p. 53.

Tyson, B. J., Dement, W. A. and Mooney, H. A. (1974): Volatilization of terpenes from Salvia mellifera. Nature, 252, 119.

U. S. Environmental Protection Agency (1977): Uses, limitations and technical basis of procedures for quantifying relationships between photochemical oxidants and precursors. Research Triangle Park, NC. EPA-450/2-77-021a.

U. S. Environmental Protection Agency (1978): Air quality criteria for ozone and other photochemical oxidants. Washington, DC. EPA-600/8-78-004.

Went, F. W. (1960): Blue hazes in the atmosphere. Nature, 187, 641.

Westberg, H. H. (1977): Analysis of evidence and viewpoints. Part IV. The issue of natural organic emissions. International Conference on Oxidants, 1976. EPA 600/3-77-116, October 1977.

Whitby, R. A. and Coffey, P. E. (1977): Measurement of terpenes and other organics in an Adirondack mountain pine forest. J. Geophys. Res., 82, 5928.

Whitten, G. Z. and Hogo, H. (1978): Users manual for kinetics, model and ozone isopleth plotting package. EPA-600/8-76-014a.

Winer, A. M., Lloyd, A. C., Darnall, K. R. and Pitts, J. N., Jr. (1976): Relative rate constants for the reaction of the hydroxyl radical with selected ketones, chloroethanes, and monoterpene hydrocarbons. J. Phys. Chem., 80, 1635.

Winer, A. M., Fitz, D. R. and Miller, P. R. (1981): Investigation of the role of natural hydrocarbons in photochemical smog formation in California. Final Report, California Air Resources Board, Contract No. A8-135-31, March.

Winer, A. M., Dodd, M. C., Fitz, D. R., Miller, P. R., Stephens, E. R., Neisess, K., Meyers, M., Brown, D. E. and Johnson, C. W. (1982): Assembling a vegetative hydrocarbon emission inventory for the California South Coast Air Basin: direct measurement of emission rates, leaf biomass and vegetative distribution. Paper No. 82-

51.6. Presented at the 75th Annual Meeting of the Air Pollution Control Association, New Orleans, LA, June 20-25.

Zimmerman, P. R., Chatfield, R. B., Fishman, J., Crutzen, P. J. and Hanst, P. L. (1978): Estimates of the production of CO and H_2 from the oxidation of hydrocarbon emissions from vegetation. J. Geophys. Res. Lett., 5, 679.

Zimmerman, P. R. (1979a): Tampa Bay Area Photochemical Oxidant Study: determination of emission rates of hydrocarbons from indigenous species of vegetation in the Tampa/St. Petersburg, Florida, area. Final Appendix C, February 2, 1979. EPA 904/9-77-028.

Zimmerman, P. R. (1979b): Testing of hydrocarbon emissions from vegetation, leaf litter and aquatic surfaces, and development of a methodology for compiling biogenic emission inventories. Final Report, March 1979. EPA 450/4-79-004.

Zimmerman, P. R. (1979c): Natural sources of ozone in Houston: natural Organics. In: Proceedings, Air Pollution Control Association Specialty Conference on Ozone/Oxidants, Houston, TX, October.

Zimmerman, P. R. (1980): Natural sources of ozone in Houston: natural organics. In: Proceedings, Specialty Conferences on Ozone/Oxidants-Interactions with the Total Environment, II, Air Pollution Control Association, Pittsburgh, PA.

X. GLOSSARY OF TERMS, ABBREVIATIONS AND SYMBOLS

ABAG: Association of Bay Area Governments

Aerial Imagery: Five overlapping frames of CIR photography taken for the randomly chosen sample cell in each of 20 polygons

AQMP: Air Quality Management Plan

BAAQMD: San Francisco Bay Area Air Quality Management District

CARB: California Air Resources Board

CDF: California Department of Forestry

CIR: Color infrared

Cover area or areal cover: Area of an individual plant as would be seen by aerial imagery (maximum cross section area). When referring to a species, it is the total area of all plants of that species

CSCAB: California South Coast Air Basin

Detection Limit: Concentration of hydrocarbons below which the corresponding gas chromatographic peak was indistinguishable from the noise

DSI: D & S Instrument, Ltd. of Pullman, Washington (where sampling canisters used in this study were purchased)

EDC: Environmental Design Consultants of Pullman, Washington

EKMA: Empirical kinetic modeling approach

EPA: U. S. Environmental Protection Agency

FID: Flame ionization detector or flame ionization detection

GC: Gas chromatography or gas chromatograph

GC-MS: Gas chromatography-mass spectrometry or gas chromatograph-mass spectrometer

Imagery area: (a) Sum of the areas of all specimens in each of five structural classes (broad-leaf and conifer, palms, shrubs, groundcover, and lawns) in the mapped area. (b) The area covered by high resolution CIR photography obtained in this study

"Knowns": Species with measured emission rates and leaf mass constants

Leaf mass: Biomass of grean leaf tissue (kg)

Leaf mass constants: Mass of dry green tissue per unit volume for a plant species (m^{-3})

LUDA: Land-Use and Land-Cover Data Analysis System (maps developed by the U. S. Geological Survey)

Mapped area: Area of imagery frame closest to the center of the sample cell (0.16 to 0.64 square kilometers)

Nadir point: "Center" point of the rectangularly shaped sample cells

NMHC: Non-methane hydrocarbons

Polygon: One of 20 urban areas defined by having a distinct reflective intensity and color on high altitude U-2 CIR imagery

PSFRES: Pacific Southwest Forest and Range Experiment Station

ROG: Reactive organic gases

Sample Cell: A randomly selected grid cell overlaid on the polygon by latitude and longitude on 1:250,000 scale U.S. Geological Survey maps

SAPRC: Statewide Air Pollution Research Center

SCAG: Southern California Association of Governments

SCAQMD: South Coast Air Quality Management District

SFBAAB: San Francisco Bay Area Air Basin

Structural Class: One of six classes of vegetation for field survey data (conifers, broad-leaf trees, palms, shrubs, grasses, and ground cover). Imagery data were grouped into five structural classes (broad-leaf trees and conifers, palm trees, shrubs, grasses, and ground cover)

Study area: Western and middle portion of CSCAB including surrounding slopes, with natural vegetation extending up to 3600 ft elevation, and encompassing 4500 km^2

Subplot: An area randomly selected area from a sample cell overlaid on a Thomas Brothers street map using streets as borders and references. These subplots were surveyed by field botanists to determine species composition and distribution

TNMHC: Total observed non-methane hydrocarbons

UCR: University of California, Riverside

"Unknowns": Species found in the field but for which leaf mass constants and emission rates were not determined

USDA: United States Department of Agriculture

USGS: United States Geological Survey

UTM: Universal Transverse Mercator (a coordinate system)

Vegetation type: One of five naturally occurring vegetation communities found in the study area (Woodland, Chamise chaparral, Chaparral, Sage and Grassland)